Deciphering the Tuzin protein of *Leishmania donovani* as a potential Diagnostic Marker and Vaccine Candidate against Visceral Leishmaniasis

Thesis submitted to University of Hyderabad for the award of

Doctor of Philosophy

In Department of Animal Biology

By

Moodu Devender

17LAPH15

Department of Animal Biology
School of Life Sciences
University of Hyderabad
Hyderabad–500046, India

March 2023

UNIVERSITY OF HYDERABAD
Central University (P.O.), Gachibowli, Hyderabad-500046

DECLARATION

I, **Moodu Devender,** hereby declare that this thesis entitled **"Deciphering the Tuzin protein of *Leishmania donovani* as a potential Diagnostic Marker and Vaccine Candidate against Visceral Leishmaniasis"** submitted by me under the supervision of **Dr. Radheshyam Maurya** and also declare that it has not been submitted previously in part or in full to this University or any other University or Institution for the award of any degree or diploma earlier.

Date:

Moodu Devender
(Ph.D. Research Scholar)
17LAPH15

University of Hyderabad
(A Central university by an act of Parliament)
Department of Animal Biology
School of Life Sciences
P.O. Central University, Gachibowli, Hyderabad-500046

"CERTIFICATE"

This is to certify that the thesis entitled **"Deciphering the Tuzin protein of *Leishmania donovani* as a potential Diagnostic Marker and Vaccine Candidate against Visceral Leishmaniasis"** submitted by **Moodu Devender** bearing registration number **17LAPH15** in partial fulfilment of the requirements for award of Doctor of philosophy in the **School of Life Sciences** is a bonafide work carried out by him under my supervision and guidance.

This thesis is free from plagiarism and has not been submitted previously in part or in full to this or any other University or Institution for award of any degree or diploma.

A. Published in the following publications:

1. Frontiers in immunology. 18 June 2021. doi: 10.3389/fimmu.2021.649359
2. The FEBS Journal 286 (2019) 3488–3503. doi:10.1111/febs.14923
3. Experimental Parasitology 236-237 (2022) 108250. doi: *org/10.1016/j.exppara.2022.108250*

B. Presented in the following conference:

1. "14th The Cytometry Society Annual Conference" Organized by University of Hyderabad, India. October 2022 (International).

Further, the student has passed the following courses towards fulfillment of coursework requirement for Ph.D.

S.No.	Course code	Name of Course	Credits	Pass/Fail
1	AS 801	Research methodology/ Analytical Techniques	4	PASS
2	AS 802	Research Ethics, Biosafety, Data Analysis and Biostatistics	4	PASS
3	AS 803	Scientific Writing and Research Proposal	4	PASS

Supervisor Head of the Department Dean of the School

ACKNOWLEDGEMENTS

I owe my first and heartiest indebtedness to my supervisor, **Dr. Radheshyam Maurya**, Associate Professor, Department of Animal Biology, School of Life Sciences, University of Hyderabad, for his expert guidance, counsel, patience, constructive criticism, and appreciation of my work. He also provided me with excellent advice throughout my research work. Working under his capable supervision and scientific expertise was indeed a huge honor. I acknowledge his advice not only related to my project but also to my personal life. His faith in me and ongoing encouragement throughout the journey helped me to develop self-confidence, which I will carry with me throughout the rest of my life as a remembrance of him.

I thank my DC members, **Prof. S. Dayananda** and **Prof. Manjula Sritharan,** for their critical comments and valuable suggestions.

I am grateful to present Dean **Prof. N. Shiva Kumar**, School of Life Sciences, former Deans **Prof. S. Dayananda**, **Prof. K. Ramaiah,** and **Prof. P. Reddanna** for providing good scientific infrastructure for the School and the Department to carry out research work.

I thank present and former Heads of the Department of Animal Biology, **Prof. Srinivasulu Kurkuti**, **Prof. Anita Jagota,** and **Prof. Jagan Pongubala,** for providing us with good equipment and facilities to carry out the work.

I thank **Prof. Kota Arun Kumar** for his helpful suggestions and comments during the progress and for all the School of Life Sciences faculties.

It is pleasant that I have an opportunity to express my gratitude **to Prof. Shyam Sundar,** BHU, for providing human VL patient serum samples used in this study.

I thank all the non-teaching office staff of the Department of Animal Biology, Animal House, and the School of Life Science for their continuous service and help.

I thank DST-SERB, DBT, UGC, ICMR, DST-PURSE, UPE II, and IoE for funding the lab. I acknowledge the infrastructure support provided by DBT-CREBB, and DST-FIST to the Dept. of Animal Biology and School of Life Sciences.

I thank the University of Hyderabad for supporting me with the BBL fellowship, DST-SERB and IoE as a Junior Research Fellowship.

I thank my lab seniors, **Dr. Jalaja Veronica** and **Dr. Bharadwaj**, for their suggestions and support.

I acknowledge my lab mates **Prince Sebastian**, **Madhulika Namdeo**, **Anjali Anand**, **Krishan Kumar,** and **Manikanta Bondada** for their help and support, and I thank all the project students who worked in our lab. They have been great lab-mates, made work in the laboratory smoother and more enjoyable.

I also want to thank all my friends from different laboratories at the School of Life Sciences, University of Hyderabad, for their cooperation and help during my doctorate tenure.

I would also thank my friends **Gandhari Shankar**, **Rajula Rajender**, **Rohit Kumar Yadav**, **Kundarapu Raju**, **Jangili Ramesh**, **Madhukar Adla, Moodu Thirupathi**, and my cousin **Lavudya Veeranna**, for their constant support and encouragement.

I want to thank **Dr. Rajan Kumar Pandey** and **Dr. Vinay Kumar** for their constant support, encouragement, and guidance throughout my journey.

I sincerely thank my supportive wife, **Mrs. Kunturi Sravanthi**, for her love and understanding and for making it possible for me to get a Ph.D. She also deserves my gratitude for never leaving my side as I faced the inevitable ups and downs while conducting my research. Her patience with my erratic emotions is evidence of her everlasting affection and commitment.

Saving the most important for the last, I owe my loving thanks and deepest gratitude to my mother **Mrs**. **Moodu Parvathi,** my father **Mr. Moodu vaagya**, my grandmother **Moodu Maaru** and grandfather **Moodu Ramulu,** and specially my brother **Mr. Moodu Venkanna** for encouraging me; in the most critical and difficult decisions throughout my life and always supported me in my endeavors. At last, I want to convey to all my family members that I am about to make their dreams a reality and give them some respect for the everlasting trust they have in me and the pains they have taken to bring me to this place today.

I offer my obeisance to "**Almighty God**" for blessing me with good health, patience, and strength to fulfill my endeavors successfully.

Moodu Devender

Table of Contents

Abbreviations

Ant-His	Anti-Histidine
AmB	Amphotericin B
APC	Antigen Presenting Cells
ATCC	American Type Culture Collection
BCIP	5-Bromo-4-chloro-3-indolyl phosphate disodium salt
BLAST	Basic Local Alignment Search Tool
BOD	Biochemical Oxygen Demand
BPL	Below Poverty Line
BSA	Bovine Serum Albumin
CaCl2	Calcium Chloride
CaCO2	Calcium Carbonate
CD	Cluster of Differentiation
cDNA	Complementary deoxyribonucleic acid
CL	Cutaneous Leishmaniasis
CLA	Crude *Leishmania* Antigen
CMI	Cell-Mediated Immunity
CO_2	Carbon Dioxide
C_T	Threshold cycle
DAPI	4',6 diamidino-2phenylindole
DC	Dendritic Cell
DCL	Diffuse Cutaneous Leishmaniasis
DD8	*Leishmania donovani* strain MHOM/IND/80/DD8
DNA	Deoxyribonucleic acid
dNTP	Deoxynucleotide triphosphate
DTT	Dithiothreitol
EDTA	Ethylene Diamine Tetra Acetic acid
ELISA	Enzyme-Linked Immunosorbent Assay
EtBr	Ethidium bromide
FASTA	Fast Alignment
FBS	Fetal Bovine Serum
GAPDH	Glyceraldehyde-3-phosphate dehydrogenase
GFP	Green fluorescent protein
gp63	Glycoprotein 63
H_2DCFDA	2',7'---dichlorodihydrofluorescein diacetate
H_2O_2	Hydrogen Peroxide
H_2SO_4	Sulphuric acid
HBSS	Hanks balanced salt solution
H-E	Haematoxylin-Eosin
HIV	*Human Immunodeficiency Virus*
HRP	Horse Radish Peroxidase
i.d.	Intra Dermal
i.m	Intra Muscular

i.v.	Intra Venal
IAEC	Institutional Animal Ethics Committee
IFN-γ	Interferon-γ
Ig	Immunoglobulin
IL	Interleukin
iNOS	Inducible Nitric Oxide Synthase
IPTG	Isopropyl β-D-1-Thiogalactopyranoside
KCl	Potassium Chloride
kDa	Kilo Dalton(s)
kDNA	Kinetoplastid deoxyribonucleic acid
Kg	Kilo gram
L. donovani	*Leishmania donovani*
L. infantum	*Leishmania infantum*
L. major	*Leishmania major*
L. maxicana	*Leishmania mexicana*
L. tropica	*Leishmania tropica*
LAT	Latex Agglutination Test
LB broth	Luria-Bertani broth
LPS	Lipopolysaccharide
M199	Medium-199
MFI	Mean fluorescence intensity
mg	Milli gram
MgCl2	Magnesium Chloride
MHC	Major Histocompatibility Complex
ml	Milli litre
mRNA	Messenger Ribonucleic Acid
MW	Molecular Weight
NaCl	Sodium Chloride
$NaHCO_3$	Sodium Bicarbonate
NaOH	Sodium hydroxide
ng	Nano gram
NK cells	Natural Killer cells
nm	Nano meter
NO	Nitric oxide
NOS	Nitric Oxide Synthase
ns	Nano seconds
OD	Optical Density
PBMCs	Peripheral Blood Mononuclear Cells
PBS	Phosphate Buffer Saline
PBS-T	Phosphate Buffer Saline-Tween
PCR	Polymerase Chain Reaction
PDB	Protein Data Bank
PE	Phycoerythrin
PI	Propidium iodide
PKDL	Post *Kala-Azar* Dermal Leishmaniasis

PMA	Phorbol 12-myristate 13-acetate
PMSF	Phenyl Methyl Sulphonyl Fluoride
PV	Parasitophorous Vacuole
RIPA	Radioimmunoprecipitation assay
ROS	Reactive Oxygen Species
RPMI	Roswell Park Memorial Institute
RT	Room Temperature
SDS	Sodium dodecyl sulphate
SDS-PAGE	Sodium Dodecyl Sulphate-Poly Acrylamide Gel Electrophoresis
Sec	Second
SEM	Scanning electron microscope
SLA	Soluble *Leishmania* Antigen
T. brucei	*Trypanosoma brucei*
T. cruzi	*Trypanosoma cruzi*
TBS	Tris Buffered Saline
TBS-T	Tris-Buffer Saline-Tween
TEMED	N,N,N',N'-Tetramethylethylenediamine
Th	T-helper
TMB	3,3', 5,5;-tetramethylbenzidine
TNF-α	Tumor Necrosis Factor-α
Tris-HCl	Tris-Hydrochloric acid
VL	Visceral leishmaniasis
WB	Western Blotting
WHO	World Health Organization
WT	Wild type
λ	Wave length
µg	Micro gram
µl	Micro litre
µM	Micro molar
µm	Micro meter
µn	Micron
Φ	Macrophage
%	Percentage
˚C	Degree centigrade/Degree Celsius

Chapter: I
Introduction

1.1 Leishmaniasis – an overview:

A protozoa parasite from the genus *Leishmania* and family Kinetoplastida, which includes more than 20 species of *Leishmania*, causes leishmaniasis. More than 90 kinds of sandflies can carry the parasite *Leishmania* (Boelaert *et al.*, 2004). The second most parasitic severe illness recognized by the WHO is leishmaniasis. Still, it poses a serious threat to public health, primarily in underdeveloped nations. There are four primary leishmaniases: cutaneous, which is the most prevalent; Mucocutaneous and visceral leishmaniasis (VL), often called Kala-azar. The disease's most lethal manifestation, called VL, affects different internal organs like the spleen, liver, and bone marrow. Additionally, it is common for patients with visceral Leishmaniasis to develop post kala-azar leishmaniasis (PKDL) as a consequence. Infected female sandflies of the genera *Phlebotomine* or *Lutzomyia* feeding on blood spread this disease by biting exposed humans (Vermelho et al., 2014). The disease impacts individuals who are among the most disadvantaged, and its occurrence is linked to inadequate housing, compromised immune systems, displacement of population, and limited financial means. The severity of this illness is made worse by factors like poor nutrition, stress, weakened immune system, poverty, famine, and war (WHO 2022). *Leishmania* parasites' natural reservoir hosts comprise more than 70 animal species, including humans. Of these, 71 countries for both VL and CL, 19 for CL, and nine for only VL cases reported as endemic. As of November 2022, data for 48 VL-endemic countries (60%) and 51 CL-endemic countries (57%) has been submitted to the WHO Global Leishmaniasis Programme for 2021. Today, almost one billion individuals are at risk of contracting Leishmaniasis because they reside in places where the disease is endemic. The World Health Organization (WHO) estimates that there are more than 30,000 new cases of VL and more than 1 million new cases of CL per year. Eight nations, including Brazil, Eritrea, Ethiopia, Somalia, India, Kenya, South Sudan, and Sudan, have been the primary reporting countries for these cases, which collectively account for more than 89% of all VL cases worldwide (WHO, 2022).

The incidence and prevalence of Leishmaniasis are influenced by a combination of factors such as the attributes of the parasite and sand fly varieties, the environmental conditions of the areas where the disease is transmitted, human behaviour and the local population's history of parasite exposure. *Leishmania* and HIV co-infected individuals have

a high chance of developing a severe clinical state as well as high relapse and mortality rates. As of 2021, leishmania-HIV co-infection cases were documented in 45 different nations. HIV infection coexists with leishmaniasis are prevalent in Brazil, Ethiopia, as well as the Indian state of Bihar, according to reports. The virulence of the parasite, the saliva's capacity to inhibit immunological function, the genetic makeup of the host, and the polymorphic outcome of VL is influenced by the various roles played by the immune response. A modernistic strategy for controlling the disease is required because it is currently impossible to prevent and manage. A good vaccination strategy can bring the disease under control. The parasite's short life cycle and the host's resistance to subsequent infections after recovering from a first infection favor the development of vaccines (Loría-Cervera and Andrade-Narváez, 2014; Kaye and Aebischer, 2011). Research advances in efficient case management and vector control are crucial for eradicating VL.

1.2 Historical Background:

Leishmaniasis affected people in prehistoric periods, according to archaeological and historical data. There are pictures of CL-like lesions that are evident on the record of the 7th century ruler Ashurbanipal. Avicenna, a Persian physician who lived in the tenth century, described Balkh sore thoroughly. After examining a patient in Turkey, Alexander Russell detailed the disease's clinical characteristics and gave it the name "Aleppo boil" in 1756. In the Americas, pottery from earlier times displays facial damage and engravings of skin lesions, which are historical and archaeological proof of CL in Peru and Ecuador from the 1st century. The diseases known as valley disease, Andean disease and white leprosy are probably CL were referenced in several manuscripts from the Spanish colonial era and the Inca Empire published between the 15th and 16th centuries (Steverding, 2017). In the latter half of the 19th century, the parasite that causes leishmaniasis was discovered independently by Borovsky, Cunningham, Leishman Vianna, Wright, Lindenberg, and Donovan. Leishman discovered new microbes in the spleen of an army soldier who had died of "dum-dum illness" in 1901. On May 30, 1903, he published his findings in "The British Medical Journal" under the heading "On the likelihood of trypanosomiasis occurring in India". Upon finding a similar organism in a smear from a patient in Madras, Charles Donovan responded to an article by Leishman that had been published in the same publication on July 11, 1903 (Bray *et al.*, 2010).

The information about Kala-Azar needed to be clarified prior to the 1820s. William Twining first listed fever and splenic enlargement as Kala-Azar symptoms. The 1st epidemic of the Leishmaniasis, which was misinterpreted as malaria and occurred in 1824–1825 at "Mahomedpore," located in Lower Bengal, around 30 miles east of Jessore, was caused by unclean village surroundings and villager behavior. A quinine-resistant second pandemic fever struck Burdwan a few years later, in 1858. Eight to ten years later, a fever with spleen enlargement, anemia, and skin darkening appeared in the southwest of Assam. Locally, this ailment was known as Kala-Azar. Ronald Ross conducted research in Darjeeling, Assam, and Upper Bengal in 1898 on Kala-Azar and believed they were all cases of the same disease. He came to the conclusion that the illness was a result of malaria and other opportunistic illnesses. Donovan discovered *L. donovani* in internal organs and peripheral circulation in 1904. Leonard Rogers cultured *L. donovani* in in vitro at 27 °C for the first occasion in 1904. Sand flies are the vector for the spread of Kala-Azar, as proven and established by British-Israeli parasitologist Saul Adler in 1942 (Gibson, 1983; Khatun *et al.*, 2017).

1.3 Taxonomical Classification of *Leishmania*

Leishmania is divided into two subgenera: (i) *Leishmania,* which is found in both the New and Old and nations, and (ii) Viannia, which is restricted to the New World only. *Leishmania* is categorized as belonging to the Trypanosomatidae family, Kinetoplastida order, and *Leishmania* genus. Figure 1.1 depicts the entire taxonomy of *Leishmania*.

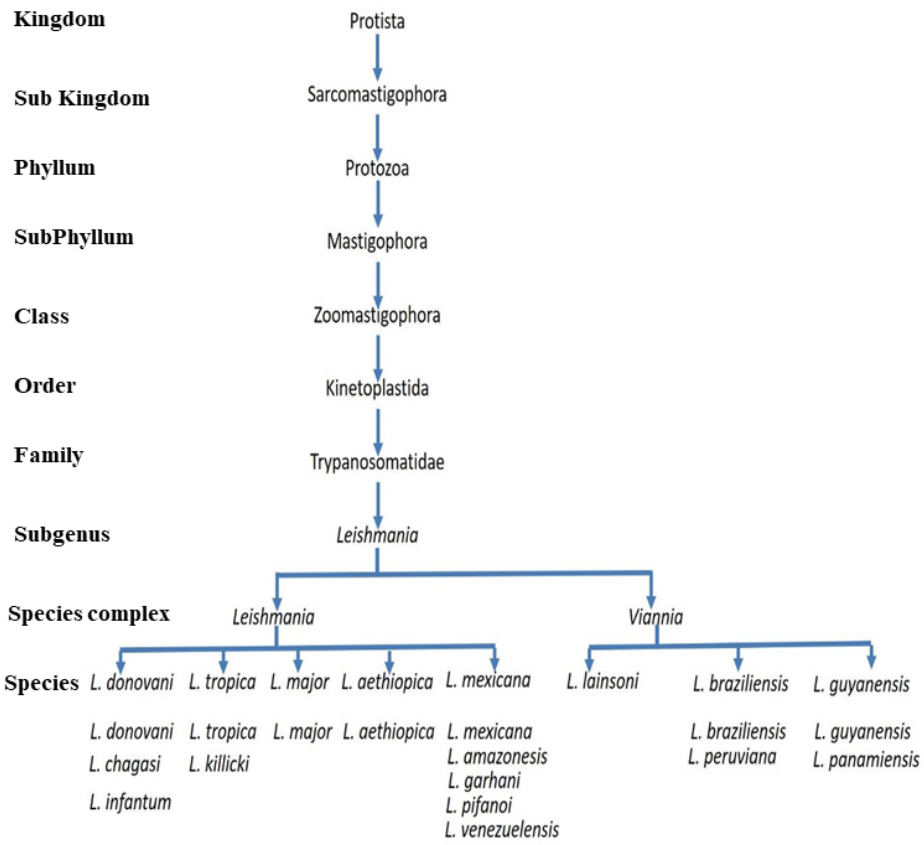

Figure 1.1: Taxonomy of *Leishmania* (Raj *et al.*, 2020)

1.4 Geographical distribution of Leishmaniasis

In total, WHO received reports of 11 743 new VL cases and 221 953 new CL cases in 2021 (11 689 domestic and 54 were imported).

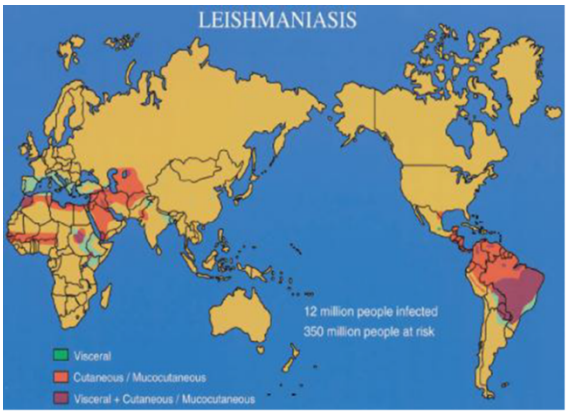

(a) Prevalence of Leishmaniasis worldwide

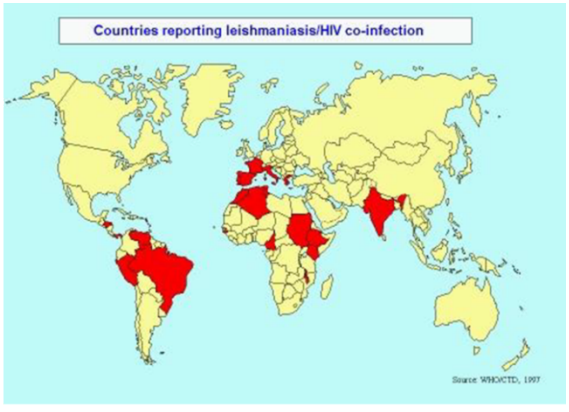

(b) VL-HIV coinfected areas

Figure 1.2: a) Status of Leishmaniasis worldwide and b) status of VL-HIV co-infection (Pal *et al.*, 2022)

1.4.1 Geographical distribution of VL

In 2021, 40% of the new VL cases were reported by EMR, followed by 33% of cases in AFR. AMR and SEAR reported 16% and 12% of cases, respectively. The regions where eco-epidemiological conditions favor the spread of VL are East Africa (which includes Ethiopia, Eritrea, Kenya, South Sudan, Somalia, Uganda, and Sudan) where 66% of VL cases globally occur, the Indian subcontinent (comprising India, Bangladesh, and Nepal) with 12%, and Brazil with 16%. Among these areas, four countries (Brazil, Kenya, India, and Sudan) have reported more than 1000 VL cases each representing 68% of all cases globally. Ethiopia, Eritrea, Nepal, Uganda, Somalia, South Sudan, and Yemen these countries reported 97% of VL cases worldwide (WHO, 2022).

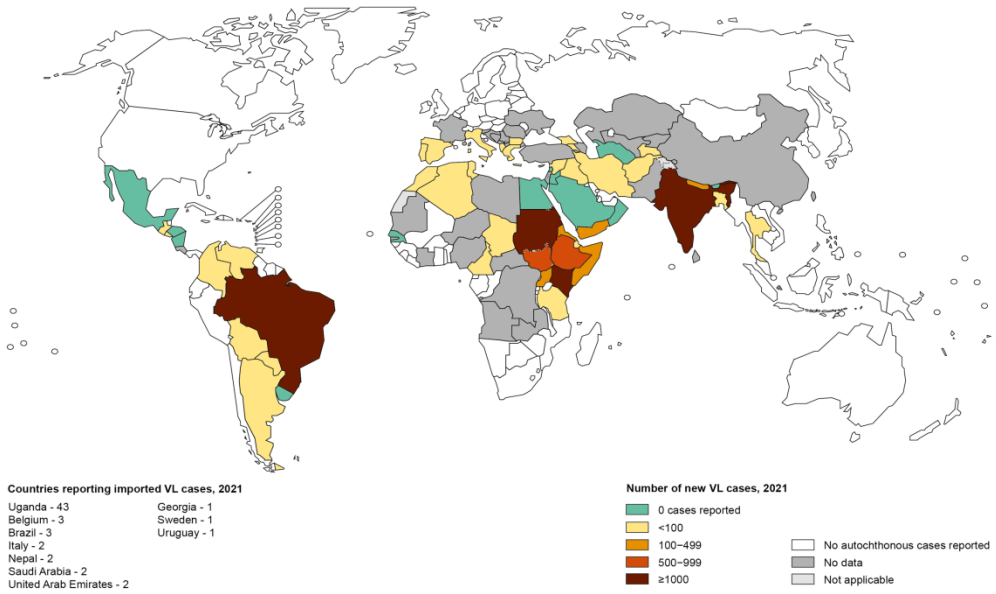

Figure 1.3: Status of endemicity of visceral Leishmaniasis worldwide (WHO, 2022)

1.4.2 Status in India

CL and VL are endemic in the Indian subcontinent, with increasing reports of PKDL cases in India. *L. major* and *L. tropica* cause CL in the northwestern states of India (herd in Punjab and Rajasthan). The hardest-hit area in Rajasthan is the Bikaner district. Historically, VL caused by *L. donovani* was widespread in India and was

nearly eradicated in 1960 due to extensive DDT spraying as part of the National Malaria Eradication Program. 130 million residents are at risk in 611 blocs (third-tier sub-national government). The number of cases is steadily declining due to the implementation of the kala-azar elimination program (Roy *et al.*, 2022).

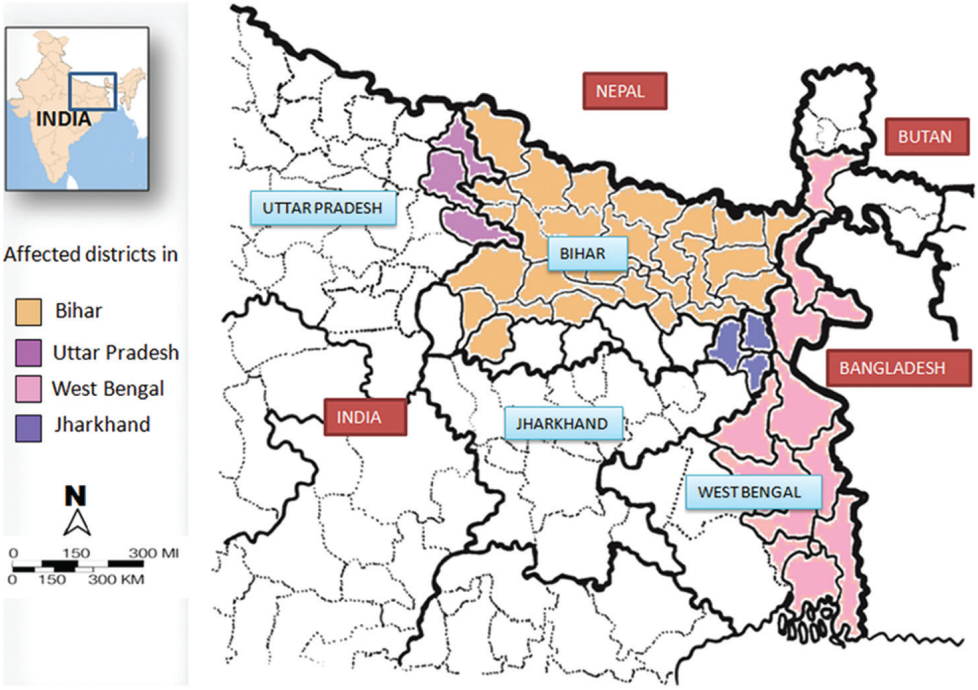

Figure 1.4: The visceral leishmaniasis hot zone of India (Muniaraj, 2014).

1.5 *Leishmania* Life cycle and morphology

Leishmania exhibits a digenetic life cycle as it undergoes distinct stages of development in both its vector are the sand fly, which is an invertebrate, and its host is a vertebrate. It comes in the amastigotes and promastigotes morphological forms.

1.5.1 Promastigote form (Invertebrate host)

In the sandfly's midgut, the parasite's promastigote stage develops, and they are motile and characterized by long and slender features, with a long flagellum and measuring about 12–20 m in size and 1.5–3.5 m in diameter (Gossage *et al.*, 2003). Mannose receptors and glycoproteins, among other molecules, are crucial for the macrophages' uptake of the promastigotes and are located in the membrane. The flagellar pouch refers to a particular indentation in the plasma membrane located at the anterior end of the parasite, which is not

enclosed by microtubules. The base of the flagellum is held in the flagellar pocket, which also facilitates the parasite's forward motion (Waller and McConville, 2002).

1.5.2 Amastigote stage (vertebrate host)

The amastigotes are immobile, non-flagellated forms in the vertebrate host, smaller than promastigotes. It divides at 37 °C via longitudinal binary fusion. Located in the parasitophoric vacuole of macrophages, this stage is ovoid in shape about 3-6 m length and 1.5 m broad. The outer membrane lacks a surface coating, but contains a polysaccharide component (Besteiro *et al.*, 2007).

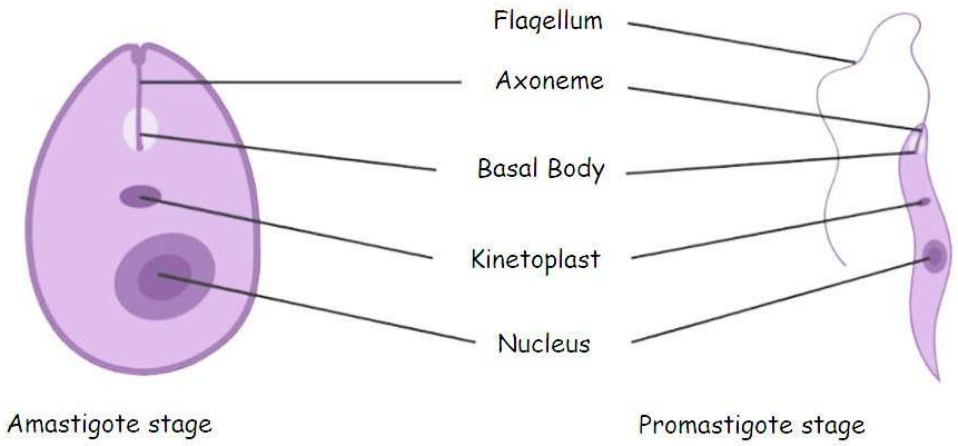

Figure 1.5: Ultrastructure representation of promastigote and amastigote stage of *L. donovani* parasite. Source: https://biologyeducare.com/*leishmania-donovani/*

1.5.3 Life cycle of *Leishmania*

While the promastigote form evolves during the insect vector (sand fly) stage, the amastigote form does during the vertebrate host stage. The promastigotes (flagellate) are present in the infected sand fly's saliva when it bites the host, and they are then transmitted to the host's blood. Immediately after the promastigotes enter the blood, they enter the macrophages by receptor-mediated endocytosis. Inside the macrophages, promastigotes are converted to amastigotes. Here they again multiply and cause the rupture of the macrophages, thus releasing the amastigotes in the blood where the other macrophages take them up. When the insect feeds on the infected host, the amastigotes enter the sand fly and are released directly into the insect's stomach. In the stomach, amastigotes immediately convert into the promastigote form. In the insect's digestive system,

promastigotes multiply through a process known as binary fission. After the multiplication of the parasites, the metacyclic form is transported from the midgut to the proboscis (Lima and Abass, 2020).

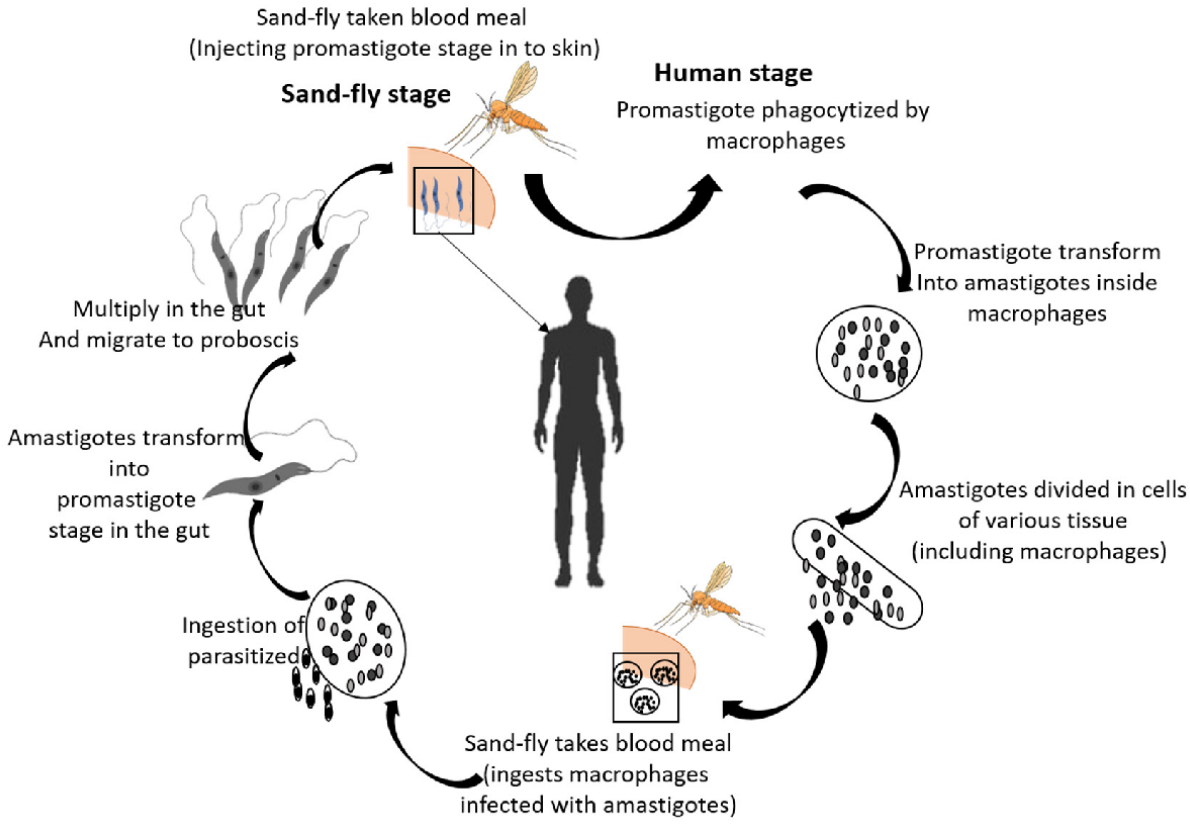

Figure 1.6: Life cycle of *Leishmania* in the mammalian host and sand fly vector (Rabaan *et al.*, 2023)

1.6 Vectors for Leishmaniasis

The sand flies spread the disease (Order: Diptera, Family: Psychodidae, Class: Insecta, Phylum: Arthropoda). The permissive vectors may contain several species of *Leishmania*, whereas the particular vectors are exclusively unique to one species. Out of the 800 species of sand flies, only 93 are known vectors. Humans are typically affected by Lutzomyia sandflies in the New World and Lutzomus sandflies in the Old World. The most studied species include *Phlebotomus argentipes* (Figure 7a) and *Lutzomyia longipalpis* (Figure 7b) (Bowles *et al.*, 2015).

A) B)

Figure 1.7: Vectors for leishmaniasis (a) *Phlebotomus argentipes* and (b) *Lutzomyia longipalpis* Source: http://www.raywilsonbirdphotography.co.uk/Galleries/Invertebrates/vectors/sand_fly.html

The sand flies reproduce in cow barns, live in cold, humid crevices, and the water's surface is where they lay their eggs. The illness is transmitted through the bites of female sand flies, whose pointed proboscis is capable of piercing the skin. Male sand flies cannot spread the illness since they only have mouth parts designed to suck plant fluids. Although the larval and pupae stages of sand flies are not aquatic, the females lay around 200 eggs on the water's surface. Under laboratory circumstances, the eggs typically hatch in 7 to 10 days then the larva develops. The pupa emerges after three weeks, and the adult flies are ready to fly after ten days. Spraying insecticides to reduce the male sand fly population is simpler because it is indoors, but managing the female population because it is outside is more complicated. The data collected in the lab could not accurately represent the time that takes place in nature. Because they travel more slowly than mosquitoes (1 m/s), they have a smaller dispersal range (Lehnhardt Pires *et al.*, 2013; Jaramillo *et al.*, 2011; WHO, 2022).

1.7 Manifestation of Leishmaniasis

Leishmaniasis can cause different types of clinical symptoms, ranging from skin ulcers to systemic infections. Cutaneous leishmaniasis, mucocutaneous leishmaniasis, visceral leishmaniasis, and dermal post-kala azar leishmaniasis are the four primary clinical forms of leishmaniasis that are frequently recognized.

1.7.1 Cutaneous Leishmaniasis

The term "cutaneous leishmaniasis" refers to the most prevalent type of leishmaniasis, appears as skin lesions, typically ulcers, on the parts of the body that are exposed. These

ulcers may persist indefinitely and can result in significant disability or social ostracism (Garrido-Jareño *et al.*, 2020). Approximately 95% of CL cases are detected in regions such as the Mediterranean, the Middle East, the Americas, and Central Asia. More than 85% of all new CL cases in 2020 were reported from just ten nations: Algeria, Afghanistan, Brazil, Iraq, Colombia, Libya, Pakistan, Syria, Peru, Tunisia, and Arab Republic. The multitude of new cases reported annually ranges from 600 000 to 1 million. Exposure to CL can result in the development of ulcers on parts of the body that are uncovered, such as the face, arms, and legs. Up to 200 lesions may be present, and each one has the potential to be very harmful. Once the ulcers have healed, they leave behind visible scars that may cause stigma, particularly for women and girls (WHO, 2022; Reithinger *et al.*, 2007).

In the old world, *L. donovani, L. major L. infantum, L. aethiopica*, and *L. tropica* are the organisms that cause cutaneous leishmaniasis. In the new world, the organisms include *L. Mexicana, L. guyanensis, L. braziliensis, L. peruviana and L. panamensis*. The characteristic of CL is the development of inflammatory skin lesions containing many parasites. The lesions can appear anywhere on the body, although they usually begin At the location of the infection, a macule, papule, or nodule gradually develops and reaches its maximum size within a week (Asilian *et al.*, 2003).

1.7.1a Diffuse cutaneous leishmaniasis (DCL)

Rarely, CL can worsen into disseminated CL, which causes extensive, non-ulcerated, non-healing nodular lesions to develop. After therapy, these lesions can reappear, spread throughout the body, leave unsightly scars, and ultimately cause death. People with DCL have a compromised cell-mediated immune response. Those who have a faulty cell-mediated immune response develop DCL. DCL is transmitted through *L. mexicana, L. aethiopica*, and *L. amazonensis* and is linked to co-infection with HIV. Lesions such as nodules, papules, or ulcers are characteristic of DCL and respond well to classical treatment (de Vries *et al.*, 2015; Mann *et al.*, 2021;WHO, 2022).

Figure 1.8: Clinical features of cutaneous Leishmaniasis (A-C), features of DCL (D); (Reithinger *et al.*, 2007; Bamorovat *et al.*, 2021).

1.7.2 Muco-cutaneous Leishmaniasis

Mucocutaneous Leishmaniasis can cause the complete or partial disintegration of the mucous membranes in the mouth, throat, and nose, particularly in regions such as Bolivia, the Plurinational State of Brazil, Ethiopia, and Peru, which account for over 90% of all cases (Vélez *et al.*, 2005).

Individuals with weakened immune systems in the Eastern Hemisphere are at risk of contracting *L. infantum, L. donovani, and L. major,* whereas in the Western Hemisphere, MCL is caused by *L. panamensis, L. guyanensis,* and *L. braziliensis*. The South American term for it is "Espundia" Strongly impacted by the lymphatic or the oral and upper respiratory tract mucosal tissues are where blood born spreading occurs. MCL might develop months to years after the onset of the cutaneous lesion. Primarily adult males who are malnourished make up the risk group, and Lymphadenopathy results in deformations of the Pharynx, Larynx, Palate, Upper Lip, Trachea, and Skin on the Nose (Robledo *et al.*, 2022). The patient undergoes severe suffering and mutilation, resulting in death due to malnutrition or bronchopneumonia. Immunological mechanisms may contribute significantly to the disfigurement. 1–10% of locally acquired CL infections in most endemic

regions resulted in MCL 1–5 years after recovery (Vélez *et al.*, 2005). In order to avoid mucosal metastases, CL must be treated as soon as possible. Usually, CL does not heal on its own and grows slowly. Pentavalent antimonials, miltefosine, and amphotericin B are the drugs of choice.

Figure 1.9: Clinical features of mucocutaneaous Leishmaniasis (Bowles *et al.*, 2015).

1.7.3 Visceral Leishmaniasis

If left untreated, visceral Leishmaniasis (VL), commonly referred to as kala-azar, has a mortality rate of over 95% for affected individuals. Spleen and liver enlargement, occasional fever attacks, anemia, weight loss, and anorexia are its hallmark symptoms. Brazil, East Africa, and India have the most instances (Chappuis *et al.*, 2007). Between 50 000 and 90 000 persons are affected by VL worldwide, yet only 25 to 45% of new cases are recorded by the WHO annually. It is one of the most severe parasite illnesses that can spread and cause fatality. More than 90% of new cases reported to the WHO in 2020 happened in just ten nations: Brazil, Ethiopia, China, Eritrea, Kenya, India, Somalia, Sudan, South Sudan, and Yemen (WHO, 2022).

L. donovani, L. chagasi, and L. infantum, typically cause VL. Human-specific *L. donovani* causes a significant rate of death in humans (Murray, 2005). It severely affects several internal organs of the body, such as the liver, spleen, and the lining of the small intestine known as the mucosa, lymph nodes, and bone marrow. Intermittent bouts of fever, significant weight loss, and extreme anemia characterize it. A drop in the number of blood cells characterizes it. It is also common among AIDS patients (Varma and Naseem, 2010; Faleiro *et al.*, 2014).

In acute forms, death is typically high. *Kala-azar* is a disease that primarily affects impoverished rural Indian people. Due to malnutrition and a weakened immune system, young children are more susceptible to sickness and exhibit severe disease symptoms (Jain and Jain, 2013). The sand fly has greater accessibility among socially underprivileged groups living on the edges of communities. Following the remission of VL, patients may experience the development of a chronic CL condition called "Post Kala-Azar Dermal Leishmaniasis", which typically requires an extended and costly treatment regimen. India and Sudan are areas where this disease is commonly found (Zijlstra *et al.*, 2017).

Figure 1.10: Clinical features of visceral Leishmaniasis (Opperdoes, 2019).
Source: https://openwho.org/courses/NTDs-visceral-leishmaniasis-east-africa

1.7.4 Post *Kala-Azar* Dermal Leishmaniasis (PKDL)

PKDL is a skin condition that often affects several body parts, such as the face, upper arms, and trunk, and develops after a person has visceral leishmaniasis. The rash associated with PKDL can appear as macules, papules, or nodules. This condition is frequently reported in the Indian subcontinent and East Africa, where the disease affects 5–10% of kala-azar patients. Although it can occur earlier, it typically occurs between 6 months and one or more years after kala-azar appear to have improved. Individuals with PKDL are thought to be sources of leishmaniasis infection (Zijlstra *et al.*, 2017; Ah *et al.*, 1992).

PKDL, which is usually noticed in people who have recovered from VL, is characterized by a flat, colorless (hypopigmented) macular rash with some faintly raised (maculopapular) or enlarged (nodular) lesions. In most cases, the PKDL recovers spontaneously in Africa but less rarely in individuals in India. It is incredibly challenging to

treat, particularly in some East African patients with a severe type of PKDL (Faleiro *et al.*, 2014; Desjeux *et al.*, 2013).

Figure 1.11: Clinical manifestations of PKDL: Patients with nodular post-kala-azar dermal Leishmaniasis (Chappuis *et al.*, 2007).

Chapter: II
Review of Literature

2.1 Infection to host macrophages

Amastigotes were ingested by the sand fly while taking the blood meal and entered the vector's lumen. Amastigotes were developed into promastigotes and multiplied through longitudinal binary fission in the lumen. The promastigotes undergo metacyclogenesis and become metacyclic promastigotes four days after ingestion. The distinguishing characteristics of these forms include their larger and narrower size, longer flagellum, and altered surface coat proteins that facilitate the parasite's adaptation and ability to infect the macrophages of the host (Späth and Beverley, 2001). Following the sandfly's next blood meal, the metacyclic promastigotes travel to the salivary glands and subsequently enter the mammalian host through the proboscis. Macrophages then phagocytose the cells. The parasite converts the amastigote form into the endocytotic parasitophorous vacuole. The cells undergo binary fission and multiply within the macrophages; eventually, they burst and release the amastigotes, infecting the surrounding macrophages. The actions mentioned above continue this cycle (Habtemariam, 2003).

2.2 Various hosts for VL

Leishmaniasis is transmitted zoonotically (through animals) and anthroponotically (through humans). The environment that sustains the survival of *Leishmania* species comprises of both sand fly vectors and vertebrate reservoir hosts. One primary reservoir host for a certain *Leishmania* species often lives in a specific focus, although other animals may become infected and become secondary or accidental hosts. The symptoms of the infection and the response displayed by the infected animals are imperceptible. Due to *L. tropica* and *L. donovani* respectively, humans have CL and VL. It is still unclear how important some hosts, including foxes, jackals, rats, badgers, and cats are in keeping *L. infantum* foci active. The *L. infantum* might live on a domestic cat (Marcondes and Day, 2019). *L. infantum*, the parasite responsible for causing VL in dogs, is easily transmitted by sand flies due to its ability to reside in both the internal organs and the outer skin layers, where a large number of parasites can be found. Dogs can also get *L. panamensis* and *L. peruviana* infections. The host's genetic makeup and immune system's Th1/Th2 balance determine an individual's vulnerability and resistance to infection. Dogs, the natural reservoirs for VL produced by *L. infantum* are the ideal animal models. Miniature rodents are frequently chosen as test

subjects for experimental VL, but dog usage is generally limited due to the expense and ethical issues (Quinnell and Courtenay, 2009).

2.2.1 Mouse/Rodent host

The recommended model for studying *L. donovani and L. infantum* infection is the mouse. A functioning *Slc11a1* gene, which encodes a phagosome component, is present in genetically resistant mice (such as CBA) infected with murine VL. It is a solute carrier localized to endosomes and lysosomes and is also known as Nramp1. It can control early infection. Due to the mutated Slc11a1 gene, susceptible strains (BALB/c) cannot inhibit the parasite's early liver-based growth (Vidal et al., 1995; Crocker et al., 1984).

Murine VL can be viewed as a subclinical infection model since susceptible mice can manage the disease, unlike the disseminated visceral disease model, and it mimics the symptoms of human VL. After an infection of the intravenous or intracardiac organs, primarily utilizing amastigotes, the cell-mediated immune response and granulomatous reaction prevent the parasite from multiplying in the liver after the first few weeks of the infection. Recently, it was demonstrated that a Pluronic F127 polymeric micelle system (ICHQ/Mic) containing clioquinol (ICHQ) could successfully treat *L. amazonensis* infection in a mouse model (Tavares *et al.*, 2020). Mice finally eliminate the virus from the liver over the course of two to three months, and it develops resistant to further infection (Murray *et al.*, 1987). When parasites are present in the spleen, it develops splenomegaly, changes the structure of the organ, and cause lymphoid follicles atrophy (Engwerda *et al.*, 2004).

The mouse and human spleens' immune responses, which are both inflammatory and regulatory in nature, may be compared. Along with IL-10 levels, TNF- α is high in the spleen (Murray *et al.*, 2000). IL-10 has suppressive effects on immune activity and is important in immunological modulation, such as preventing tissue damage from excessive inflammation. High levels of TNF-α stimulate the production of IL-10, which protects against the tissue damage that TNF-α cause. However, IL-10 contributes to the longevity of the parasite by preventing macrophage activation (Belkaid *et al.*, 2001).

2.2.2 Hamster host

The use of mice infected with *L. donovani* can accurately depict the initial phase of parasite growth, subsequent immune system suppression, and subclinical infection. However, there is currently no mouse model available that can replicate the progression of active visceral leishmaniasis in humans; it causes the sickness to become more severe. The clinical and pathological features of VL in hamsters closely mimic an active human disease. Due to an infection caused by *L. donovani* at a systemic level the hamster develops a persistently rising visceral parasite load, progressive hepatosplenomegaly, cachexia, hypergammaglobulinemia, pancytopenia, and finally passes away. Sadly, a scarcity of immunological reagents prevents further extensive research using the hamster model (Melby *et al.*, 2001a).

Hamsters can acquire progressive VL, much like humans, which can be fatal. Hamsters produce more Th1-associated cytokines including IFN- γ, TNF-α, and IL-2 in the spleen, but the amount of human-like activation of IL-4 m-RNA is surprisingly low (Melby *et al.*, 2001b). In comparison to humans, hamsters don't produce nearly as much NO. The expression of NOS2 mRNA is down regulated in *L. donovani* -infected hamsters in response to IFN- γ, which may be connected to lower NOS2 promoter activity (Perez *et al.*, 2006).

2.2.3 Human host

The symptoms of human VL can vary from a deadly infection affecting internal organs to a condition where the person has no apparent symptoms, but has leishmania-specific antibodies or a positive skin test for *leishmania* antigen. The exact causes of VL are still largely unknown. Some but not all subclinical or asymptomatic patients' peripheral blood mononuclear cells (PBMCs) react to stimulation with leishmanial antigen (LAg) by producing IFN-γ, IL-12, and IL-2 (Carvalho *et al.*, 1992). In naturally exposed healthy individuals, neutralising IL-12 cytokine prevents both proliferation and IFN-γ production (Costa *et al.*, 2012).

Cachexia, severe splenomegaly, hypergammaglobulinemia, and a gradual rise in the visceral parasite burden are the hallmarks of active human VL. However mice with *L. donovani* infection, the most prevalent VL model, do not manifest an apparent, progressing illness. Additionally, mice generate NO, an effector mechanism that is unclear in the antibacterial action of human macrophages, to limit *Leishmania* infection. The clinical and

pathological features of human visceral leishmaniasis were surprisingly replicated in Syrian hamsters infected with *L. donovani*. Further investigation into the disease mechanisms in hamsters revealed notable differences from the murine model. Despite observing a robust Th1-like cytokine reaction (including IL-2, TNF-α/lymphotoxin, and IFN-γ) in the liver, bone marrow, and spleen of hamsters, the parasite continued to replicate unchecked in these organs, indicating a deficiency in macrophage effector function. There was no sign of mRNA or enzyme activity related to inducible NO synthase (iNOS, NOS2) observed in the spleen and liver tissue during the course of the infection.

On the other hand, the infected mice's spleens exhibited readily detectable levels of NOS2 mRNA and enzyme activity (Melby *et al.*, 2001a). It is impossible to account for hamsters with low NOS2 expression by the NOS2 gene being absent, producing excessive amounts of IL-4, or having deficient TNF-/lymphotoxin production (which is another strong indication for NOS2 induction), or the earlier prevalence of deactivating cytokines such as TGF-β and IL-10. Although hamsters are a trustworthy model for testing new drugs against VL, this strategy is constrained by a lack of reagents (De Trez *et al.*, 2009).

Unexpectedly, new research has shown that blood cells from whole blood from VL patients—rather than isolated PBMCs—maintain the ability to generate IFN-γ in response to soluble *Leishmania* antigen. Initially, there was a connection between VL and a bias towards Th2 response characterized by elevated levels of IL-13 and/or IL-4. However, according to the majority of studies, there is no clear indication of Th2 skewing in human VL (Ansari *et al.*, 2011). IFN-γ mRNA is upregulated in the spleen and bone marrow during the early stages of infection. These findings demonstrate that additional mechanisms, rather than Th2 skewing, are implicated in the aetiology of VL. The pathogenesis of VL has been demonstrated in clinical studies to involve the contribution of IL-10, and the patients with the active VL have higher levels of IL-10 in their blood as well as in their lymph nodes, bone marrow, and spleen (Nylén and Sacks, 2007). Whole blood cell cultures can show signs of IL-10 after *Leishmania* antigen stimulation, but not in PBMCs obtained from individuals with VL (Ansari et al., 2011). The host macrophages are conditioned by IL-10 to allow the parasite to remain in VL.

Additionally, it reduces the synthesis of TNF-α, and NO, which prevents the destruction of amastigotes. In addition, IL-10 makes macrophages resistant to activation

cues. Inhibiting IL-10 in the serum prevents parasite multiplication in macrophages in human VL and improves the IFN-γ response in PBMC that has been activated with an antigen (Nylén and Sacks, 2007). Recent studies demonstrate that IL-10 neutralization has a host-protective impact on lesional tissue, demonstrating that excessive IL-10 production directly contributes to the pathogenesis of human VL (Ansari *et al.*, 2011).

2.3 Immune response in visceral leishmaniasis

Leishmania parasites can only be successfully removed from an infected host with the assistance of several significant immune system players. After a sand fly bite, the fight between the promastigotes and the amastigotes begins as they enter the bloodstream and lasts until they are housed within the macrophages. The eradication of parasites and disease onset will be influenced by *Leishmania*'s ability to alter and/or evade host immune systems. The host's defensive mechanisms necessary for parasite eradication include components of the immune systems, both innate and adaptive (Ikeogu *et al.*, 2020). Cellular and immunological processes leading to *Leishmania* infection are poorly understood. Studies have shown that animal models of leishmaniasis can partially imitate some of the immunopathological features of the human disease, albeit with certain limitations. This enables researchers to explore and identify regulatory factors linked to resistance or susceptibility to *Leishmania* and their effects on the infected host. Despite significant variances between experimental and human leishmaniasis, the interplay between the innate and adaptive immune systems and the nature of cell-mediated responses generated are crucial factors determining the disease progression in both cases (Kaye and Scott, 2011**;** dos Santos Meira and Gedamu, 2021).

2.3.1 Innate immunity

The course of the disease may be predicted based on the early innate immune response against parasite infection, such as an increase in immunoregulatory cytokines response and slowing the spread of infections and parasite proliferation. *Leishmania*, an opportunistic pathogen, modifies various host characteristics to help them survive inside the phagolysosomes of macrophages. Host dendritic cells and macrophages can phagocytize parasites after the parasites penetrate the skin. However, parasites prevent phagocytic killing by controlling the breakdown of the parasite's proteins. On the other hand, parasites utilizes

the powerful immune opsonin complement protein C3b to sped up the parasite engulfment process by phagocytic cells (Sharma and Singh, 2008). NK cells, phagocytes that are either mononuclear or polymorphonuclear, and various components such as TLRs, complement proteins, IL-1, and myeloid differentiation factor 88 (myd88) are all included, are usually involved in the front-line defensive response known as innate immunity against any pathogenic agent (Hawn *et al.*, 2002)**.** Like the mouse model, early *Leishmania* infection defense in humans involves NK cell-mediated pathways. In naive individuals, it is hypothesized that NK cells have a role in maintaining the recovery process in addition to the initial response (Carvalho *et al.*, 2012).

The importance of NK cells in the innate immune response becomes evident when considering that mice challenged with *L. major* experience a reduction in NK cell numbers, a decrease in IFN-γ production, and a rise in parasite burden within seven days. TNF-α and IFN-γ work together to activate infected macrophages to create NO, a powerful cytostatic and cytotoxic chemical that eliminates various intracellular infections in a mouse model, including *Leishmania* (Müller *et al.*, 1991).

Activated polymorphonuclear leukocytes also eradicate the pathogen, principally utilizing the oxidative burst. The function of NO as an anti-leishmanial agent is demonstrated by the observation that IFN-γ dependent activation of macrophages leads to NO production, resulting in parasite death. Susceptibility to *Leishmania* infection is increased by null mutation of the NOS2 gene, which impedes NO production and impairs macrophage function. In resistant mice models, suppression of iNOS leads to an increase in iNOS expression and NO production, rendering them sensitive to *Leishmania* infection (Bogdan and Röllinghoff, 1999)**.** Nevertheless, most studies demonstrate anti-leishmanial activity in the liver and spleen through an iNOS-dependent mechanism (Perez *et al.*, 2006). Nevertheless, most studies demonstrate anti-leishmanial activity in the liver and spleen through an iNOS-dependent mechanism (Arunima Biswas, Arijit Bhattacharya, 2011). A fascinating aspect of the innate immune system is the induction of apoptosis through FasL in macrophages that have been infected with *Leishmania* (Huang *et al.*, 2013)**.** Hence, macrophages are distinct cells involved in the parasites' survival and demise (Gurung and Kanneganti, 2015).

2.3.2 Humoral immune response

The development of antigen-specific antibodies distinguishes the humoral response, a subset of adaptive immunity. Anti-leishmanial antibodies are a crucial component of the serological diagnosis of human leishmaniasis. Despite the anti-leishmanial antibodies' low levels in CL and high amounts in VL, the scientific community first thought they played no part in protection. Several investigations have shown conflicting findings, indicating that their involvement in pathogenesis or prevention still needs to be better understood. According to the immunoglobulin isotypic pattern analysis, the IgM, IgE, and *Leishmania* antigen-specific IgG were detected in high concentrations during active disease (Conde *et al.*, 2022). In the case of VL, increased antibody titers also serve as a marker for the severity of the disease (Melby *et al.*, 2001a). The significance of humoral immunity during *Leishmania* infection in humans needs to be clearly understood. Despite the scarcity of information on the precise function of IgG subclasses, a few studies have shown their significance in developing or preventing disease. The increased IL-10 activity and decreased IFN-γ activity was related to the higher IgG1 and IgG3 titers in human VL (i.e., decreased IgG2 titers). IFN-γ levels are in fact, correlated with IgG2 titers, supporting its function in host defense (Costa *et al.*, 2012).

2.3.3 Cell-mediated immune response

In acquired immunity, the distinguishing feature is cell-mediated immunity, which is mainly controlled by T-cells. In the case of leishmaniasis, the effector function is mainly carried out by CD4+ T-cell subset while the CD8+ T-cell subset primarily functions as memory cells (Reiner and Seder, 1995). Contrarily, Tregs are mostly linked to disease progression impacted by ongoing infection (Belkaid *et al.*, 2001). Th1 polarisation and the resulting copious IFN-γ production are the primary mediators of protection against human cutaneous and visceral infection. On the other hand, mucocutaneous and chronic lesions occur as a result of increased IL-4 and IL-10 production. After recovering, the volunteers who were exposed to the disease are protected from reinfection both in endemic and experimental settings due to their immunity (Ghalib *et al.*, 1993). IL-4 production was not directly correlated with the active VL but rather with the predominate levels of IL-10 and persistent levels of IFN-γ (Kharazmi *et al.*, 1999). In contrast to IFN-γ and IL-10 cytokines, macrophage-deactivating cytokines were also linked to the pathogenesis of all clinical types

of leishmaniasis. One indication of the immunological dysfunction caused by *L. donovani* during active VL is the inability of lymphocytes to produce cytokines when re-stimulated with leishmania-specific antigen. The decrease in T-cell microenvironment lymphocytes in the spleen and lymph nodes provides further evidence to support the aforementioned assertion regarding patients with VL (Veress *et al.*, 1977).

As a result, it offered convincing proof of the importance of cell-mediated immunity, and the vital part cytokines play in leishmaniasis. Nevertheless, ongoing TNF-α levels (Ansari *et al.*, 2011) and an imbalance in the production of IL-10 are frequently linked to the emergence of the clinical form of PKDL. However, the pathogenesis of VL is linked to an enhanced Th2 response specific to *Leishmania* and an increase in the number of cells that present antigen, which inhibits the protective T-cell response. After recovering, the volunteers who were exposed to the disease are protected from reinfection both in endemic and experimental settings due to their immunity (Kharazmi *et al.*, 1999). Studies have shown that active VL patients had prominent IL-10 m-RNA upregulation in their bone marrow, lymph nodes, spleen, and plasma (Murray *et al.*, 2002). On the other hand, the decrease in IL-10 mRNA expression points to the illness cure (Burns *et al.*, 1993). A proper equilibrium between IL-10 and IL-12 is essential for treatment, etiology, or both (Sharma and Singh, 2008). Important classical Th2 cytokine IL-4 is produced in VL and is typically associated with treatment resistance (Sundar et al., 1997; Dunning, 2009). IFN-γ and IL-4 were undoubtedly increased but dramatically decreased after the cure during active VL. Moreover, IL-13 increases when a disease is active, but its levels drop after successful treatment. Instead of IL-13, IL-10 is mainly linked to disease relapse, and during human VL, IL-10+ IFN-+ generating antigen-specific T cells have a significant impact (Kemp *et al.*, 1999).

Additionally, to lessen the dreadful consequences of VL brought on by the parasite, the host regulates the Th17 response. The significant IL-10 production in keratinocytes raises the possibility that PKDL-related skin complaints are involved. It makes sense for a VL patient with elevated plasma IL-10 levels (Gasim *et al.*, 1998). The concentration of IL-10 in the skin and plasma can serve as an indicator for predicting the severity of PKDL pathogenesis and the probability of VL advancing to PKDL. This is supported by the fact that during active PKDL there is a robust T-cell response to parasite antigens and that in

response to crude *L. donovani* antigens, PBMCs release large levels of Th1 and Th2 cytokines (Zijlstra, 2016). Figure 2.1 illustrates the function of the innate and adaptive immune cells in either protecting the host from infection or contributing to the progression of illness in VL.

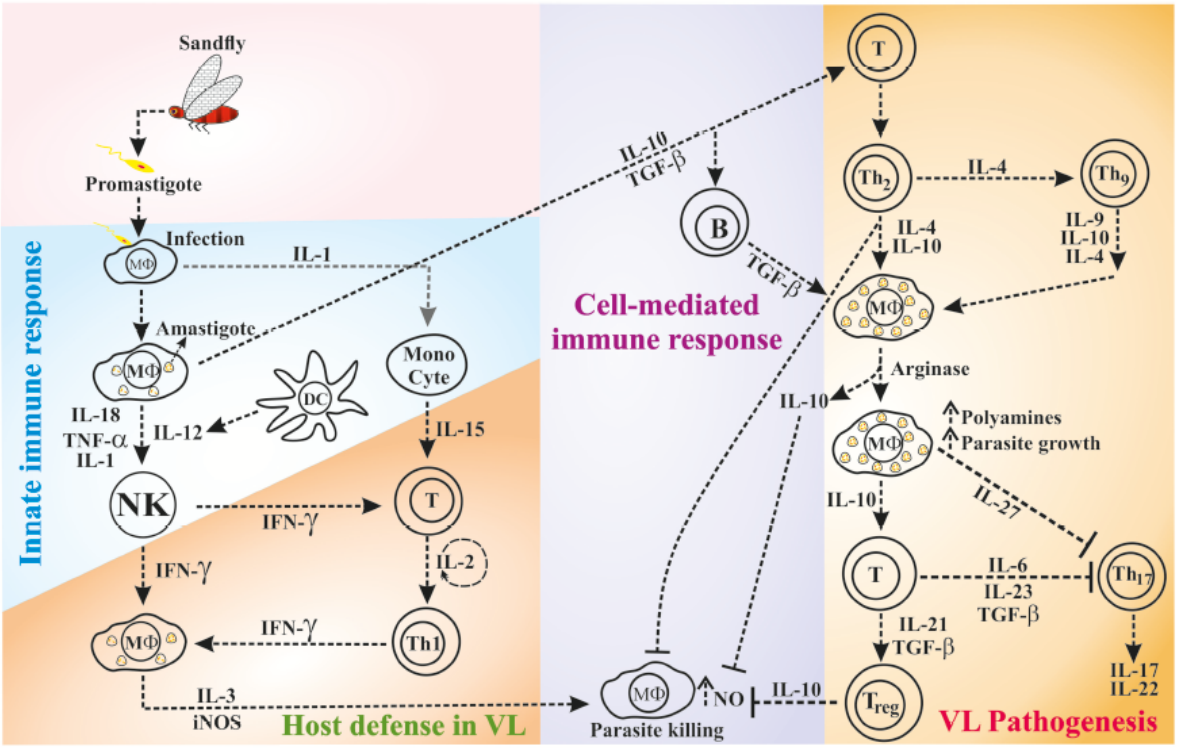

Figure 2.1: The involvement of innate and/or adaptive immune cells in the host's defense or development of the disease in VL (Dayakar *et al.*, 2019).

2.4 Th1/Th2 paradigm

The interactions between Th1 and Th2 cells are mutually reinforcing. Antigens trigger immune responses, but humoral and cell-mediated reactions are not always equally activated. The strength of the secondary response is typically influenced by the first response, which typically dominates. Based on the cytokine pattern displayed in the animal at the stage of infection, it is possible to anticipate whether such a Th1 or Th2 response will manifest in the mouse model. In other words, the early cytokine environment determines whether the response is polarised towards one T-cell subset or the other. IFN-γ and IL-12, for example, are known to encourage the maturation of Th1 responses, while IL-4 and IL-10 support the formation of Th2 responses, according to studies using human and murine in

vitro cells. In CL, Th1 or Th2 subset polarisation occurs very early in infection (3 days in mice). Even though it damages the host, the immune response is halted in either Th1 or Th2 after it is generated (Kemp *et al.*, 1999).

Th1 cells induce the secretion of IL-12 by macrophages and dendritic cells, which is a potent cytokine that activates cell-mediated immunity. In contrast, Th2 cells produce immune cytokines that assist B lymphocytes in generating antibodies. Recently, a new population of T cells, known as Th3 cells, has been identified that release the TGF-β is an immune cytokine that possesses both activating and inhibiting properties. Both Th1 and Th2 cells can reciprocally suppress each other's activity. While TGF-β is generally associated with promoting the release of mucosal IgA antibodies (a Th2 response) and suppressing Th1 cell activity, Th3 cells have the ability to decrease the activity of both cell types (Asad *et al.*, 2019). Macrophages are rendered inactive by TGF-β and IL-10, which also prevents the secretion of IL-12. IFN-γ, in contrast, prevents IL-10 from being released. The equilibrium of cytokines in humans is regulated by the regulator, autoantibodies, steroids, hormones, and prostaglandins. In mice and humans, VL produced by *L. donovani* has not been associated with the distinct Th1/Th2 pattern of disease progression seen for *L. mexicana and L. major*. The proposal states that disease vulnerability in VL is determined by the absence of a Th1 response rather than the presence of a Th2 response (Miralles *et al.*, 1994). IL-4 can act as a precursor for the generation of IL-12, according to several studies. The Trim levels of IL-4 may also be required to maintain IFN-γ production by activated T cells and its effects on the production of innate IL-12 and Th1 differentiation. Additionally, it has been demonstrated that IL-4 is essential for sustaining IFN-γ production after pharmacological therapy (Hurdayal and Brombacher, 2014).

2.5 Chemotherapy against Leishmaniasis

Leishmaniasis can only be treated with chemotherapy, which remains crucial in managing the disease in endemic regions. Due to its status as a neglected tropical disease, only a few drugs are available to combat it, some of the treatments that are included are meglumine antimoniate and sodium stibogluconate (which are pentavalent antimonials), as well as miltefosine and liposomal amphotericin B, paromomycin and pentamidine. However, these drugs have significant limitations (Mbongo et al., 1998), such as high toxicity, prolonged

use, high cost, and drug resistance. Despite this, there is a need for new treatments and approaches that can overcome these challenges. Miltefosine is among the most promising oral medications, with minor side effects, and has been approved for treating visceral Leishmaniasis. Unfortunately, commercial drug resistance testing is unavailable, and repeat biopsies and serological testing are generally not recommended (Mann *et al.*, 2021).

In 1912, Vianna brought trivalent antimonials to Brazil as a treatment for CL and MCL, whereas in Italy, Di Cristina and Caronia introduced them for the treatment of VL in 1915. Urea stibamine, the first safer pentavalent antimonial, was introduced by Brahmachari in 1922 and remained the primary treatment option for leishmaniasis. However, antimonials were found to be ineffective against VL cases in Bihar in the 1980s due to drug resistance, high costs, and toxicity issues. Miltefosine (2004), Paromomycin (2006), and liposomal AmB (1996) have been approved for VL treatment. As the need for safe and efficient medications is urgent, new compounds are expected to be discovered (WHO, 2022). Antileishmanial medications that are specifically used to treat leishmaniasis include a range of drugs such as pentavalent antimonials, AmBisome® (manufactured by Gilead Sciences in California, USA), Glucantime® (manufactured by Aventis in France), Pentostam® (manufactured by GlaxoSmithKline in the UK, or the generic version from Albert David in India), Impavido® (made by Paladin Labs), and Pentam® (manufactured by Abbott in Illinois, USA). These medications consist of active ingredients such as meglumine antimoniate, amphotericin B, sodium stibogluconate, miltefosine, and pentamidine, respectively (Monzote, 2009).

Miltefosine, an oral medication, is now the most effective therapeutic option. A significant development in antileishmanial chemotherapy was praised (Figure 2.2A). The FDA has approved this phosphatidylcholine derivative for treating all forms of leishmaniasis. It has been discovered that it controls *Leishmania* parasites by causing apoptotic cell death. Miltefosine and Ambisome together have also been examined and shown to be helpful; however, severe side effects call into question their extraordinary efficacy (Sundar and Olliaro, 2007). Its teratogenicity, lengthy terminal residency impairs, and time is the significant compliance of this medication, and time (Annang *et al.*, 2015). It has a long half-life of 152 hours which facilitates the development of clinical resistance (Paris *et al.*, 2004).

The pentavalent antimonial medications prevent amastigotes from producing glycolytic enzymes or oxidising fatty acids. Stibogluconate of sodium (Pentostam) (Figure 2.2B) and meglumine antimoniate have been used to treat Leishmaniasis for over five decades. Despite concerns about increasing resistance in disease-endemic areas, these drugs remain the preferred first-line treatment options (Carter *et al.*, 2006). The leading causes of acquired resistance are the widespread overuse of these medications due to their accessibility in areas with endemic diseases and parasites' lack of drug activation—moreover, several genes found in clinical isolates resistant to antimonial hint at a complex mechanism of resistance (Basselin *et al.*, 2002).

Antimonials have limited uses due to their toxicity, side effects, including hepatotoxicity, cardiac arrhythmia, severe pancreatitis, and increasing drug resistance (Kato *et al.*, 2014; Teng *et al.*, 2021).

Paromomycin is an antibiotic that possesses aminoglycosidic properties and exhibits both anti-leishmanial and antibacterial effects (Figure 2.2C). A phase II trial conducted in Tunisia and France demonstrated the safety of using the paromomycin-gentamycin combination (WR279,396) to treat cutaneous leishmaniasis (Thakur *et al.*, 2000).The primary mechanism of action of this drug remains unknown, although its ability to interact with the negatively charged leishmanial glycocalyx suggests that mitochondria may be its primary target. Studies have also shown that paromomycin binds to the 50S and 30S ribosomal subunits without interfering with IF3's connection with the 30S subunit. However, in vitro reports have demonstrated drug resistance in *L. tropica* and *L. donovani* (Jhingran *et al.*, 2009).

Pentamidine is an aromatic diamine that is considered a second-line treatment for leishmaniasis (Figure 2.2D). While the exact route of action of this drug remains unknown, it is thought to enter *L. donovani* promastigotes through arginine and polyamine transporters (Basselin *et al.*, 2002). Studies have demonstrated that pentamidine resistance in *L. amazonensis* and *L. donovani* promastigotes is due to decreased drug uptake or increased efflux, and it is reported to inhibit mitochondrial topoisomerase II. However, pentamidine is highly toxic and can cause nephrotoxicity, hypoglycemia, and hypotension. Although the mechanism behind pentamidine resistance is unclear, the intracellular ABC protein PRP1 is

thought to confer resistance in the intracellular stage of *Leishmania* (Coser *et al.*, 2020). Due to its suboptimal efficacy and toxicity, pentamidine is rarely used (Tiuman *et al.*, 2011)

The polyene fungal antibiotic, Amphotericin B, disrupts the ion balance of the *Leishmania* cell membrane by interacting with its abundant ergosterol component. This interaction creates holes in the membrane, ultimately resulting in the death of the cell (Figure 3E). As a second-line drug for leishmaniasis, Amphotericin B (AmBisome®, Gilead Sciences, CA, USA) exhibits a high affinity for ergosterol, the predominant sterol of the leishmanial cell membrane, thereby abrogating macrophage-parasite interaction (Colombo *et al.*, 2003). In Bihar, where antimonials have failed in more than 60% of patients, Amphotericin B is used as the first-line treatment. Common side effects include chills, rigidity, and fever, while nephrotoxicity can prevent the medication from being effective. Hypokalemia and myocarditis are two other rare but severe side effects. Patients receiving Amphotericin B should be provided with adequate hydration and additional potassium (Balasegaram *et al.*, 2012).

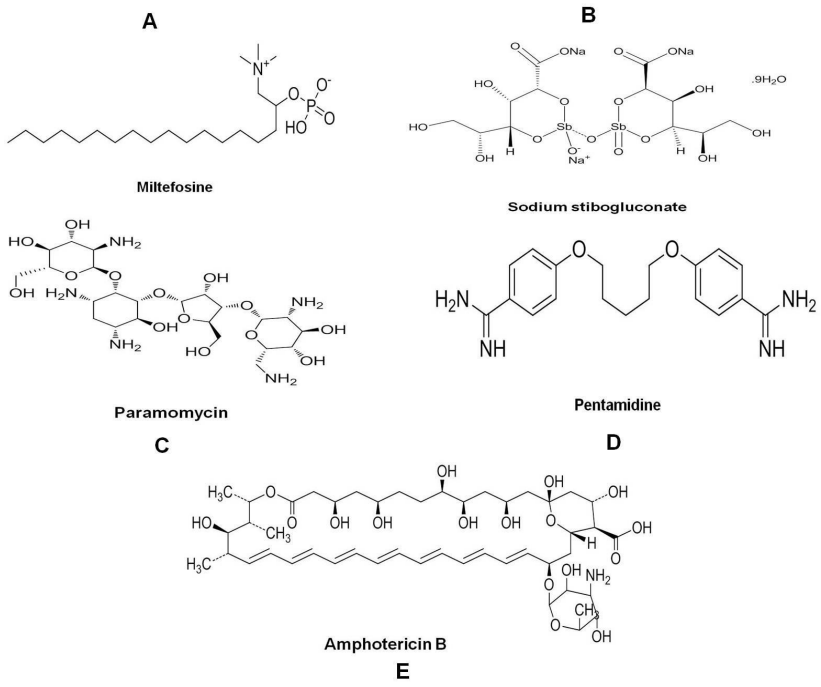

Figure 2.2: Molecular structures of antileishmanial drugs. A) Miltefosine, B) Sodium stibogluconate, C) Paramomycin, D) Pentamidine, and E) Amphotericin B.

2.6 Diagnosis for Visceral Leishmaniasis

VL is a chronic febrile illness that frequently starts with splenomegaly before progressing to wasting, anemia, and death from bleeding or a secondary bacterial infection. Early detection and efficient treatment are critical to controlling this condition. Noninvasive, quick diagnostics that recognize VL as a marker of cure in peripheral health clinics may impact the management of VL in endemic communities. Parasite identification, a highly specialized technique, is the primary way to diagnose VL. A buffy coat or peripheral blood smear is microscopic and examined as the initial noninvasive test. In the event of a negative result, the same technique is carried out on splenic or bone marrow samples, and this is still the most accurate method of diagnosis utilized in East Africa and the Indian subcontinent (Mugasa *et al.*, 2010).

2.6.1 Diagnostic workflow for visceral leishmaniasis

When making a diagnosis, it's crucial to take into account the patient's immune system function and the origin of the *Leishmania* infection, particularly if rK39 testing is used. A step-by-step approach to testing could involve preliminary PCR and serology tests on peripheral blood, along with microscopy and/or culture. Additional testing methods like microscopy or culturing may be included if needed. For patients with compromised immune systems, using multiple serologic tests may be beneficial. If the diagnosis remains inconclusive, invasive testing using PCR and microscopy (and possibly culture) may be carried out on tissue samples such as bone marrow or lymph nodes. Invasive testing is also necessary in cases where test results are uncertain, such as low-level positive serology and quantitative PCR results. To achieve a high degree of certainty in confirming or ruling out the condition, the results of various tests should be combined with pre-test probabilities. It's important to note that not all positive *Leishmania* tests indicate VL due to the low specificity of certain assays. In cases where there is a strong clinical suspicion despite the initial negative *Leishmania* test (even if the initial bone marrow aspiration was negative but turned positive upon repetition), repeating the tests has been found to be beneficial. Serologic testing may not be effective for patients experiencing a VL relapse as antibodies can persist in the body for years after treatment. In such situations, direct parasitologic testing and quantitative PCR, if possible, can be useful (Thakur *et al.*, 2020).

The initial sign of infection manifests as a mild redness at the bite location. Subsequently, the parasites trigger an inflammatory response, and the infection commences. The redness can either advance into an open ulcer or extend to internal organs such as the liver and spleen. Several factors influence the inflammatory reactions incited by parasites, including the type of parasite, the host's immune system, the strain of the parasite, and other unidentified variables (Reithinger and Dujardin, 2007). Therefore, early diagnosis of leishmaniasis is essential in preventing the progression of severe clinical symptoms and potential patient mortality. The conventional diagnostic approach involves microscopic examination of amastigotes in tissues obtained via aspiration from organs such as the spleen, liver, lymph nodes, and skin. Parasite cultures can also be developed from these sites. However, this diagnostic method is uncomfortable for patients undergoing aspiration, and the process of isolating parasites from cultures is time-consuming, expensive, and challenging to execute (Mugasa *et al.*, 2010). Different diagnostic approaches for leishmaniasis have been devised, each exhibiting different levels of precision in detecting the disease. These methods comprise parasitological techniques, such as parasite culture, microscopy, and histopathology, as well as serological and molecular diagnostic techniques (Cunningham *et al.*, 2012)**.**

2.6.2 Parasitological methods of diagnosis

In eco-epidemiological research, the most favored method for identifying leishmaniasis is through the use of parasitological diagnostic techniques (de Vries *et al.*, 2015). Laboratory diagnosis can be achieved by directly examining Giemsa-stained smears of lesions obtained through scraping, biopsies, or impression smears for the presence of amastigotes (Chappuis *et al.*, 2007). Aspirates of the spleen or bone marrow are the most often used samples. However, other samples, such as lymph nodes, liver biopsies, and peripheral blood with buffy coats, can also be used to detect amastigotes. Splenic aspirates showed the highest sensitivity of all the samples (93-99%) (Srivastava *et al.*, 2011). *Leishmania* parasites are commonly found in splenic aspirates, but their evaluation carries a high risk of bleeding in the hands of untrained personnel. Blood cell and tissue aspirates have 100% sensitivity in vitro cultures(Thakur *et al.*, 2020). The most sensitive diagnostic method is the examination of splenic aspirates, which has a sensitivity rate of 93-99%. Parasite cultures developed from

splenic and bone marrow aspirates are highly specific. It is only used in research laboratories since it is extremely tedious, expensive, and time-consuming (Singh and Sundar, 2015).

Laboratory animals such as mice, hamsters, guinea pigs, and rodents can be injected with parasites. However, this diagnostic method is not typically employed as a primary diagnostic procedure since it can take several months for the parasites to become evident in these species (Sundar S, 2002). The most preferred and first-line diagnostics for identifying the illness are parasitological techniques. However, the limited sensitivity of parasitological techniques, the need for technical skills to carry out the procedure, and additional dangers related to the tests are drawbacks (Reithinger and Dujardin, 2007).

2.6.3 Immunological methods of diagnosis

Immunological procedures were designed to address the shortcomings of parasitological methods of diagnosis. However, a very low humoral immune response characterises in Mucocutaneous and CL. Due to the relatively low amounts of circulating antibodies in areas where CL is common, immunological tests are not routinely used, and the potential variability in specificity, particularly in areas where cross-reactive parasites such as Trypanosoma cruzi are present (Singh and Sundar, 2015). Nevertheless, hyperimmunoglobulinemia is only seen in the case of VL, and numerous antibody detection techniques have been developed to diagnose VL (Boelaert *et al.*, 2004). Additional methods employed in the diagnosis of the disease comprise of the indirect fluorescent antibody, western blot, , direct agglutination and ELISA (Varani *et al.*, 2017).

Fluorescent antibody test

In this assay, an antibody is combined with a fluorescent marker to create a reporter molecule that binds to a target molecule with high specificity and is quick and straightforward to analyze. The test can be conducted either directly, where the labeled antibody attaches to the antigen, or indirectly, where a secondary polyclonal antibody binds to the prepared antigen and attaches to the primary antibody. This test, which uses promastigotes to identify anti-leishmanial antibodies, is one of the most widely used. However, cross-reactions with trypanosomal sera have been noted. The antigen promastigote reduces cross-reactions with trypanosomal sera (Thakur *et al.*, 2020).

Direct agglutination test (DAT)

The DAT is an easy, trustworthy, economical, and semi-quantitative test. DAT has received approval in several nations, including India, Nepal, Kenya, Sudan, Brazil, Bangladesh, and Ethiopia. In order for this test to work, *Leishmania* promastigotes must clump together after being exposed to anti-leishmanial antibodies, which results in agglutination of promastigote (Elmahallawy *et al.*, 2014). The test can be utilised in laboratories and fields because it is affordable and simple. According to numerous studies, the direct agglutination test's sensitivity and specificity are 70.5-100% and 53-100%, respectively. Furthermore, it has drawbacks because of its lengthy 18-hour incubation period and the demand for serial dilution of serum or blood (Kumar *et al.*, 2020).

Fast Agglutination Screening Test (FAST)

The Fast Agglutination Screening Test (FAST) has been designed to rapidly detect antibodies against the *Leishmania* parasite in both serum samples and blood samples collected on filter paper (in less than 3 hours) (Ababa and Ababa, 2001). According to reports, FAST has sensitivity and specificity ranges between 91.1 and 95.4% and 70.5% and 88.5%, respectively (Hailu *et al.*, 2006).

Enzyme-linked immunosorbent assay (ELISA)

ELISA frequently detects antileishmanial antibodies, and the antigen employed is mainly responsible for their sensitivity and specificity. Previously crude or soluble antigens of parasites were utilized in ELISA, but because of cross-reactivity, it is now given minor importance in diagnosis. With the advancement of technology, many recombinant antigens have been developed for diagnosing VL, with rK39 ranking as the most effective (sensitivity: 67–100%; specificity: 93–100%) (Singh and Sundar, 2015) Compared to rK26 and rK9, the rK39 antigen was the most suitable. Furthermore, a 100% specific and sensitive recombinant antigen KE16 has been cloned from Indian *L. donovani*. For the detection of the cutaneous form of the disease, as well as mucocutaneous and VL, recombinant HSP83 demonstrated superior results in terms of specificity and sensitivity when compared to crude *L. major* antigens (Mohapatra *et al.*, 2010). Even though ELISA is a technique with improved specificity and sensitivity, only advanced laboratories may utilize it due to the necessity for specialized personnel, complex technologies, and electricity (Elmahallawy *et*

al., 2014). There is also a commercially available dipstick called rK39 (FDA approval). It is based on a surface antigen recombinant that is extremely specific for VL. It is especially pertinent for use in the field (Sundar *et al.*, 1998).

Immunoblotting

It has been shown that serodiagnosis employing immunoblotting of soluble antigens is extremely sensitive and specific. The test's specificity is 98-100%, while its sensitivity ranges from 90 to 98%. The band pattern obtained in immunoblotting can be used to estimate the disease stage. However, its application is restricted by its high cost, lengthy tenure, and requirement for complex equipment and a very skilled workforce (Elmahallawy *et al.*, 2014).

Immunochromatographic assay (IC) or Immunochromatographic test (ICT)

Based on the rK39 antigen, IC is an immunochromatographic test that is reliable, quick, and simple. In VL patients, rK39's sensitivity and specificity were observed to vary depending on the population. Brazil's sensitivity and specificity were 90% and 100%, whereas India's were 100% and 93-98% (Sundar S, 2002). This test can also be utilized in fields because it is efficient, affordable, and produces results that are positive (Elmahallawy *et al.*, 2014).

Latex agglutination test (LAT)

The LAT assay is a newly developed method for quickly identifying anti-leishmanial antibodies. In this study, both A2 antigens from the amastigote form and crude promastigote antigens were utilized Sensitivity was 88.4% and specificity was 93.5% when measured against DAT. During a study evaluating the efficacy of the kala-azar latex agglutination test (Katex), it was observed that the test has a specificity of 100%, while its sensitivity is moderate at 75%. Due to its decreased sensitivity, KAtex cannot be used in environments with limited resources (Thakur *et al.*, 2020).

Xenodiagnosis

This technique involves in exposing the infected tissues or lesion to the sandfly and allowing the vector to bite it, then looking for *Leishmania* flagellates in the vector's gut. *L. donovani* was administered intradermally to the ear pinna of BALB/c mice (Sadlova *et al.*, 2015).

Although Xenodiagnosis is considerably more straightforward to use than other procedures and exhibits excellent sensitivity, it cannot distinguish between various *Leishmania* species. In addition, it takes much time and is only possible with the animal or insect (Akhoundi *et al.*, 2017).

2.6.4 Molecular methods

Molecular diagnostic techniques are increasingly used to diagnose VL. A recent systematic study found that polymerase chain reaction (PCR) testing on bone marrow, peripheral blood, or buffy coat samples had good sensitivity (>95%), with no significant differences in PCR performance between *L. donovani* in Asia, East Africa, and *L. infantum* in the Mediterranean. However, PCR results on blood from cases of *L. infantum* infection in Latin America were scarce, but they suggest a similar performance in this region. Real-time PCR data were also limited, but they indicate comparable performance to traditional PCR. Therefore, PCR on blood may serve as an initial non-invasive step in the diagnostic process. However, specificity was modest (63%–76%) in well-conducted investigations. On the one hand, this may indicate a poor choice of the gold standard, resulting in missing real cases. On the other hand, it also indicates that a significant percentage of people without VL in endemic areas are PCR-positive (asymptomatic *Leishmania* infection). Thus, a positive test should be assessed with a robust clinical case definition and other tests such as serology, ideally. Quantitative PCR's high parasite burdens further support the VL diagnosis (van Griensven and Diro, 2019).

2.7 Vaccine development for Leishmaniasis

An active acquired immunity to a specific infectious disease is provided by a biological component known as a vaccine. One of the practical and affordable strategies for preventing infectious diseases is vaccination (Raman *et al.*, 2012). Treatment of Leishmaniasis entirely depends on chemotherapy. The urgency to have a secure and efficient vaccine for leishmaniasis has increased because of the harmful effects of present therapies, the development of drug-resistant strains, and the rising cases of the disease in people with weakened immune systems. Extensive attempts have been undertaken to create a vaccine to prevent cutaneous and visceral leishmaniasis. Nonetheless, there is insufficient credible proof of acquired protective immunity in humans following recovery from visceral

leishmaniasis. Furthermore, due to the asymptomatic nature of most human infections and the lack of a reliable animal model that mimics the human disease, the situation is complicated.

Leishmanization, which involved inoculation with live, virulent parasites, was a successful vaccine against leishmaniasis in the past but was abandoned in many countries due to logistical and safety issues. Killed vaccines made up of crude parasite antigens have been developed and classified as first-generation vaccines, but their average efficacy value was low. Therefore, the need for an effective vaccine against leishmaniasis remains urgent (Coelho *et al.*, 2008).

The next generation of vaccines for Leishmaniasis are being developed using various approaches. Second-generation vaccines are based on live vaccines, purified *Leishmania* antigens, and recombinant antigens. Many *Leishmania* recombinant proteins have been tested intensively in recent years, either alone or in combination, as polyproteins or chimeras. However, none of these vaccines have yet reached phase III clinical trials. DNA vaccines are also under development and testing, which have the advantage of stability, low production costs, efficient generation of immune response, and sustained expression of relevant antigens. Furthermore, a single DNA construct can produce multiple antigens (Abdellahi *et al.*, 2022).

There are many different types of vaccinations in their preliminary stage; some include DNA or RNA (genetic), killed (inactivated), subunit, attenuated, recombinant, toxoid, semi-virus particles, and vaccines made from toxoids (Ghorbani and Farhoudi, 2018). The ability to use it for therapeutic and preventative purposes, ease of transportation and low cost are the qualities of an ideal leishmaniasis vaccine. It should also provide immunity against most parasite strains, require little repetition to maintain long-term immunity against disease strains, and be inexpensive. Multi-antigen vaccines must produce the best immunity against the parasite to achieve these aims, which have been discovered in modern times. In addition to first-, second-, and third-generation vaccines, live vaccines for *Leishmania* are also available and need to evaluate at clinical setting (Deris *et al.*, 2022). Despite many years of research and progress in identifying immunogenic parasite antigens and developing vaccine technologies, a single vaccine candidate capable of providing the

level of protection required for a disease-elimination program has yet to be identified. The pace of the development of a vaccine for Leishmaniasis has been slow (Ikeogu *et al.*, 2020).

There are currently three types of vaccines in development: (i) vaccines made from live-attenuated or heat-killed parasites, (ii) the most advanced vaccines designed for managing human leishmaniasis are based on these recombinant molecules, including subunit vaccinations, vaccines containing recombinant proteins, GM parasites produced by viruses or bacteria, and vaccines with recombinant proteins. In human clinical trials, LEISHF1, LEISHF2, and LEISHF3 are polyproteins of assorted specified *Leishmania* antigens. In experimental canine models, protein Q, another poly-antigenic molecule, has been discovered to protect against CanVL. This vaccine (LETIFEND®) has just been licensed in Europe to prevent canine leishmaniasis (Iborra *et al.*, 2018). (iii) The virus produces immunogenic proteins and plasmid DNA is used in vaccine development. Developing vaccines for VL has been a significant challenge due to incomplete understanding of the immune mechanism that inhibits the pathogen. Studies on the host immune response during VL have primarily relied on mouse models since human studies require invasive techniques (Faleiro *et al.*, 2014). Vaccines are a safer and more cost-effective alternative to chemotherapy, with no adverse effects observed. While immunomodulators have potential therapeutic benefits, they are currently not being employed. Several animal vaccinations appear to be successful; however, human immunization experiments have proved unsatisfactory. Canine leishmaniasis has been prevented with remarkable effectiveness by vaccines like CaniLeish® and Leishmune®. These vaccinations, approved for use in animals, have been demonstrated to protect dogs, preventing the zoonotic spread of leishmaniasis to humans (Ikeogu *et al.*, 2020).

2.8 Background study

Tuzin is a transmembrane protein that is rarely conserved and its function is not well understood. It is found in *Trypanosoma* and *Leishmania* species (Jackson, 2010). The Tuzin gene is present in multiple copies and is often found adjacent to the δ amastin gene, a transmembrane glycoprotein, abundant in quantity and essential for cell function after infection, has been detected on the cell surface of trypanosomatid parasites. Throughout the evolution of δ amastin, the connection between Tuzin and δ amastin genes has remained

intact, suggesting a robust functional association between these two gene families (Kangussu-Marcolino *et al.*, 2013).

The gene named Tuzin was initially discovered in *Trypanosoma cruzi* and therefore named as such. *T. cruzi* harbors a series of two interchanging genes in tandem repetition, with one coding for amastin and the other for Tuzin. Amastin is a highly expressed glycoprotein found on the surface of amastigotes (Jackson, 2010), whereas the function and location of the Tuzin protein are still unknown despite being identified in *Trypanosoma cruzi*. Tuzin is considered a rare protein, while Amastin is an abundant surface protein in amastigotes. The 5' UTR and spliced leader addition site of Tuzin combine to significantly decrease its expression (Teixeira *et al.*, 1995), which is a pseudogene in both *L. major* and *L. braziliensis* but not in *L. donovani* and *L. infantum*. Genes that are distributed differently among various *Leishmania* species encode proteins that are involved in host-pathogen interaction and parasite survival in host macrophages. *L. infantum* is primarily linked with visceral Leishmaniasis, in certain subspecies, cutaneous Leishmaniasis may also be triggered by it. According to research, *L. infantum* strains obtained from cutaneous patients were not capable of causing visceral infection, unlike strains from visceral patients. This suggests that the disease manifestation is determined by the genetic variations among *L. infantum* subspecies. Variations in species-specific genes, pseudogenes, and the levels of virulence and stage response gene expression may all play a role in the disparities in disease pathology (McCall and Matlashewski, 2010). It is noteworthy that in pathogenic *Leishmania* species, the chromosomal location of amastin genes is frequently linked to Tuzin (Raymond *et al.*, 2012). Additionally, amastin is crucial to the parasite after infection, and the function of the Tuzin (LdBPK_080750) gene product is unknown in *L. donovani.* Hence, we are interested in characterizing the function of Tuzin (LdBPK_080750) in *L. donovani* infection.

Our understanding of the causes of visceral Leishmaniasis is still limited, but recent progress in genomic research, immunology, and animal models is shedding light on this disease (McCall and Matlashewski, 2010). Tuzin, a pseudogene present in *L. braziliensis* and *L. major* causing cutaneous and mucocutaneous Leishmaniasis respectively, is not found in *L. donovani* and *L. infantum*, which cause visceral Leishmaniasis. The comparison of genomes among different species of *Leishmania* has indicated that the primary factors shaping their genomes are gene loss and the formation of pseudogenes. On

the other hand, genes with differential distribution among species encode proteins that play a crucial role in host-pathogen interaction and parasite survival within host macrophages (Vélez *et al.*, 2005). According to (McCall *et al.*, 2013), although both the vector and host contribute to the development of symptomatic disease, the characteristics of the parasite are the most important factor in differentiating between cutaneous and visceral disease (Peacock *et al.*, 2007) found that out of over 8,000 genes in *L. major, L. braziliensis, L. donovani,* and *L. mexicana*, only 19 genes were specific to *L. donovani* and absent or present as pseudo genes in cutaneous species. To explore how specific genes can enhance the survival of parasites in the visceral organs and The genes were introduced into *L. major* and the parasite load in the liver and spleen of BALB/c mice was observed (Zhang *et al.*, 2018; Matlashewski *et al.*, 2013)..

The field's primary method for diagnosing visceral Leishmaniasis is currently the rapid strip test that relies on the rk39 antigen. However, it is concerning that a significant percentage of healthy individuals from areas where the disease is prevalent also test positive for this antigen, up to 20-32%. Therefore, it is crucial to find an alternative antigen that is more specific and has a comparable level of sensitivity to the rk39 antigen (Srivastava *et al.*, 2011). In mice, the surface antigens of the leishmanial Amastin protein sequences elicit a high level of immunogenicity compared to other antigens (Stober *et al.*, 2005) and Induce potent immune reactions in humans, specifically in relation to visceral Leishmaniasis (Khamesipour *et al.*, 2006). Information is accessible regarding the prospective utilization of amastin proteins and their homologs for detecting active visceral Leishmaniasis. A set of 11 amino acids that form the amastin signature sequence are present in all *Leishmania* amastin homologs, specifically in the peptides that correspond to the first extracellular domain of *Leishmania* amastin surface protein, indicating a highly conserved sequence (Rochette *et al.*, 2005). It may be feasible to create a diagnostic kit using Tuzin as an antigen, which could have similar effects to other antigens. Tuzin has a distinct quality that is exclusive to *Leishmania*, making it impossible for cross-reactivity with other joint illnesses like malaria and tuberculosis, particularly in regions where Leishmaniasis is common (Rafati *et al.*, 2006).

In this context, exploring the function of the Tuzin (LdBPK_080750) gene, which is a pseudogene in *L. major* but functional in *L. donovani,* will shed light on its role in virulence

and infectivity in the visceral organs. Alternatively, since Tuzin is a close homolog strongly associated with the amastin gene family, substantial evidence supports amastin family members for its role in diagnosing Leishmaniasis. In order to clarify protective immunity in BALB/c mice against the *L. donovani* challenge, The immune-boosting properties and ability to provide protection of Tuzin as a DNA vaccine were documented and exhibited (Lakshmi *et al.*, 2014). Developing a dependable vaccine for *Leishmania* has been a challenging undertaking with minimal advancements. To make Tuzin a viable option for a VL vaccine and diagnostic, we are interested in understanding its role in *L. donovani* infection. Since Tuzin is a pseudogene in *L. major* but a functional gene in *L. donovani* which causes VL will help us understand how it affects virulence and infectivity in the visceral organs. Tuzin may contribute to Leishmania's pathogenesis and be a candidate for both a diagnosis and a vaccination.

Our study was categorized into the subsequent goals based on this

1. To evaluate the Tuzin protein as a candidate for the potential diagnostic marker for Visceral Leishmaniasis.
2. To evaluate the immune response induced by Tuzin protein in *L. donovani* challenged BALB/c mice.
3. To determine the role of the Tuzin gene in the survival and infectivity of *L. donovani* by knockdown approach.

Chapter: III
Materials and Methods

Objective 1: To evaluate the Tuzin protein as a candidate for a potential diagnostic marker for Visceral Leishmaniasis.

3.1.1 General chemicals and reagents

All the biochemical and immunochemical materials used in the investigation were of high purity and analytical quality. These included M-199 media, RPMI, $CaCl_2$, $MgCl_2$, D-glucose, sodium bicarbonate, Betain, Ficoll 400, Protease inhibitor cocktail, Propidium iodide (PI), Freund's complete adjuvant, and Freund's incomplete adjuvant, Trypsin from porcine Pancreas, BCIP/NBT solution (premixed), formaldehyde, which were all procured from Sigma-Aldrich, USA. Additionally, other materials such as skimmed milk, glycine, Tris buffer, SDS, glycerol, hydroxyurea, triton X-100, acrylamide, NaCl, kanamycin sulfate, peptone, tween-20, agar agar, yeast extract powder, ammonium bicarbonate, Giemsa stain, sodium lauryl sulfate, NADPH, ponceau S, ethidium bromide, coomassie Blue G-500, β-mercaptoethanol, PMSF, immersion oil for microscopy, BSA, TEMED, EDTA, bis-acrylamide, Formaldehyde 37%, isopropyl alcohol, isobutanol, glacial acetic acid, G148 sulfate, Trypan blue, Yeast extract, Kanamycin sulfate, Agar Agar, and Peptone were purchased from Himedia. Finally, EDTA, Sodium phosphate monobasic anhydrous, 2-Mercapatoethanol, HEPES buffer, KCl, Trypsin, and Acrylamide were purchased from SRL.

Restriction enzymes, Enzyme buffers, T4 DNA ligase, Electroporation cuvettes and SnakeSkin® dialysis tubing (3.5K MWCO) were procured from Thermo Fisher Scientific Inc, Agarose (Lonza), Serological pipettes, dishes, and cell culture flasks purchased from Corning India. FBS (Gibco). Trizol-T-Reagent (Ambion/RNA), Griess assay kit was purchased from Invitrogen. Chemiluminescent reagent/ fento LUCENT PLUS –HRP (G-Biosciences), TMB/H_2O_2 (GeNai), Penicillin/Streptomycin antibiotic mixture (Gibco), Phusion High fidelity DNA (Biolab), Proteinase K (Thermo scientific). The products included are the 1st strand cDNA synthesis kit from TakaRa called PrimeScript, a 1 Kb DNA step ladder from GCC Biotech, a broad range protein molecular marker from GeNei, a prestained protein ladder from Purogene, and VECTASHIELD® PLUS antifade mounting medium containing DAPI from Vector Laboratories. The kit used for plasmid purification,

PCR, and gel clean-up was obtained from Macherey-Nagel, while the DNA extraction kit was acquired from Qiagen and the RNA isolation kit was purchased from Sigma

Antibodies: His-Tag Mouse HRP conjugated Abs (Cell Signalling tech), Goat Anti-mouse FITC (GeNei), Goat-Anti- Human IgG-HRP (GeNei), B-Tubulin Ab (Invitrogen), Goat pAb to mouse IgG 1 HRP, Goat pAb to mouse IgG2a HRP (Abcam), Anti–mouse CD8a, Anti-Mouse CD4, Anti-Mouse CD3 (eBiosciences), Goat Anti Human IgG- HRP (GeiNei).

3.1.2 Growth media for bacterial culture

3.1.2a Luria Bertani broth (LB)

In order to prepare the medium, 10 grams of peptone, 5 grams of NaCl, and 5 grams of yeast extract were dissolved in 800 milliliters of double-distilled water. The solution's pH was subsequently adjusted to 7.4 by utilizing 10N NaOH, and the final volume was then brought up to 1000 mL, and the medium was sterilized through autoclaving at a pressure of 15 pounds for 15 minutes.

3.1.2b LB agar plate

15 g of Agar-agar was added to each liter of LB broth and autoclaved to sterilize it. A specific antibiotic solution (kanamycin 50 µg/mL) was added and placed into 100 mm plates (20-30 mL per plate) after the media had been chilled to 50 °C. The plates were held in the laminar flow for at least 30 minutes to solidify and dry.

3.1.3 Cultivating *Leishmania*

3.1.3.1 Culture medium for *Leishmania* donovani promastigotes

The powder weighing 12.5 grams was combined with 900 mL of double-distilled water to produce the growth medium. The mixture was stirred gently until the powder dissolved completely, and 0.35 g of sodium bicarbonate was then added. An incomplete medium was created by bringing the pH of the solution to 7.4 and adding double-distilled water to fill the remaining volume to 1 L. In order to prepare a full medium, 150 mL of FBS that had been heat-inactivated and 10 mL of penicillin/streptomycin solution were mixed with the incomplete medium. The remaining volume was then topped up with the incomplete

medium, and the resulting mixture was passed through a 0.22 µm pore-size membrane filter. The complete medium was then stored at 4 °C until it was needed

3.1.3.2 Parasite culture

The promastigote strain (MHOM/IN/80/Dd8) of *L. donovani* was acquired from the ATCC, located in the United States. These parasites were cultivated in a Medium-199 that consisted of 15% heat-inactivated FBS, 4 mM $NaHCO_3$, 20 mM HEPES (pH 7.4), 100 U/mL of penicillin, and 100 mg/mL of streptomycin at a temperature of 25 °C ± 1 °C. The quantification of parasites was performed by immobilizing them with 4% formalin and then counting them with a hemocytometer.

3.1.3.3 In vivo

Leishmania DD8's virulence was controlled in BALB/c mice by passage over time. A dose of $1x10^8$ promastigotes in PBS was injected intravenously into each mouse. Parasites were found in the lesions on the infected spleen of BALB/c mice one month after infection. The spleen was removed under sterile conditions, homogenized by hand, and splenocytes were cultured in 10% FBS containing M-199 at 25 °C. Freshly transformed promastigotes were observed under the microscope. The suspension was centrifuged at 100 x g for 10 min at 4°C to remove splenic debris, and the parasites were sub-cultured in fresh M199 medium. The parasites in stationary phase were collected, purified through pelleting, washing twice, and then suspended in PBS at a concentration of $1x10^8$ cells/mL. Next, a volume of 100 µL containing freshly transformed promastigotes (also at $1x10^8$ cells/mL) was injected into the tail vein of mice aged between 6 and 8 weeks.

3.1.5 Isolation of Genomic DNA

Promastigote cells of *L. donovani* were cultivated until they reached the exponential phase. Next, the cells were harvested by centrifuging them at 2500 rpm for 10 minutes and then rinsed two times with PBS (pH 7.4) to eliminate the medium. These cells were utilized for the isolation of genomic DNA, which was performed using a Sigma kit following the manufacturer's guidelines. The genomic DNA's quality was evaluated through the use of electrophoresis on a 1% agarose gel, and it was subsequently used to amplify the LdTuzin gene.

3.1.6 Primers designing

The *Leishmania donovani* Tuzin sequence (FASTA format of 993 bp) was picked up from the GENBANK database (Gene ID: LDBPK_080750) and designed specific primers for cloning into pET 28a vector. Restriction enzyme analysis of the Tuzin sequence was performed by using the NEB Cutter tool. Two non-cutters, *HindIII* and *BamHI*, for the digestion were selected. Primer sequences are created for amplifying particular gene segments, and both forward and reverse primers are included. These primers have restriction enzyme sites incorporated into their sequences. The design of the primers involves the addition of *HindIII* and *BamHI* restriction sites at the 3' and 5' ends, respectively. The melting point and other properties of both primers were checked by using the OligoCalc tool. The primers which were used for cloning are shown in Table 3.1.

Table 3.1: primers list which was used for cloning

Primer	Sequence	Restriction enzyme
Tuzin FP	5’- GCCGGATCCATGATTCCTGGAGTCGTC -3’	*BamH*I
Tuzin RP	5’- ATAAAGCTTTACGCCCGCCGCGGCCT -3’	*Hind*III

3.1.7 PCR Amplification of Tuzin gene

To amplify the Tuzin gene (LdBPK_080750) from genomic DNA, PCR was performed using Phusion High Fidelity Taq polymerase in a verity 96-well thermocycler from Applied Biosystems. A 25 µL PCR reaction mixture was created by combining template DNA, 10 pmol of each Tuzin forward and reverse primers, 0.2 mM dNTPs, and 1 U of Taq DNA polymerase. A preliminary denaturation stage at 98 ºC for 1 min was followed by 35 cycles of denaturation at 95 ºC for 30 sec, annealing at 64 ºC for 45 sec, and extension at 72 ºC for 1 min. The final extension step of the reaction was carried out at a temperature of 72 ºC for duration of 5 minutes. Electrophoresis was used to confirm the amplification of the Tuzin gene on a 1% agarose gel, and afterward, the amplified product was obtained from the gel and subjected to purification utilizing a Nucleo Spin kit in accordance with the guidelines provided by the manufacturer.

3.1.8 Isolation of pET-28a plasmid

The pET-28a plasmid was obtained by extracting it from *E. coli* DH5α cells. To do this, the glycerol stock of pET-28a along with the *E. coli* DH5α cells were cultured in 10 mL of LB broth media and allowed to incubate overnight at 37 °C. After washing the cell pellet twice, following the manufacturer's instructions, a NucleoSpin kit was used to extract the plasmid from the pellet.

3.1.9 Double digestion of vector and gene of interest

The isolation of the pET-28a plasmid from DH5α cells was carried out using a NucleoSpin kit as per the manufacturer's protocol. Furthermore, the amplified gene was obtained from the agarose gel by using a gel elution kit. The same restriction enzyme BamHI double digested both plasmid and gene and *HindIII* in different Eppendorf, and then incubated at 37 ºC for 3 hours. Finally, double digested construct were run on 1% agarose gel and isolated by gel extraction.

3.1.10 Preparation of Competent Bacterial cells

To obtain competent bacterial cells, a single colony was cultured in 5 mL of LB medium (without antibiotic) at 37 ºC in a shaking incubator overnight. To start a secondary culture, 500 µL of the primary culture was transferred into 50 mL of fresh LB medium (without antibiotic), using the resulting primary culture. After that, the secondary culture was maintained at 37 °C in a shaking incubator until the OD600 reached 0.4–0.5. The centrifugation process was used to harvest the cells at a 2000 rpm for 5 minutes at a temperature of 4 ºC. The resulting pellet was then suspended in 2 mL of 0.1 M $MgCl_2$. The cells were centrifuged once more, and the pellet was then resuspended in 5 mL of 0.1 M $CaCl_2$ and incubated for 1-2 hours on ice. The resulting pellet was centrifuged once more and then suspended in a cold solution containing 15% glycerol and 0.1 M $CaCl_2$. The cells were eventually separated into 100 µL aliquots and stored at a temperature of -80 ºC for subsequent utilization.

3.1.11 Transformation

To carry out the transformation process, 100 µL of competent cells that had been frozen were thawed on ice for a short duration, and then combined with 20 ng of plasmid DNA. The mixture was then placed on ice for 30 minutes, following which the cells underwent a heat shock treatment for 90 seconds in a water bath at 42 °C. After the immediate heat shock, the microtubes were promptly chilled for 5 minutes. Afterwards, the mixture was provided with 1 mL of recently prepared LB media that did not contain any antibiotics. It was then placed in a shaking incubator for one hour at 37°C. Following this, the pellet was mixed with 100 µL of fresh LB media and spun at 2000 rpm without antibiotics. To acquire the transformed colonies, the transformed culture was positioned on a kanamycin-containing agar plate and left to incubate overnight at 37 °C.

3.1.12 Ligation and transformation

The ligation reaction was performed by incubating with a double-digested vector and double-digested insert in the ratio of 1:3 and 300U of ligase, 1X ligase buffer in a volume of 10 µL. This ligated mixture was then incubated at 22 °C overnight. The the ligated reaction was mixture transformed into *E. coli* DH5α competent cells by heat shock methpd. Briefly, 100 µL of DH5α competent cells were taken and thawed on ice for 30 min, and then added the ligation reaction mixture to these cells. Heat shock was applied for 90 seconds at 42 ºC. Tubes were placed on ice for 2 min, and then added 1 mL of fresh LB media was placed. This mixture was incubated at for 1 h at 37 ºC with 180 rpm. The cells were pellet down at 5000 rpm for 5 minutes, and removed 800 µL supernatant. The pellets were resuspended in the remaining media and plated on LB-Agar containing kanamycin as a selection marker, and the plate was incubated at 37 ºC for overnight.

Analysis of Tuzin-pET-28a recombinants screening of the positive transformants was performed by colony PCR method, double digestion, and checking the presence of the resistance gene in the construct.

3.1.13 Colony PCR

The process of colony PCR involved picking colonies from the master plate and streaking them onto another LB-kanamycin plate to create a replica plate. After incubating the plate at

37 ºC for 12 hours, the colonies was harvested by scraping the cells and transferring them into 1.5 mL centrifuge tubes with 20 µL of sterilized water. Subsequently, the tubes were subjected to 95 º C temperatures for 10 minutes in dry bath and then centrifuged for 5 minutes at 13,000 rpm. The resulting supernatant was used to obtain 1 µL of plasmid DNA, which was then subjected to PCR in a 12.5 µL reaction volume. In the PCR procedure, a total of 35 cycles were performed, each consisting of denaturation for 30 seconds at 98 ºC, annealing for 30 seconds at 64 ºC, and extension for 1 min at 72 ºC. The final step of the process involved an extension at 72 ºC for 5 minutes. To verify the amplification, a 1% agarose gel was loaded with the amplified gene.

3.1.14 Confirmation by PCR

For the confirmation of the clone, PCR was performed using forward, reverse primers in 25 µL reaction volume containing pET-28a Tuzin construct as a template and the same reaction mixture with an empty vector as a template for negative control. Amplification was checked on 1% agarose gel.

3.1.15 Double digestion for clone confirmation

The colonies which appeared optimistic in colony PCR were further subjected to double digestion. Briefly, the transformants were picked up from replica plates and grown for 12 hours in 30 mL LB media containing 30 µL of kanamycin (50 mg/mL) at 37 ºC, 200 rpm speed, then centrifuged for pellet down and washed with 1X PBS. The construct was isolated from the pellet using a kit; the purity and integrity of the plasmids were checked on 1% agarose gel. These plasmids were subjected to double digestion by Hind III and Bam HI. Dropout of insert checked on 1% agarose gel.

3.1.16 Expression of recombinant Tuzin protein

To express the Tuzin protein, the positive clone was first transformed into *Escherichia coli* Rosetta (DE3) strain using heat shock method and plated onto an LB agar plate containing kanamycin and chloramphenicol. After being incubated overnight at 37 ºC, a solitary colony was chosen and added to a new batch of LB broth, which was then continuously shaken at 200 rpm and incubated overnight at 37 ºC. The secondary culture was then raised from the first culture in freshly LB broth until the OD600 reached 0.4-0.5. To standardize the

experiment, a portion of the culture was extracted as an uninduced control, while the rest of the culture was induced using IPTG with specific time, temperature, and concentration. The cells were subsequently centrifuged, and the resulting pellets were washed with 1X PBS before being suspended in 2X loading dye and heated. Following this, the samples were loaded onto 10% SDS-PAGE and subjected to Coomassie blue staining for analysis.

3.1.17 Determination of protein solubility

To determine the protein solubility, the log phase of the *E. coli* Rosetta culture was induced overnight at 25 ºC with 0.5 mM. After induction, after centrifuging, the cells were collected, and the resulting sediment was subjected to further treatment with lysis buffer after adding PMSF and DNase. Following sonication and centrifugation, the soluble fraction was separated from the insoluble fraction, which was subsequently resuspended in lysis buffer. Both fractions were then subjected to 12.5% SDS-PAGE analysis.

3.1.18 Protein purification in denaturing condition

To isolate the protein in denaturing conditions, the IPTG-induced culture of 500 mL was gathered via centrifugation for 10 minutes at 6000 rpm and rinsed for two times with 1X PBS. The resulting pellets were then suspended in a guanidinium lysis buffer (6 M Guanidine HCl, 20 mM Sodium phosphate pH 7.8, and 500 mM NaCl), gently agitated for 15 min at RT, sonicated on ice, and centrifuged for 15 min at 4500 x g. The collected supernatant was utilized for purification by adding it to a pre-prepared Ni-NTA purification column, which was allowed to bind at RT for 30 minutes with mild agitation. After binding, denaturing binding buffer, which has a pH of 7.8, was used to wash the column. It contains 20 mM sodium phosphate, 8 M urea, and 500 mM NaCl. Subsequently, the column was successively washed with denaturing wash buffers of pH 6.0 and pH 5.3. To elute the protein, denaturing elution buffer (pH 4.0) containing 500 mM NaCl, 8 M Urea, and 20 mM Sodium phosphate was added, while the column was clamped vertically and the cap removed from the lower end. To remove urea, the eluted protein was dialyzed for 6 hours at 4 ºC against 150 mM NaCl, 10 mM Tris (pH 8.0), and 0.1% Triton X-100.

3.1.19 Protein Immunoblotting

To conduct protein immunoblotting, the protein samples underwent SDS-PAGE separation and were subsequently transferred onto a nitrocellulose membrane using a Bio-Rad Trans-blot SD semi-dry transfer cell. Nonspecific binding sites were blocked by submerging the membrane in a 5% BSA or skimmed milk solution that was made in TBS (150 mM NaCl, 20 mM Tris, pH 8.0) for a period of 1 hour. Next, the membrane was subjected to an overnight incubation with a primary antibody that had been suitably diluted in a blocking solution. Following this, the membrane was washed thrice using a TBST buffer (20 mM Tris, 150 mM NaCl, and 0.1% w/v Tween 20) and was then exposed to a secondary antibody that had been conjugated with HRP for a period of 1 hour at RT. The TBST buffer was used to wash the membrane again, and the respective protein bands were visualized using the FemtoLUCENT™ PLUS-HRP Chemiluminescence Detection System and the Chemidoc system.

3.1.20 Antibody raising against Tuzin

In order to generate an antibody against Tuzin, the recombinant Tuzin protein was purified and its concentration was determined. Afterwards, around 50 µg of the recombinant Tuzin was combined with Freund's complete adjuvant in equal amounts and vigorously mixed using a sterile syringe needle to create an emulsion. The resulting emulsion was then administered to a BALB/c mouse through subcutaneous injection. The mouse was later injected with the first and second booster doses prepared similarly, and the whole blood was drawn on the 30th day from the mouse retro-orbitally. The serum was isolated and preserved at a temperature of -80 ºC until it is needed for future applications.

3.1.21 Western blotting by anti-Tuzin antibody

The SDS-PAGE analysis was performed on both the recombinant Tuzin protein and *Leishmania donovani* (DD8) crude lysate protein samples, which were later, transfer onto a nitrocellulose membrane. A primary antibody, acquired from mice immunized with Tuzin protein, was used at a 1:300 dilution and left to incubate overnight at 4 ºC. Following that, the membrane underwent a washing step before being subjected to a secondary antibody. The secondary antibody used was anti-mouse IgG antibody conjugated with HRP, and it was

diluted to a concentration of 1:10,000. FemtoLUCENT™ PLUS-HRP Chemiluminescence Detection System visualized the respective protein bands using the Chemidoc system.

3.1.22 Immunofluorescence assay to localize the Tuzin protein in parasite

The *Leishmania* parasites were suspended in 4% formaldehyde in PBS for 20 min at RT to fix them. The fixed parasites were then washed 3 times with 1X PBS and allowed to attach to glass coverslips and air-dried. Once air-dried, they were treated with ice-cold methanol (-20 ºC) for 5 minutes, then blocked with 1% BSA in PBS for 30 minutes. Afterward, an anti-Tuzin primary antibody (Tuzin protein raised mouse serum) was added in a 1:200 dilution and allowed to incubate for 1 hour. The coverslips were subjected to a secondary antibody after three washes in 1% PBS with 0.1% Tween 20 (Goat anti-mouse IgG antibody with FITC) in a 1:300 dilution. After that, they were subjected to three more rinses with 1% PBS solution containing 0.1% Tween 20 and finally, they were fixed onto glass slides using Vectashield, a mounting medium that includes DAPI. Finally, the slides were examined under a confocal microscope to detect fluorescence (Veronica *et al.*, 2019).

3.1.23 Evaluation of Tuzin potency by ELISA

By utilizing the checkerboard titration technique, we identified the most effective concentrations of sera, antigens, and anti-human serum conjugates. Polystyrene plates were coated with 150 ng/well of antigen that had been diluted in 0.1 M bicarbonate buffer (pH 9.6) and left to incubate at 4°C for overnight. Afterward, the plates underwent three washes with a washing buffer consisting of 1% PBS and 0.1% Tween 20. Next, any non-specific binding sites were blocked by a blocking buffer containing 1% BSA in PBS (pH 7.4) buffer) for two hours at 37°C. Serum samples were diluted to 1:500 in a dilution buffer (0.1% BSA, 0.1% Tween 20 in 1X PBS), and duplicate aliquots of 100 µL were added for each sample, including positive and negative control sera. The plates were then incubated at 37 °C for one hour and washed three times. To the plates, we added peroxidase-conjugated anti-human IgG that had been diluted 1:15000 (100 µl/well), and they were then incubated at 37 °C for one hour prior to being washed 5 times. After washing, we added 100 µL of TMB (substrate solution) to each well and stopped the reaction after 15 minutes by adding stop solution (1N sulphuric acid). We then read the plate at 450 nm in a microplate reader (Zhang *et al.*, 2018).

Serum samples were obtained from two sources: the Kala-azar Medical Research Center in Muzaffarpur, Bihar, and the Department of Medicine at the Institute of Medical Sciences, Banaras Hindu University in Varanasi, India, under the guidance of Professor Shyam Sundar.

The cutoff value was calculate using below formula

$$Cutoff = X_{neg} + 0.13\, X_{pos}$$

The average value of the negative controls is referred to as X_{neg}, while X_{pos} denotes the average value of the positive controls

The sensitivity and specificity was calculated based on cutoff value using following formulas (Trevethan, 2017).

$$\text{Sensitivity} = \left(\frac{\text{True Positive}}{(\text{True Positive} + \text{False Negative})} \right) \text{X } 100$$

$$\text{Specificity} = \left(\frac{\text{True Negative}}{(\text{False Positive} + \text{True Negative})} \right) \text{X } 100$$

Objective 2: To evaluate the immune response induced by Tuzin protein in *L. donovani* challenged BALB/c mice

3.2.1 Parasites

The parasites used in the study, *Leishmania donovani* DD8 (MH0M/IN/80/DD8), were acquired from the ATCC (American Type Culture Collection), United States. To cultivate these parasites, a complete M-199 Medium was utilized, which contained 15% heat-inactivated FBS, 4 mM $NaHCO_3$, and penicillin (100 U/mL) and streptomycin (100 mg/mL) at a pH of 7.4. The parasites were cultured in a BOD Incubator at a temperature of 25 ^oC.

3.2.2 Experimental Animals

We purchased female BALB/c mice from Sainath Agencies at Hyderabad when they were 6 to 8 weeks old and kept in the university's animal facility. IAEC (Institutional Animal Ethics Committee) approval was taken from Animal Ethics Committee, University of Hyderabad and criteria were followed in all trials. The mice were maintained at RT with a natural light cycle and fed standard rodent food and water.

3.2.3 Immunization and Infection of Female BALB/C mice with *L. donovani*

A total of twenty-five mice were randomly assigned to five groups, each containing five mice. Group 1: Healthy control, Group 2: Immunized with only adjuvant, Group 3: Infected control, which is given only PBS while the immunization process and then challenged with parasites; group 4: Immunized with adjuvant and then challenged with parasites and Group 5: Immunized with Tuzin protein and challenged with parasites. 40 μg of Tuzin protein was immunized to BLAB/c mice through a subcutaneous route. Two booster doses were given with a two-week gap between each administration. Mice were exposed to *L. donovani* parasites in the form of metacyclic promastigotes four weeks after receiving the last booster dosage (Figure 3.2.1). In brief, the highly infectious phase of a metacyclic parasite was acquired by subjecting a stationary promastigote culture to Ficoll gradient centrifugation. The parasites were subsequently introduced into mice through the tail vein using sterile procedures. After duration of eight weeks, the mice were humanely put to death with

Chloroform, and peripheral blood was collected via the intra-cordial route. The sterile collection of both the spleen and liver was done for subsequent experiments. Biopsies of the spleen were obtained in order to evaluate the presence of parasites.

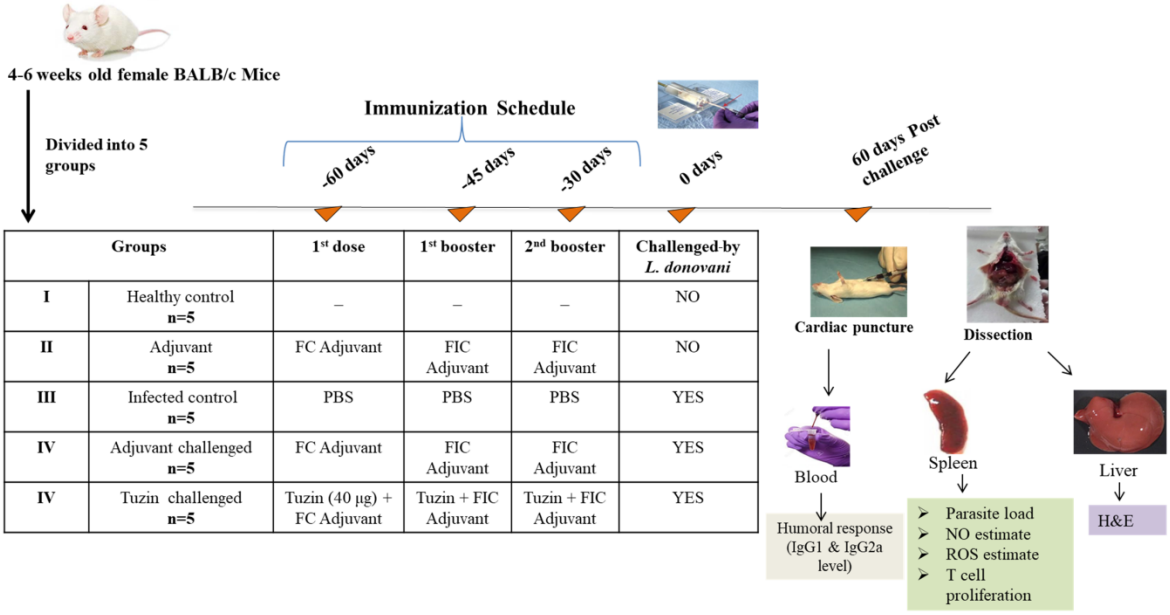

Groups		1st dose	1st booster	2nd booster	Challenged-by *L. donovani*
I	Healthy control **n=5**	_	_	_	NO
II	Adjuvant **n=5**	FC Adjuvant	FIC Adjuvant	FIC Adjuvant	NO
III	Infected control **n=5**	PBS	PBS	PBS	YES
IV	Adjuvant challenged **n=5**	FC Adjuvant	FIC Adjuvant	FIC Adjuvant	YES
IV	Tuzin challenged **n=5**	Tuzin (40 µg) + FC Adjuvant	Tuzin + FIC Adjuvant	Tuzin + FIC Adjuvant	YES

Figure 3.2.1: Illustration of in vivo experiments using a schematic

3.2.4 Determination of Parasite burden in BALB/c mice

To measure the parasite burden in mice exposed to *L. donovani* groups, the liver and spleen were collected.

3.2.4.1 Microscopic method

Briefly, Touch biopsy was performed on a glass slide using a mouse spleen, and the slide was then allowed to dry for a short while. The slide's cellular material was methanol-fixed for 5 minutes and then stained for 30 minutes using Giemsa stain (HiMedia). Next, with distilled water, the stain was gradually removed while maintaining the slide's angle. After drying, the slides were visualized under the light microscope to count the parasites. For all infected and Tuzin-challenged groups, the intracellular amastigote parasites were counted in 100 macrophages (Pandey *et al.*, 2022).

3.2.4.2 Real-Time PCR

DNA extraction:

To prepare a single-cell suspension from the mice liver, it was homogenized using a cell strainer. After homogenizing the liver sample, a mixture of 100 µL of tissue lysis buffer with 20 µL of proteinase K was added to 80 µL of the sample. The resulting mixture was then incubated overnight at 56 ^{0}C to ensure full lysis. Next, The QiAmp DNA Mini Kit (Qiagen) was utilised in accordance with the directions provided by the manufacturer.

Standard curve:

A standard curve was utilized to determine the level of parasite load, wherein *Leishmania* DNA was subjected to serial dilutions. The QIAamp DNA mini kit was used to extract the DNA of *Leishmania donovani* from 1×10^8 promastigotes, resulting in a stock solution. Upon elution in 100 mL of H_2O, the concentration was determined to be 10^6 parasites/mL, assuming near-perfect extraction efficiency (as 120 *Leishmania* parasites contain 10 pg of DNA). The DNA stock solution was subjected to ten-fold serial dilutions, resulting in eight points on a curve that spans 0.1–10^6 parasites (Sudarshan *et al.*, 2011).

qPCR experiment:

To quantify the *Leishmania* parasite in patient blood, SYBR Green-based qPCR was used, with a target region of the parasite's kinetoplast DNA for accurate sensitivity. The final volume of the PCR was 20 µL, consisting of SYBR Green master mixture (2×) from Takra, MiliQ water, DNA template, and forward and reverse primers. The real-time PCR system was used to conduct the amplification, with thermal cycling parameters consisting of an initial incubation for 2 minutes at 50 ^{o}C followed by denaturation for 10 min at 95 ^{o}C for 10, and 40 cycles for 15 seconds at 95 ^{o}C, and 1 minute at 60 ^{o}C for each. The ABI SDS software was used to create standard curves, mean values, and amplification plots, and the melting temperatures of each amplicon were calculated using the same software. Negative controls, including a healthy control and no template controls, were included in each plate to address contamination concerns (Nicolas *et al.*, 2002).

3.2.5 Quantitation of serum IgG1 and IgG2a

The level of IgG1 and IgG2a antibodies in mouse sera from different experimental groups was measured using the standard indirect ELISA method. The procedure involved coating 96-well ELISA plates with 100 ng/well of recombinant Tuzin protein and incubating them overnight at 4 ºC. Subsequently, the plate underwent a washing procedure and was blocked with 1% BSA at room temperature for duration of 2 hours. Subsequently, the plate was incubated with diluted sera at a 1:100 dilution and kept at 37°C for an hour. Following this, the plate was rinsed with PBS-Tween 20. Next, HP-conjugated rat anti-mouse IgG1 and IgG2a antibodies were added (dilution 1:10000, Abcam®) were introduced to their corresponding wells and incubated for 1 hour at 37 ºC. After an additional washing procedure, 100 µL of a substrate consisting of 1X TMB/H_2O_2 was introduced and left to incubate for 30 minutes at room temperature in the absence of light. A micro plate reader (TECAN) was used to measure the colour intensity at 450 nm when the reaction was stopped by adding 50 µL of Stop solution (1N H_2SO_4).

3.2.6 Histopathological studies

Samples of liver tissue were gathered from all mouse groups and preserved in a saline buffer containing 10% formalin (composed of 100 mL of 40% formaldehyde, 9 g NaCl, and 900 mL of water) for Histopathological examination. These tissue samples were later transported to the LV Prasad Eye Institute in Hyderabad, where they underwent hematoxylin-eosin (H-E) staining. To ascertain the quantity of granuloma formations and degenerative/necrosis changes, the resulting slides were scrutinized with a light microscope (Leica) (Salguero *et al.*, 2018).

3.2.7 Nitric Oxide (NO) quantification

The splenocytes from all mouse groups were grown in 12-well plates containing a complete RPMI medium. The cells were incubated with and without 80 µg/well soluble *leishmania* antigen (SLA) for 72 h at 37°C in a CO_2 incubator. The resulting supernatant was collected and examined for NO levels. In order to perform this task, 100 µL of the supernatant from the culture was combined with 100 µL of Griess reagent, is composed of 2.5% v/v phosphoric acid along with 1% w/v sulphanilamide and 0.1% w/v naphthyl

ethylenediamine-HCl. The mixture was then allowed for 30 minutes at RT. The samples were then analyzed for absorbance at 540 nm, and the nitrite levels were determined using standard curves produced from various concentrations of $NaNO_2$ (10-100 μM).

3.2.8 Reactive Oxygen Species (ROS) Analysis

Intracellular ROS levels were measured using a cell-permeable dye known as H2DCFDA (2,7-dichlorodihydrofluorescein-diacetate). To carry out this measurement, splenocytes from various groups of mice ($2x10^6$ cells/well) were were incubated for 3 days in a CO_2 incubator, either with or without SLA (80 μg/well), to observe the effect on their culture. The supernatant was used to estimate NO, cytokines, and cells for ROS analysis, while the cell pellet was washed with PBS and subsequently incubated with 10 μM of H_2DCFDA in PBS in the dark for 30 minutes at RT. Using flow cytometry (specifically, the BD LSR FortessaTM instrument and FACSDiva software), the measurement of the green fluorescence of H_2DCFDA was taken and represented as a bar graph displaying Mean Fluorescence Intensity (MFI)

3.2.9 Cytokine expression analysis

3.2.9.1 RNA isolation and cDNA preparation

Following the manufacturer's instructions, RNA was extracted from splenocytes in all mouse experimental groups using the QIAGEN RNeasy mini kit. After using 1 μg of total RNA, cDNA was synthesized using the Takara Prime script 1st strand DNA synthesis kit. The resulting amplified cDNA was stored at a temperature of -80 ºC for future use

3.2.9.2 Real time quantitative PCR

Using cDNA as a template, the targeted genes were amplified with their respective primers (listed in Table 3.2.1) using SYBR Premix Ex Taq (2X) from Takara. The PCR reaction was prepared as per the kit instructions using SYBR Green PCR master mix, 1X SYBR green, primers, and cDNA templates. Real-time PCR was carried out using 40 cycles of activation for 2 min at 95 ºC, followed by denaturation for 15 sec at 95 ºC, and annealing for 30 seconds at 60 ºC. The StepOnePlus™ software from Applied Biosystems was used to analyze the real-time PCR results. The relative fold expression of the target gene was

measured using the $2^{-\Delta\Delta ct}$ technique. The mean±SD from two independent experiments were used to calculate the relative expression.

Table 3.2.1: Primers used for the RT-PCR

Primer		**Sequence (5'-3')**
IFN-γ	FP	TCAAGTGGATAGATGTGGAAGAA
	RP	TGGCTCTGCAGGATTTTCATG
IL-10	FP	GGTTGCCAAGCCTTATCGGA
	RP	ACCTGCTCCACTGCCTTGCT
GAPDH	FP	CAAGGCTGTGGGCAAGGTCA
	RP	AGGTGGAAGAGTGGGAGTTGCTG

3.2.10 CFSE proliferation assay

Flow cytometry was used to evaluate the proliferative capacity of T cells in all mouse groups through CFSE staining. The process involved isolating splenocytes from the mice and incubating them in 15 mM CFSE for 10 minutes in RPMI 1640 without FBS. Following treatment, the cells were cooled in ice-cold RPMI 1640 containing 10% FBS, rinsed, and seeded in 24-well tissue culture plates at a concentration of $2x10^6$ cells per well. The cells were then cultured for five days at 37 °C with 5% CO_2, either with or without SLA stimulation (80 µg/well), within a CO_2 incubator. Afterwards, the cells were gathered, washed with PBS, and then exposed to anti-mouse CD3-FITC, anti-mouse CD8-APC and, anti-mouse CD4-PE staining, which were left to incubate for 30 min at 4 °C. Subsequently, the cells were rinsed and suspended in FACS staining buffer prior to acquisition using flow cytometry (BD LSR FortessaTM using FACSDiva software). FlowJo software was then used to analyze the T cells population (Karmakar *et al.*, 2021).

Objective 3: To determine the role of Tuzin gene in survival and infectivity of *L. donovani* by knockdown approach

3.3.1 Cloning of Tuzin gene in pEGFP-C1 vector in sense and anti-sense orientation

In order to comprehend how the Tuzin gen works for the *L. donovani* parasite's infectivity and virulence, the vector pEGFP-C1 (mammalian expression vector) was used in these studies. The tuzin gene cloned either in sense or antisense orientation into the pEGFP-C1 vector.

Leishmania donovani Tuzin sequence (in FASTA format, 993 bp) was taken from the GENBANK database and used to create primers for Tuzin overexpression (OE) and knockdown (KD). Table 1 lists the primers utilized for OE and KD cloning.

Table 3.3.1: Primers for the cloning of Tuzin overexpression and knockdown

Primer	Sequence	Restriction enzyme
FP for OE	5'- GCCAAGCTTATGATTCCTGGAGTCGTCT -3'	Hind*III*
FP for OE	5'- ATAGGATCCTAACGCCCGCCGCGGCCTT -3'	*BamHI*
FP for KD	5'- GCCGGATCCATGATTCCTGGAGTCGTC -3'	*BamHI*
RP for KD	5'- ATAAAGCTTTACGCCCGCCGCGGCCT -3'	*Hind*III

The Tuzin gene was cloned into pEGFP-C1 vector in sense and anti-sense orientation for overexpression and knockdown, respectively. Briefly, the Tuzin gene was amplified from genomic DNA by PCR; simultaneously, the pEGFP-C1 vector was isolated from *E. coli* DH5α cells. Both the vector and gene were double digested and then ligated by DNA ligase enzyme at 22 ºC for overnight. The *E. coli* DH5α competent cells were transformed with the ligated reaction mixture using the heat shock method. Verification of the clone was carried out through colony PCR and double digestion.

3.3.2 Transfection

Isolated the plasmid from the respective source and quantified. The active late log phage *Leishmania donovani* promastigote culture was taken and centrifuged for 10 minutes

at 3000 rpm. The pellet was rinsed twice using 5 mL of HBSS buffer before being washed with electroporation buffer (EPB) that had been filtered. EPB contains 21 mM HEPES, 5 mM KCl, 137 mM NaCl, 6 mM glucose, and 0.7 mM Na_2HPO_4. Resuspended the pellets in 1 mL of EPB and counted the parasite using a neubauer chamber. After taking 4 x 10^7 cells, pellet it down and resuspend in 400 mL of EPB and cytomix buffer (10 mM $K2HPO_4$, 5 mM $MgCl_2$, 120 mM KCl, 0.1 mM $CaCl_2$, 25 mM HEPES and 2 mM EDTA, pH 7.6) in 4:1 ratio and kept on ice. At the same time, the gene pulser was activated with the following specifications: a voltage of 450 V, capacitance of 50μF, resistance of □, and duration of 5 ms. To the cell suspension, 10-50 μg of plasmid was added and mixed well, then transferred into 0.2 mM transfection cuvette (Bio-Rad). The electroporation chamber was used to expose the cuvette to a pulse, after which it was promptly placed on ice for 10 minutes. The parasites that underwent electroporation were then moved to 5 mL of M199 media without the drug and left to incubate overnight in a BOD incubator set at 25 ^oC. Added G418 antibiotic after 24 h to select transfectant cells in the medium at an initial concentration of 10-20 μg/mL G418 antibiotic and incubate for 4-5 days. The drug concentration increased gradually from 20-50 μg/mL. Once the parasites survive at maximum drug concentration, the parasites are used for further studies (Veronica *et al.*, 2019).

3.3.3 PCR to confirm the Tuzin level in parasite

The RNA extraction from splenocytes of all mouse experimental groups was performed using the QIAGEN RNeasy mini kit accordance with the instructions provided by the manufacturer. Subsequently, 1 μg of the extracted RNA was utilized for cDNA synthesis, employing the Takara Prime script 1st strand DNA synthesis kit, and the resulting amplified cDNA was stored at -80 ^oC to be used later. To conduct PCR, a particular Tuzin primer was utilized along with cDNA acting as a template.

3.3.4. Western blotting by anti Tuzin antibody

An equal number of stationary phase parasites (1x10^8 cells) were taken and added 500 μL of 2x loading dye and mixed, then boiled at 95 ^oC for 10 min. The prepared sample of all groups was loaded equally on SDS-PAGE to resolve. Using the Trans-blot SD semi-dry transfer cell, the sample was transferred from the gel onto the nitrocellulose membrane

(Bio-Rad). After transfer, the membrane was exposed to Tuzin immunized rabbit serum primary antibody at a 1:300 dilution overnight at 4 ºC. Subsequently, incubation was performed with a secondary antibody, (anti-rabbit IgG antibody conjugated with HRP), diluted at a ratio of 1:10000. FemtoLUCENT™ PLUS-HRP Chemiluminescence Detection System visualized the respective protein bands using the Chemidoc system.

3.3.5 Growth curves

The $0.5x10^6$/mL stationary phase cells were seeded in duplicate in a 12-well culture plate and counted on alternate days for 11 days using a hemocytometer and trypan blue to examine the growth rate of WT, Tuzin OE, and Tuzin KD parasites in equal cells (Shailendra Yadav et al 2020).

3.3.6 Scanning Electron Microscopy (SEM) Analysis

The effect of Tuzin overexpression and knockdown on the morphology of the parasite was investigated using SEM. The process involved the collection of promastigote parasites, followed by washing them with PBS and fixing them with 2.5% glutaraldehyde in PBS. The fixed cells were then placed on coverslips coated with L-lysine and left to incubate for 45 minutes. After this time, non-adherent cells were eliminated, and the coverslip was washed using sterile filtered PBS. The cells were then post-fixed with 1% OSO4 in distilled water for 45 minutes, and washed again with PBS and distilled water. To dehydrate the samples, graded series of ethanol (v/v) 25%, 50%, 75%, and 95% were added in ascending order for one minute each, followed by 100% anhydrous ethanol for 10 minutes. The SEM processing of the dried samples involved mounting them on metallic stubs using bioadhesive carbon tape and applying a coating of gold and palladium via sputtering. Imaging was then performed using a scanning electron microscope (Philips XL30 ESEM) (Gluenz *et al.*, 2015)(Kumar *et al.*, 2021).

3.3.7 Immunofluorescence assay to localize the Tuzin protein in parasite

The *Leishmania* parasites were synchronized one day before with 5 mM hydroxyl urea. Subsequent day culture was centrifuged and washed the pellets with 1X PBS two times, then counted the parasites and took $1x10^7$ cells from all groups (DD8 WT, Tuzin OE, Tuzin KD, and DD8+pEGFP-C1 vector) and fixed in the suspension of 4% formaldehyde in PBS at RT

for 20 min. The parasites that were fixed were rinsed 3 times with 1X PBS and left to adhere to the glass coverslips before being air-dried. Following air-drying, ice-cold methanol (-20 ºC) was added and allowed to sit for 5 minutes, after which it was blocked for 30 minutes with 1% BSA. The specimen was subjected to incubation with an anti-Tuzin primary antibody (Rabbit serum) at a dilution of 1:200 for one hour. Afterward, the sample underwent four washes using 1% PBS with 0.1% Tween 20 and was then subjected to incubation with a secondary antibody (Alexa Fluor 555-conjugated anti-Rabbit IgG antibody) at a 1:200 dilution. The coverslips were washed four more times with 1% PBS containing 0.1% Tween 20. Finally, the coverslips that were ready for use were affixed onto glass slides that had been cleaned, utilizing mounting media containing DAPI within Vectashield. Subsequently, they were observed using a confocal microscope to observe the fluorescence (Veronica *et al.*, 2019).

3.3.8 THP-1 culture and differentiation

The National Center for Cell Science (Pune, India) provided THP-1 suspension cells, which were cultured in sterile 25 cm^2 culture flasks containing RPMI 1640 media with 10% heat-inactivated FBS and 1% penicillin-streptomycin. The flasks were maintained at 37 °C and 5% CO_2, with the cells maintained at a density of $1x10^6$ cells/mL and the culture media was replenished every two to three days. In order to induce infection, the THP-1 cells were cultured in a 6-well plate with a density of $1x10^6$ cells/mL in complete media, followed by treatment with 25 g/mL of PMA from Sigma-Aldrich. Afterward, the cells were subjected to a 24-hour incubation period at 37°C and 5% CO_2 to activate them. This process differentiated the THP-1 cells into macrophage-like cells and improved their phagocytic abilities (Gatto *et al.*, 2020). Prior to culturing the cells, their viability was assessed using Trypan Blue. Upon being stimulated with PMA, the cells exhibited characteristics of macrophages, including changes in morphology and attachment to the culture plates**.**

3.3.9 Phagocytic activity to determine the infectivity

Before infection, the sterile coverslips were placed in a 6-well culture plate. The experiment involved seeding THP-1 cells in a culture plate with a concentration of $1x10^6$ cells/mL in complete RPMI media. These cells were then treated with PMA (25 ng/mL) and incubated

for 24 hours at 37°C in CO_2 incubator, during which they developed into macrophage-like phenotypes. To remove nonadherent cells, the cells were washed with incomplete RPMI media twice. Then, new media was added, and the macrophages were infected with stationary phase parasites from different groups (DD8 WT, Tuzin OE, Tuzin KD parasites) at a 1:10 ratio ($1x10^7$ cells). The cells that had been infected were placed in a CO_2 incubator at a temperature of 37 ºC with 5% CO_2 for 8 hours. Any parasites that had not entered the cells were removed by washing with PBS, and the cells that were still infected were left to incubate in fresh medium for another 16 hours. Once this incubation was complete, the media was removed and the cells were washed several times with filtered 1X PBS. The coverslips were fixed on the slide using nail polish and then processed for Giemsa stain (Himedia) (Dayakar *et al.*, 2016). The Leica light microscope was used to count the number of infected macrophages and the quantity of amastigotes present within 100 macrophages. The phagocytic index was determined using the following formula (Santulli-Marotto *et al.*, 2015).

PI = (Total number of engulfed cells/Total number of counted MΦ) X (Number of MΦ's containing engulfed cells/Total number of counted MΦ) X 100

Chapter: IV
Results and Discussion

Objective 1: To evaluate the Tuzin protein as a candidate for the potential diagnostic marker for Visceral Leishmaniasis

4.1 Cloning and in silico analysis of *L. donovani* Tuzin

The *L. donovani* Tuzin gene was identified in NCBI with the gene id: LDBPK_080750. On chromosomal number 8, there is a single open reading frame gene with a length of 993 bp identified as the putative Tuzin sequence of *L. donovani*. The 334 amino acid residue polypeptide with a molecular mass of approximately 38 kDa is encoded by the tuzin gene. The PCR product of Tuzin was cloned into pET-28a vector **(**Figure 4.1.1**)**, generating an expression construct for expression of N-terminally His-tagged *Ld*Tuzin protein.

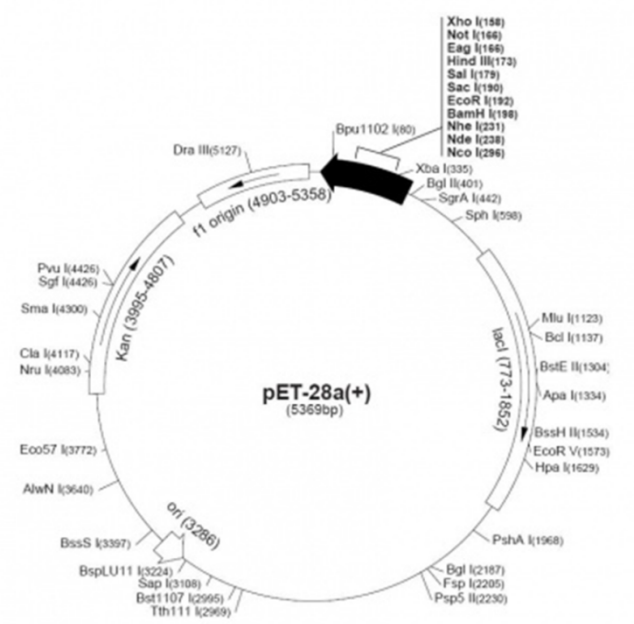

Figure 4.1.1: pET 28 a vector (Add gene)

The Multiple sequence alignments of *L. donovani* Tuzin (XP_003858638.1)with *L. infantum* (XP_001463413.1), *L. major* (XP_001686384.1), *Leishmania braziliensis* (XP_001564521.2) *and Trypanosoma cruzi* (RNC59122.1) (Figure 4.1.2). The similarity was found in 90.07% of *L. infantum*, 45.98% of *L. major*, 40.24% of *L. braziliensis, and* 26.26% of *Trypanosoma cruzi* (Table 4.1.1). The Tuzin protein may be used as a distinct protein for diagnosis and vaccination candidates because it was not discovered in humans.

Table 4.1.1 compares *L. donovani* Tuzin protein sequence with the Tuzin sequence from other species

S.No.	Gene name	Organism	Identity	Length	Accession
1	Putative tuzin	*Leishmania infantum*	99.07%	342	XP_001463413.1
2	Putative tuzin	*Leishmania major*	45.98%	559	XP_001686384.1
3	Putative tuzin	*Leishmania braziliensis*	40.24%	584	XP_001564521.2
4	Tuzin	*Trypanosoma cruzi*	26.26 %	574	RNC59122.1

Figure 4.1.2: Multiple sequence alignment of Tuzin sequences from *L. donovani* with *L. infantum, L. major*, *Leishmania braziliensis and Trypanosoma cruzi*.

The Tuzin protein's location was discovered using an *in silico* analysis using the PSIPRED service. The findings suggested that the Tuzin protein is a transmembrane protein where the N-terminal is situated in the cytoplasm and the C-terminal is positioned in the extracellular area (Figure 4.1.3 A & B).

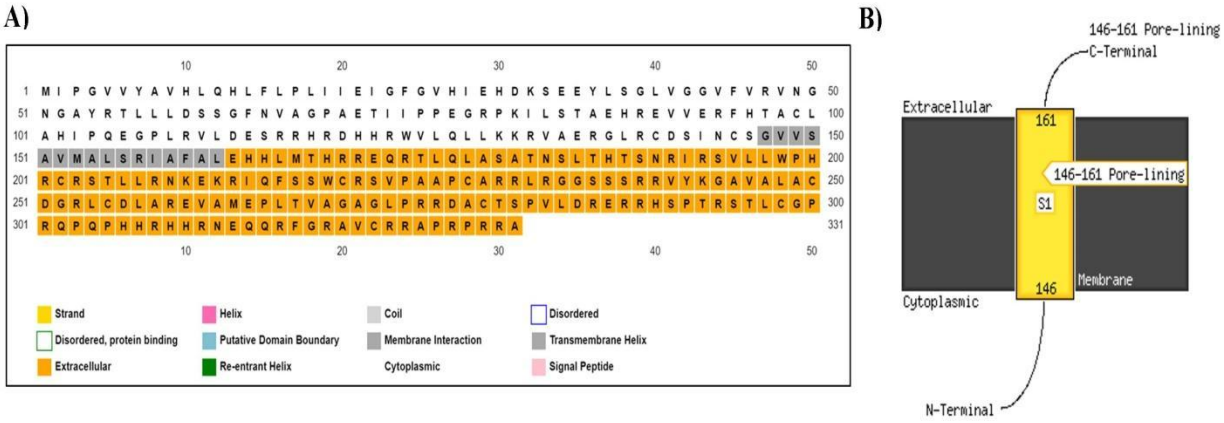

Figure 4.1.3: Tuzin protein localization using in silico technique: (A) the grey color AA was used to represent the transmembrane portion, the yellow color AA was used to represent the extracellular portion, and the colorless portion represented the cytoplasmic portion. (B) A schematic representation of Tuzin localization was created using the PSIPRED server (PSIPRED Workbench (ucl.ac.uk)).

4.1.2 Generation of pET28a-LdTuzin construct

Gradient PCR was performed in 12.5 µL reaction volume to find the optimal annealing temperature (Ta). At Ta of 62 ºC maximum amplification of the expected band size of ~ 993 bp of *Ld*Tuzin was observed (Figure 4.1.4A). The amplified product was purified from 1 % agarose gel. The insert (*Ld*Tuzin) and vector pET28a were double digested using *BamHI* and *HindIII* enzymes, and ligation was performed. After transforming the ligated mixture into competent *E. coli* DH5α cells, a few colonies were selected for screening. In colony PCR, other than one colony, all colonies were found to be positive (Figure 4.1.4B), which showed the amplification of the expected band size of *Ld*Tuzin (~ 993 bp). Clone 1 was selected and subjected to double digestion using *BamHI* and *HindIII* for further confirmation. The clone released a ~ 993 bp band of *Ld*Tuzin along with a pET28a vector

backbone of ~ 4.5 kb, as shown in Figure 4.1.4C. Finally, the positive clone of pET28a-*LdTuzin* was confirmed by the sequencing. The confirmed clone was transformed into competent *Escherichia coli* Rosetta (DE3) strain cells by heat shock method.

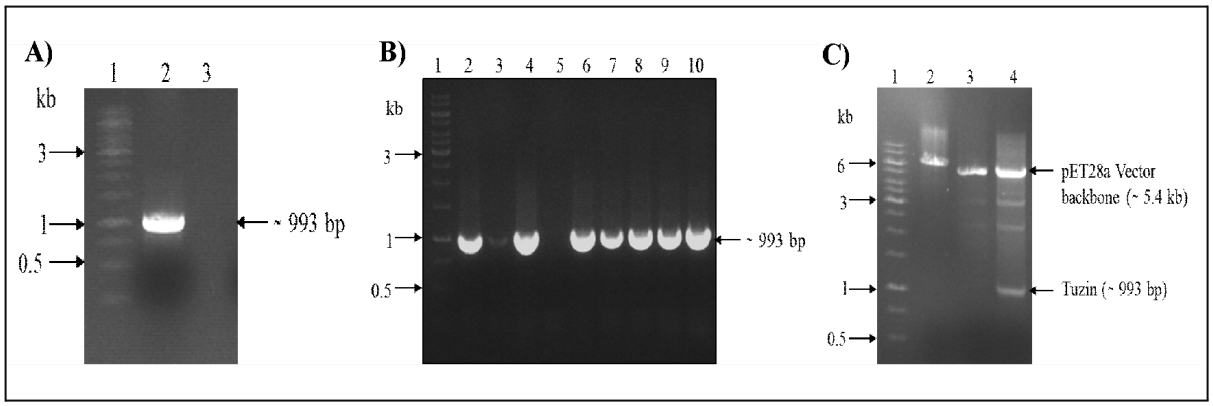

Figure 4.1.4: Construction of pET28a−LdTuzin construct. 1% of Agarose gel showing (A) Amplification of the Tuzin gene from *L. donovani* gDNA by PCR, Lane1: DNA ladder, Lane 2: Tuzin gene amplification, and Lane 3: Negative control (without genomic DNA). (B) Screening of *L. donovani* pET28a−LdTuzin clones by colony PCR; Lanes 1: DNA ladder, lane 2&3: Positive control (with genomic DNA) and negative control respectively; Lanes 4-10: PCR amplified products of colony 1 to 7 respectively. (C) Confirmation of positive clones by double digestion with *BamHI* and *HindIII*. Lanes 1-4: DNA ladder, Single digested clone, single-digested empty vector, and double-digested clone, respectively.

In order to express the recombinant protein, the Tuzin gene was successfully cloned into the pET-28a vector, verified by double digestion, and effectively transformed into *E. coli* Rosetta (DE3) competent cells.

4.1.3 Expression, purification, and confirmation of recombinant Tuzin

The expression was checked by using different concentrations of IPTG and different temperatures, and induction time points. The protein expressed when induced by 0.5 mM IPTG for at 25 °C for 24 h shown in Figure 4.1.5A. An anti-His-Tag antibody was utilized for performing Western blotting, after loading the crude lysate from purified, induced, uninduced, and wild-type protein onto a 12.5% SDS-PAGE as mentioned in the methodology. We got a specific band in IPTG-induced cell lysate (Figure 4.1.5B).

The protein was assessed to identify if it was present in soluble or insoluble fractions. Our analysis showed that the protein was located in the insoluble fraction,

specifically in the inclusion bodies, which was confirmed through SDS-PAGE (Figure 4.1.5C). Subsequently, we purified the protein using a Ni-NTA affinity chromatography column under denaturing conditions, followed by dialysis as per the protocol mentioned above. Upon loading the purified protein on SDS-PAGE, we observed no non-specific clear band **(**Figure 4.1.5 D**)**.

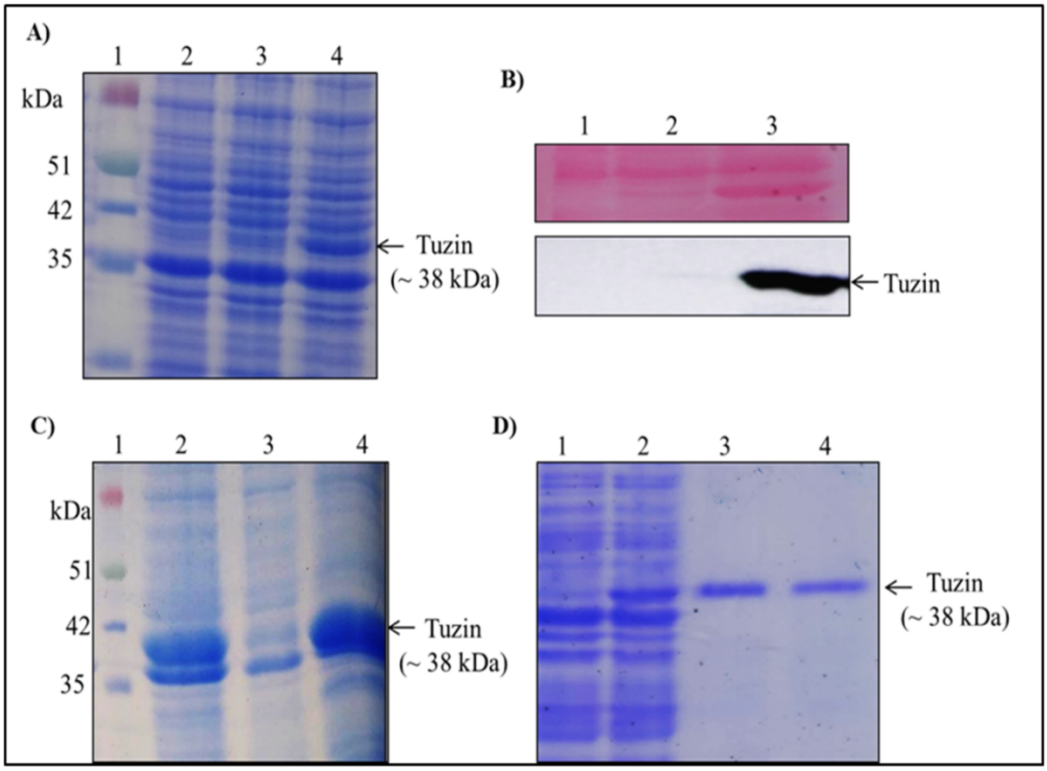

Figure 4.1.5: Induction, expression, and purification of recombinant Tuzin protein. (A) Coomassie blue staining of 12.5 % SDS-PAGE showing expression of recombinant Tuzin protein in *E. coli*. Rosetta (DE3) with 0.5 mM IPTG induction at 25 °C for 24 h. Lane 1: Pre-stained protein ladder, 2: wild-type cell lysate, 3: uninduced cell lysate, and 4: 0.5 mM IPTG-induced cell lysate. (B) Western blot: the resolved protein sample was separated in SDS-PAGE, then transferred to PVDF membrane, and performed western blot using anti-His Tag antibody. Lane 1: wild type, lane 2: uninduced, and lane 3: 0.5 mM IPTG-induced lysate. (C) Fractionation of Expressed Rosetta (DE3) lysate; lane 1: Pre-stained protein ladder, lane to sonicated crude lysate of expressed cells, 2: soluble fraction (supernatant) and 3: inclusion bodies (pellet) and (D) purified Tuzin protein; Lane 1: uninduced and lane 3: 0.5 mM IPTG induced lysate, 3: purified protein and 4: dialyzed protein

The expression of the recombinant protein was achieved at 25 °C with 0.5 mM IPTG, resulting in the successful production of LdTuzin with a molecular weight of approximately 38 kDa, which matches the expected theoretical molecular weight. Subsequently, the protein was verified via western blot utilizing an anti-His tag antibody, purified under denaturing conditions, dialyzed, and finally quantified through the BCA method.

4.1.4 Antibody generation against Tuzin and confirmation by western blot

After dialysis, the protein was purified and an antibody against Tuzin was generated in mice, following the procedure described previously. Subsequently, blood was drawn and left undisturbed at RT for 10-15 minutes to allow clotting. After centrifuging the serum at 3000 x g for 10 minutes at 4 ºC, it was collected into a new tube and kept at a temperature of -80 ºC until its utilization.

As mentioned in the methodology, the protein samples were moved from SDS-PAGE onto a PVDF membrane and carried out in western blotting. Figure 4.1.6 shows western blot results of crude induced protein and purified protein and got a band in both samples with anti-Tuzin antibody (Tuzin immunized mice serum); it confirms that the antibody against Tuzin was successfully raised, then we want to check the expression of Tuzin in *L. donovani* parasite, for that the crude *leishmania* parasite lysate was loaded on SDS-PAGE, then performed the western blot, and we found the band at 38 kDa size (Figure 4.1.6B) it confirms that Tuzin was expressing in *leishmania* parasites.

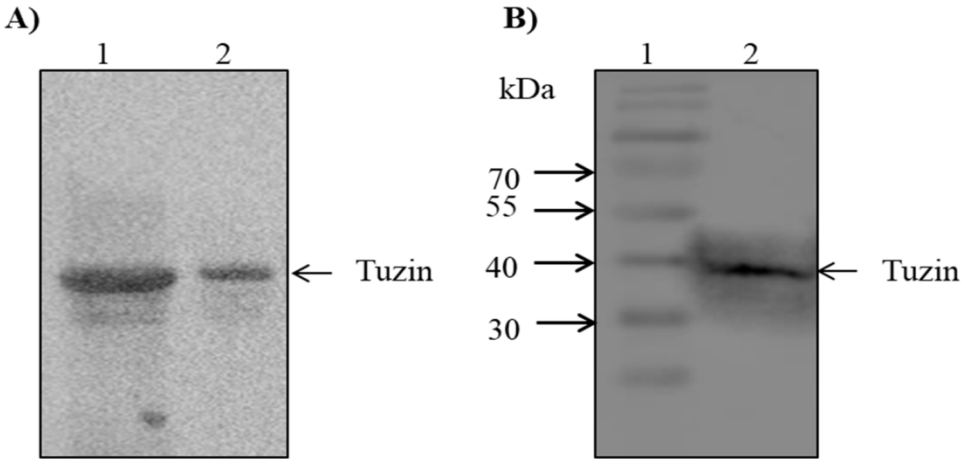

Figure 4.1.6: Western blot analysis by anti-Tuzin antibody: (A) Lane 1- Recombinant expressed crude protein, and Lane 2- Purified protein (B) Lane 1 Protein ladder, and lane 2: *Leishmania donovani* crude lysate

4.1.5 Confirmation of Tuzin in *L. donovani* by confocal microscopy

The expression of Tuzin was assessed in both stages of *L. donovani* using an immunofluorescence assay. The use of methanol permeabilization enabled the binding of both primary and secondary antibodies to Tuzin. Control (without anti-Tuzin antibody) exhibits no FITC fluorescence in either the promastigote or amastigote phases (Figure 4.1.7 A&C). But in the presence of an anti-Tuzin antibody (immunized mice serum) at a 1:300 dilution, FITC fluorescence was observed in both stages (Figure 4.1.7 B&D), indicating that the Tuzin protein was probably localized at the membrane in the parasite.

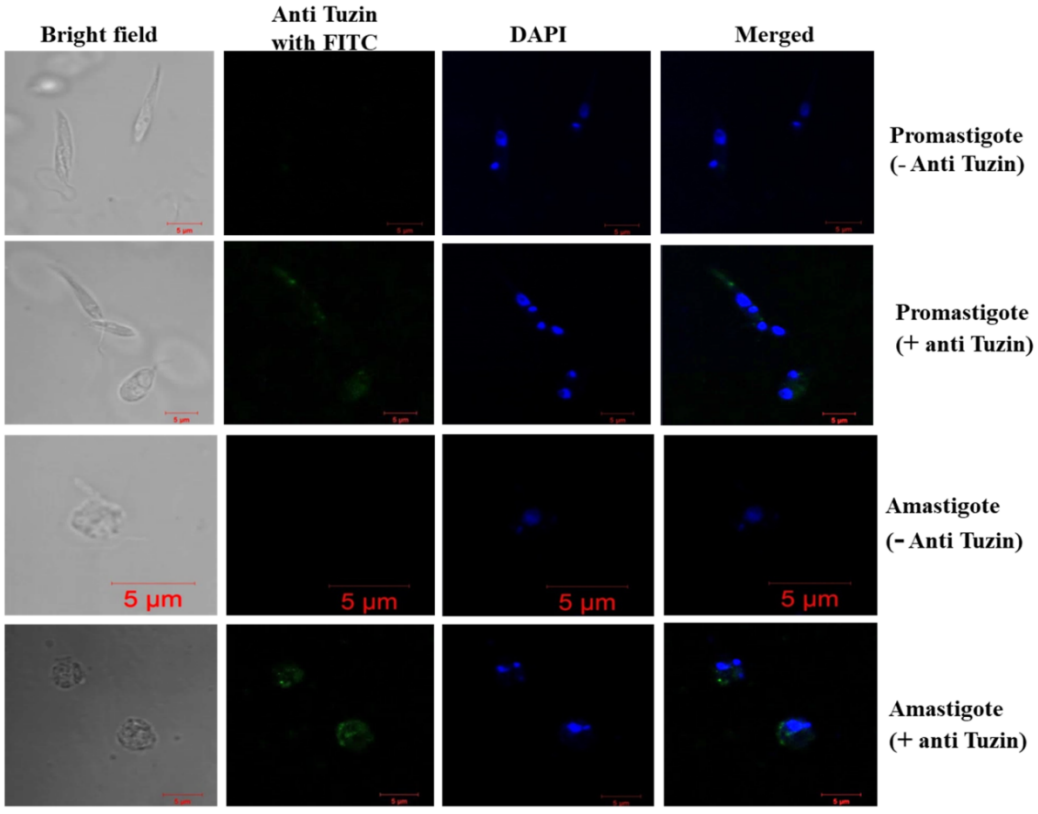

Figure 4.1.7: A) Immunofluorescence assay for protein localization: Panel 1- Bright field; Panel 2- anti-Tuzin with FITC fluorescence; Panel 3- DAPI fluorescence; Panel 4- merged. A and B- Promastigote control (without anti-Tuzin antibody) and test (with anti-Tuzin antibody), respectively; C&D- Amastigote control and test, respectively.

4.1.6 Evaluation of Tuzin protein as a diagnostic marker for the detection of VL

Despite efforts to find novel diagnostic techniques, a procedure with adequate VL diagnosis effectiveness still needs to be improved. Still Microscopy method is Gold standard for VL which is invasive process. rK-39 strip test is the only test is Non-invasive process but it lacks of high sensitivity and specificity and giving 15-20% false positive results, Therefore, it is essential to adopt reliable techniques that are affordable, practical to apply in the field, and for disease control. Tuzin is a rare trans-membrane protein with immunogenic properties. Tuzin could play a part in *Leishmania* pathogenesis and serve as a possible option. The antigen (150 ng/well Tuzin) was diluted in 0.1 M bicarbonate buffer (pH 9.6) and added 100 µL at a time to the ELISA plates, and ELISA was carried out using various patient serum on Day 0 (n = 100), Day 15 (n = 51), Day 30 (n = 50), and Day 6 of treatment (n = 25), along with endemic control (n = 50), healthy control (n =25) and different disease patient serum (n=25). The reading on the plate at 450 nm was measured using a microplate reader. One-way ANOVA (Tukey's multiple comparisons) was used to generate the results using Graph Pad Prism. According to the findings, compared to other groups, VL patients had anti-Tuzin antibody titers that were significantly higher. The level of anti-Tuzin antibody titer was significantly reduced upon the treatment (Figure 4.1.8). The cutoff value, specificity, and sensitivity were calculated using the above-mentioned formula in methodology and found a cutoff value of 0.3372.

Table 4.1.2: Accuracy of Enzyme linked immunosorbent assay (ELISA)

Accuracy	ELISA	95% CI
Sensitivity	85.00%	76.47% to 91.35%
Specificity	92.00%	73.97% to 99.02%

The ELISA results show that the anti-Tuzin antibody titer was significantly higher in the VL patient serum than in the treated patient. The measurement of sensitivity and specificity of Tuzin protein against anti-Tuzin antibody in human patient serum was 85% and 92 %, respectively; it inferred that the Tuzin protein could be a potential diagnostic marker in case of active Visceral Leishmaniasis. This data suggested further studies to increase the sensitivity and specificity of Tuzin as a diagnostic marker.

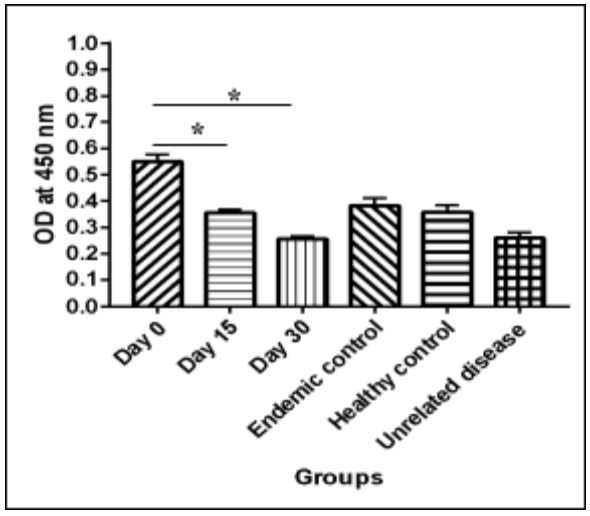

Figure 4.1.8: Evaluation of Tuzin potency by ELISA: The multiple comparision of one way ANOVA (Newman-Kelus Multiple comparison test). It shows mean significance of $p<0.01$ at $p<0.05$.

Tuzin protein's immunogenic properties led to the selection of this antigen as a potential diagnostic candidate in the current investigation. The Tuzin protein's location was found using an in silico investigation with the PSIPRED program. The results demonstrated that the Tuzin protein was transmembrane, with the protein's cytoplasmic N-terminus and extracellular C-terminus, respectively. The Tuzin gene from *Leishmania donovani* was cloned into the pET28a vector, followed by transformation into *E. coli* Rosetta (DE3) strains to express the recombinant Tuzin protein. The expressed protein was purified, and antibodies were raised against it. Finally, the presence of the Tuzin protein was confirmed using western blot analysis.

Additionally, the Tuzin protein was expressed in both stages of the *L. donovani* parasite, according to localization studies of tuzin in parasites. Using ELISA to test the recombinant Tuzin protein's diagnostic capacity with VL sera, the results revealed that the anti-Tuzin antibody titer was much more significant in the serum of VL patients than in that of treated patients. Tuzin protein may be possible to diagnose active VL because it showed 85% and 92% sensitivity and specificity against anti-Tuzin antibodies in human patient serum, respectively. These findings recommended additional research to improve the sensitivity and specificity of Tuzin as a diagnostic marker.

Objective 2: To evaluate the immune response induced by Tuzin protein in *L. donovani* challenged BALB/c mice

4.2.1 Measurement of spleen size and parasite burden

In visceral leishmaniasis, Splenomegaly and Hepatomegaly are the hallmarks of the disease, so we collected the spleen, measured the size of all groups, and found that Tuzin immunized mice spleen size was small when compared with infected control (Figure 4.2.1A and B). This result inferred that the Tuzin vaccine induces parasite elimination. Then spleen biopsies were used to prepare the glass slides by dabbing to determine the parasite burden in the spleen; Giemsa was used to stain the prepared slides. The number of intracellular amastigotes parasites was counted for 100 macrophages of each mouse. We observed that the infected control mice had a significantly higher parasite load in comparison to mice immunized with Tuzin protein ($P<0.05$) **(**Figure 4.2.1C). The results showed that the Tuzin-vaccinated mice could clear the parasites more efficiently than its control, suggesting that Tuzin had a protective role in these mice.

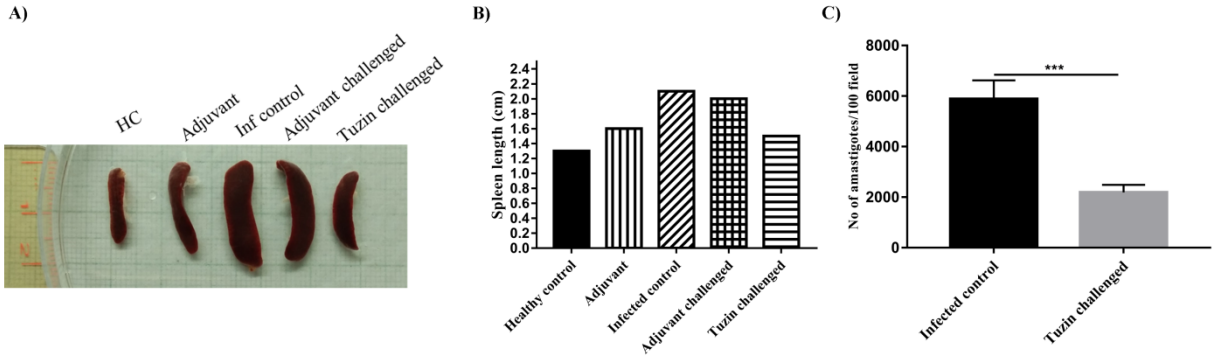

Figure: 4.2.1: Measurement of spleen size and parasite load: A) spleens from all the different mice groups were isolated and measured by using scale, (B) Bar graph of spleen size in length, and (C) Intracellular amastigote in spleen using Giemsa staining: The graph shows the amastigote numbers for 100 macrophages. The values are showing significance difference between infected control and Tuzin challenged group were calculated using unpaired student t-test (***$P<0.05$**)**.

4.2.2 Estimation of parasite load by q RT PCR

In order to execute RT-PCR with appropriate kDNA primers, the genomic DNA was extracted from mouse liver homogenate. The standard curve was plotted with the various dilutions of genomic DNA to determine the parasite burden as mentioned in methodology. In qRT-PCR, equal amounts of DNA from different groups of mice were used as a template. The parasite load was determined for each group using GraphPad prism. A standard curve was created using the Ct values of *L. donovani* gDNA at different concentrations (Figure 4.2.2). The parasite count in each group was determined by calculating the linear regression of the Ct values and interpolating the Ct value of the Adjuvant infected, infected, and Tuzin vaccinated groups with the x value. The results of the qRT-PCR analysis indicated a significant reduction in parasite load in the Tuzin-challenged mice group compared to the infected control group (Figure 4.2.2 B).

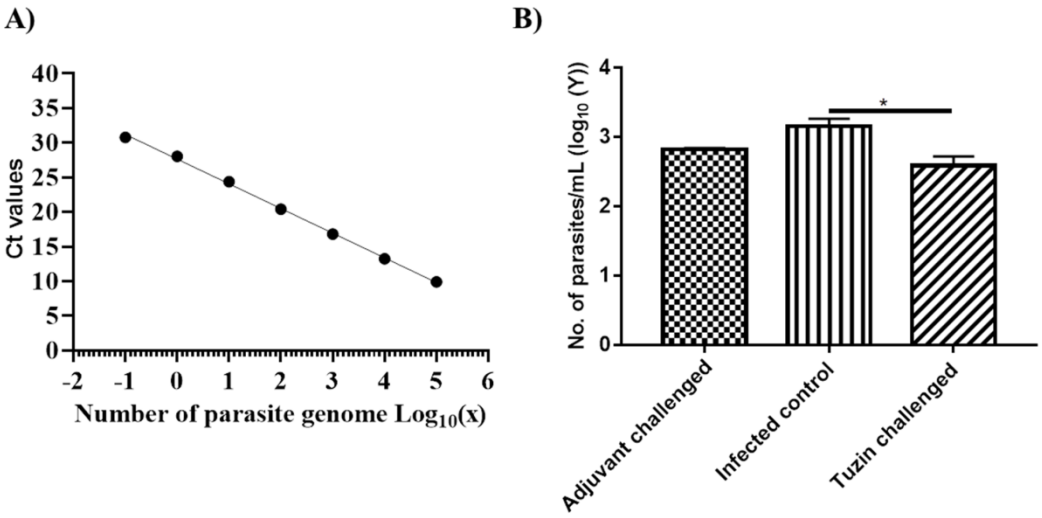

Figure 4.2.2: Parasite load by RT PCR: (A) Standard curve (B) Parasite load by qRT-PCR: The significance difference between infected control and Tuzin challenged group were calculated using unpaired student t-test (*P<0.05).

4.2.3 Quantitative analysis of serum IgG1 and IgG2a mediated Humoral immune response of Tuzin

We examined the humoral immune response produced in the vaccinated animals and compared it to that of the control mice. Sera from all groups of mice were tested by ELISA, following the protocol, for *Leishmania*-specific IgG1 and IgG2a titers eight weeks after the

challenge. Compared to the control groups, tuzin-vaccinated mice had more significant IgG2a titers (Figure 4.2.3A), whereas the IgG1 titers were seen to be less comparable in the mouse groups that had received the Tuzin vaccination (Figure 4.2.3b). The Tuzin-vaccinated animals had greater levels of IgG2a antibody; it can be shown that during parasite infection, the immune responses were biased towards a cell-mediated immune response. The data presented here are mean ± SD for each group. Infected control and Tuzin-challenged groups (***P<0.05) were calculated using an unpaired t-test.

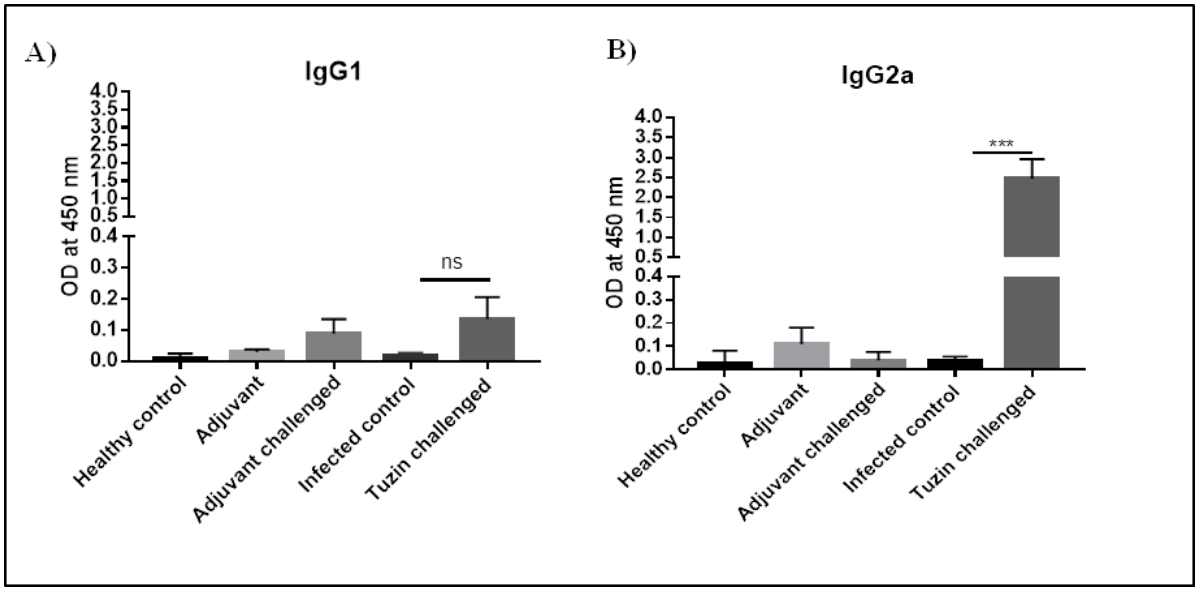

Figure 4.2.3: ELISA for quantifying IgG1 and IgG2a: Serum from different mice was collected at eight weeks post-infection. (A) Level of IgG1. (B) Level of IgG2a. The data are presented as the mean ± SD for each group. Significant differences between infected control and Tuzin immunized (*** P<0.05) were calculated using an unpaired t-test.

4.2.4 Tuzin vaccination enhanced the production of NO and ROS in BALB/c mice

Macrophage activation and generating harmful oxygen metabolites, such as superoxide anion (O^{-2}), Nitric oxide (NO), and hydrogen peroxide (H_2O_2), which kills the parasites, are necessary to remove the *leishmania* from the macrophages. Our results implied that the anti-leishmanial cell-mediated immunity (CMI) responses were responsible for Tuzin protein immunization's protective effects against VL in mice. The supernatant was collected from the splenocytes culture to estimate the NO level, and cells were used for ROS analysis

by flow cytometry, as mentioned above protocol. The Tuzin-vaccinated mice group showed an increased NO production trend upon stimulation with CLA compared to infected groups (Fig.14 A). The ROS level was estimated by flow cytometry, and the graph was plotted with MFI and found that the ROS level in Tuzin immunized mice group showed an increased trend than the infected control group (Fig 14B).

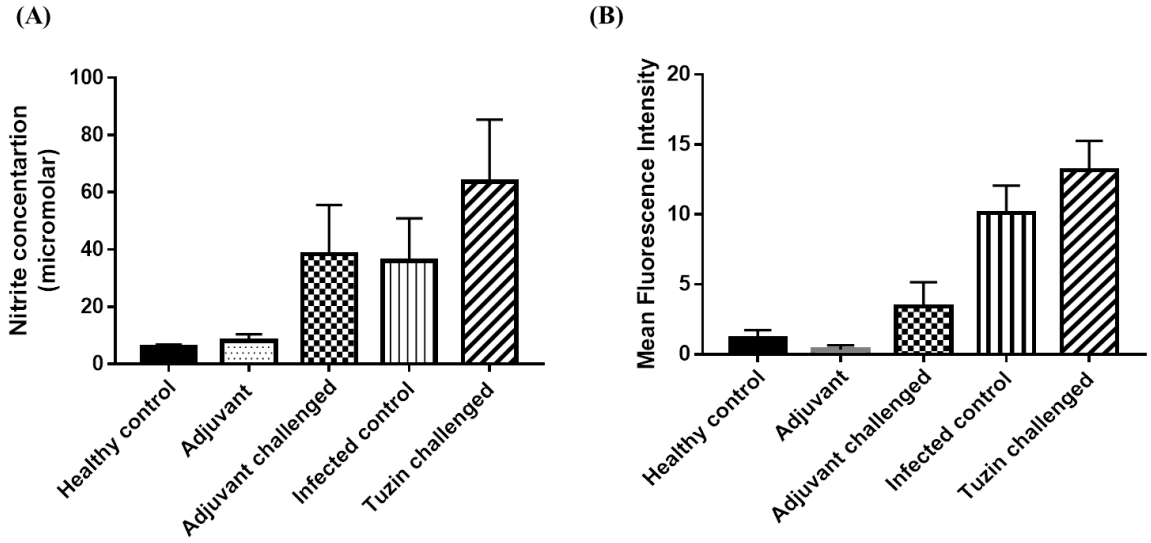

Figure 4.2.4: Determination of Nitric oxide (NO) and reactive oxygen species (ROS): Splenocytes from a different group of mice were cultured in the presence and absence of CLA. (A): Production of nitric oxide at eight weeks post-challenge; the nitrite level of the sample was calculated using standard curves made from various concentrations of $NaNO_2$. (B): The ROS estimation at eight weeks post-challenge. The green fluorescence of H_2DCFDA was measured using flow cytometry, and Mean Fluorescence Intensity (MFI) was represented as a bar graph.

4.2.5 Tuzin prevents granuloma formation

The T cells infiltrate and grow into a granuloma during the infection, which contains amastigotes and is eventually eliminated. Histological analysis of liver in different group of mice did at 8 weeks post infection. The granulomas were counted per 50 fields and found the significant difference between infected control and Tuzin challenged group calculated using unpaired student t-test (*$P<0.05$). In Tuzin challenged group showed a significant decrease of size and less numbers of granulomas compared to infected control (Figure 4.2.4).

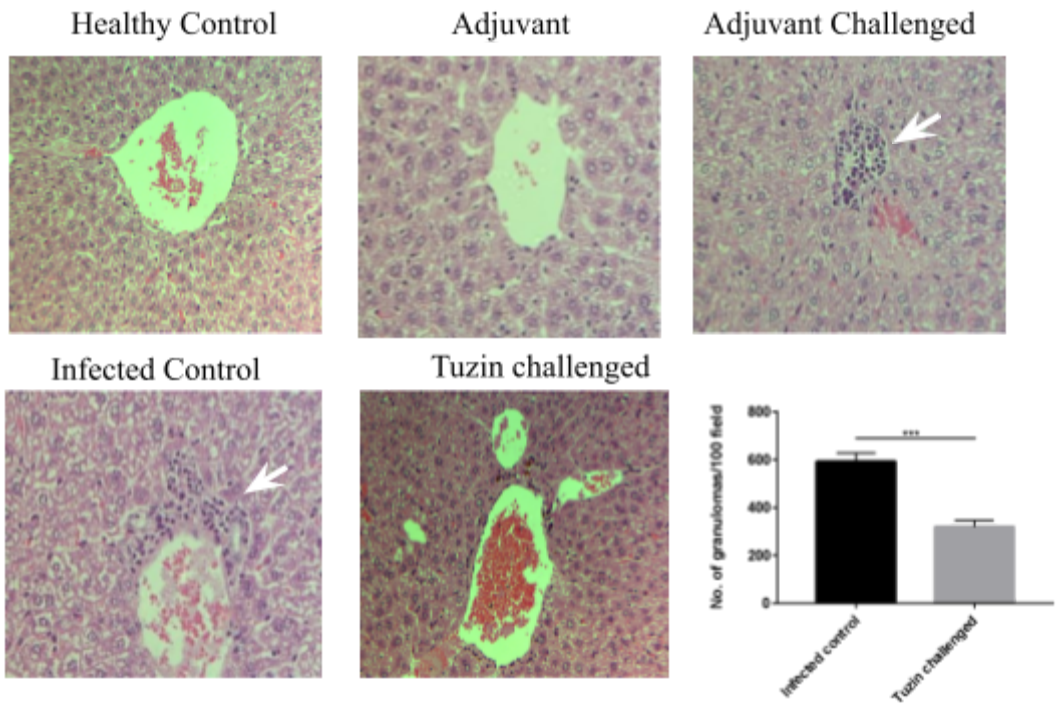

Figure 4.2.5: Histological analysis of liver and spleen in different group of mice: Eight weeks after infection, a histological analysis was conducted and the results were presented in the form of a bar graph. The graph revealed that the group that was challenged with Tuzin displayed a significantly lower number of granulomas as compared to the infected control group.

4.2.6 Tuzin down regulate the IL-10 cytokine to improve the host immune response

The quantitative real-time PCR of mice-specific cytokine genes was performed to know the gene expression level of various cytokines in different experimental groups of mice. *Leishmania* pathogenesis and host defense depend heavily on cytokines. In order to recover from visceral leishmaniasis (VL), T-cell immunity must be induced, preferably through Th1 immune responses. The activation of T cells by IL-12 leads to the production of IFN-γ, which brings about the death of parasites through the action of NO. On the other hand, the presence of IL-10+ regulatory T cells (Tregs) is linked to the development of VL in humans, as they decrease the anti-parasitic effect of M1-type macrophage activation and Th1 response. This is in contrast to the abundance of Th2 type cytokines, such as IL-10, TGF-β, and IL-4. In the progression of the VL clinical disease, higher levels of IL-10 are more

critical than a deficiency in IFN-γ. In killing the intracellular parasites, IL-10 substantially resists IFN-γ mediated macrophage activation while somewhat inhibiting IFN-γ production. The analysis of cytokines showed that the expression of the anti-inflammatory cytokine IL-10 was noticeably decreased in the Tuzin vaccinated group in comparison to the control group (Figure 4.2.6A). While the IFN-γ level remained unchanged (as shown in Figure 4.2.6B), the presence of IL-10 cytokine is essential for the survival of parasites within the macrophages of the host organism. The result is indicating that Tuzin suppresses IL-10 functions by promoting the protective immunity in mice.

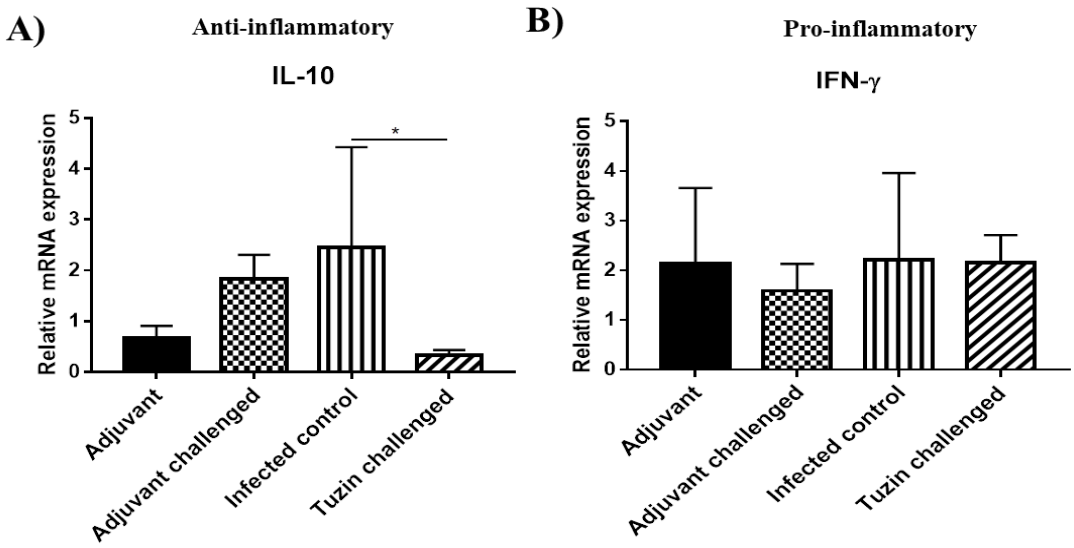

Figure 4.2.6: The relative expression of cytokines at mRNA level using RT-qPCR: A) level Anti-inflammatory cytokines (IL-10) and (B) level of Pro-inflammatory cytokine (IFN-γ)

4.2.7 Vaccination with Tuzin significantly increases the IFN- γ/IL-10 ratio

The survival of intracellular parasites during visceral leishmaniasis is determined by the ratio of IFN-γ to IL-10. If the ratio is low, the parasites are able to survive. Conversely, when the ratio of IFN-γ to IL-10 is elevated, the immune response switches to the Th1 immunological phenotype (Jajarmi *et al.*, 2019). The Tuzin vaccinated group showing significant increase in IFN-γ/IL-10 ratio (**Figure 4.2.7**) denotes that the immune response towards Th1 type promoting the protective immunity.

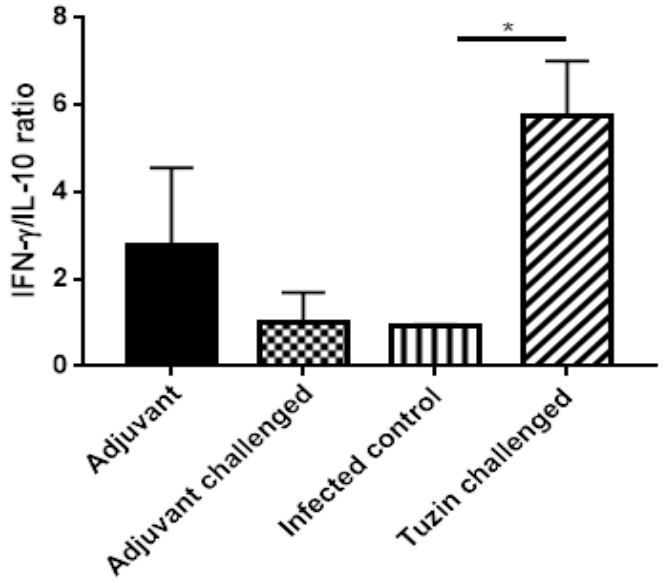

Figure 4.2.7: Determination of IFN- γ/IL-10 ratio in mice splenocytes

4.2.8 Ag-specific T cell proliferation response in Tuzin vaccinated BALB/c mice

In order to determine if T cells can undergo proliferation after being exposed to *Leishmania* antigen again, spleen cells from experimental groups of mice were isolated, labeled with CFSE, stimulated with *Leishmania* antigens, and incubated for five days at 37 °C in a CO_2 incubator. Flow cytometry was used to analyze the CFSE profile of cells that had been stimulated with antigens for five days, after being stained with anti-CD3, anti-CD4, and anti-CD8 antibodies (Figure 4.2.8). FlowJo analysis showed that Tuzin-immunized challenge mice exhibited lower proliferative capacity in all CD3+ T cells, including CD4 and CD8, compared to the infected control and uninfected adjuvant group. There was no notable disparity observed in the proliferation of T cells between the groups that received Tuzin vaccination and the ones that were infected and served as a control. Yet further research is required to comprehend the underlying mechanism.

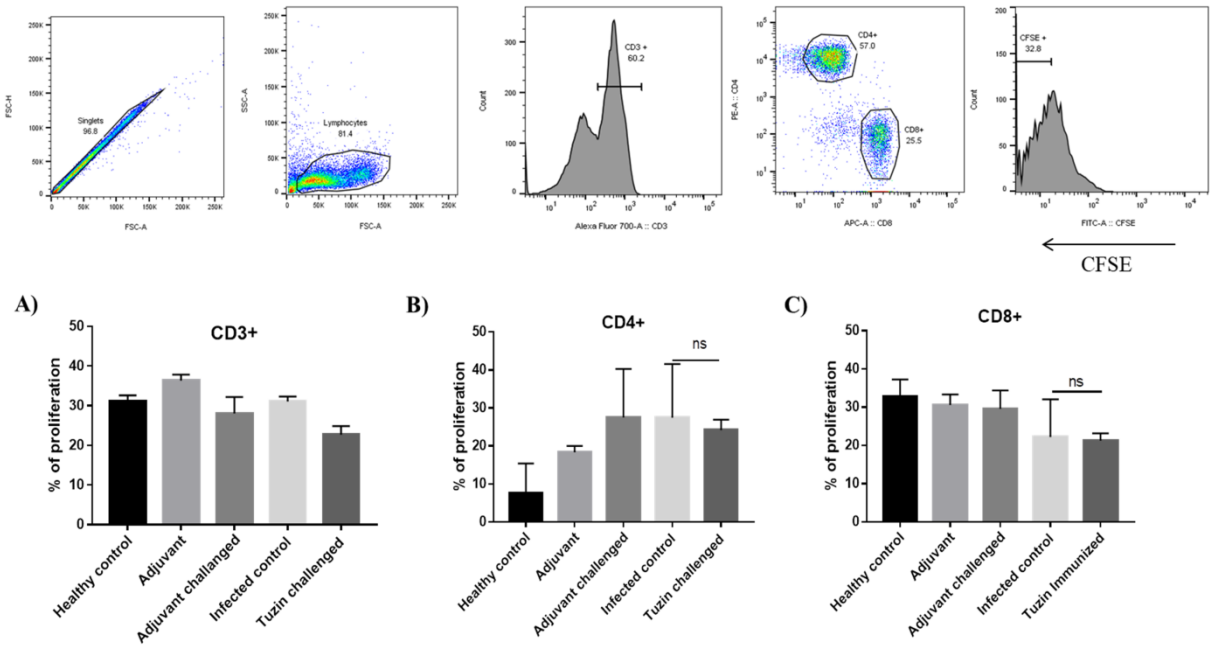

Figure 4.2.8: T cell proliferation of antigen-specific T cells after eight weeks of post-challenge: The cells were analyzed by flow cytometry, in which CFSE dilution on particular gated cells was used as the readout for Ag-specific proliferation (A) Percentage proliferation of CD3+, (B) Percentage proliferation of CD4+, and (C) Percentage proliferation of CD8+.

Despite significant efforts to develop a suitable vaccine for the prevention and treatment of leishmaniasis, the disease continues to pose a threat to human life. It is essential to identify potential candidates that can stimulate protective responses against *Leishmania* to develop vaccines and prevent this disease (Kedzierski, 2010). Research indicates that resistance against leishmaniasis is provided by Th1 cytokines, whereas Th2 cytokines worsen the condition (Reiner and Locksley, 1995). Vaccinations that consistently favor Th1 responses over Th2 responses have been found to control the disease in susceptible mice (Kemp *et al.*, 1993). In murine visceral leishmaniasis, the deficiency of IL-12 production and the promotion of IFN-γ have been linked with resistance to infection in experimental and clinical VL, respectively. Conversely, IL-4, a Th2 cytokine, was observed to be prevalent in the blood samples of VL patients, and susceptibility was found to be associated with IL-10 (Lakshmi *et al.*, 2014). The mixed cytokine responses involved in immune reactions to leishmaniasis, as with any infection, are intricate and multifaceted (Kumar and Nylén, 2012). Therefore, a Th1 polarized immune response may be a better indicator of a

protective antigen than the absence of a Th1 or Th2 response (Basu *et al.*, 2009). *Leishmania donovani* is a type of protozoan that invades tissue macrophages and has a preference for infecting normal mice such as BALB/c and C57BL/6. The ability of these mice to develop resistance against *L. donovani* relies on the activation of T cells, the production of cytokines of the Th1 cell type, and the activation of mononuclear phagocytes (Murray, 2001). The figure 4.2.9 showing the overview of immune response from *L. donovani* infected BALB/c mice.

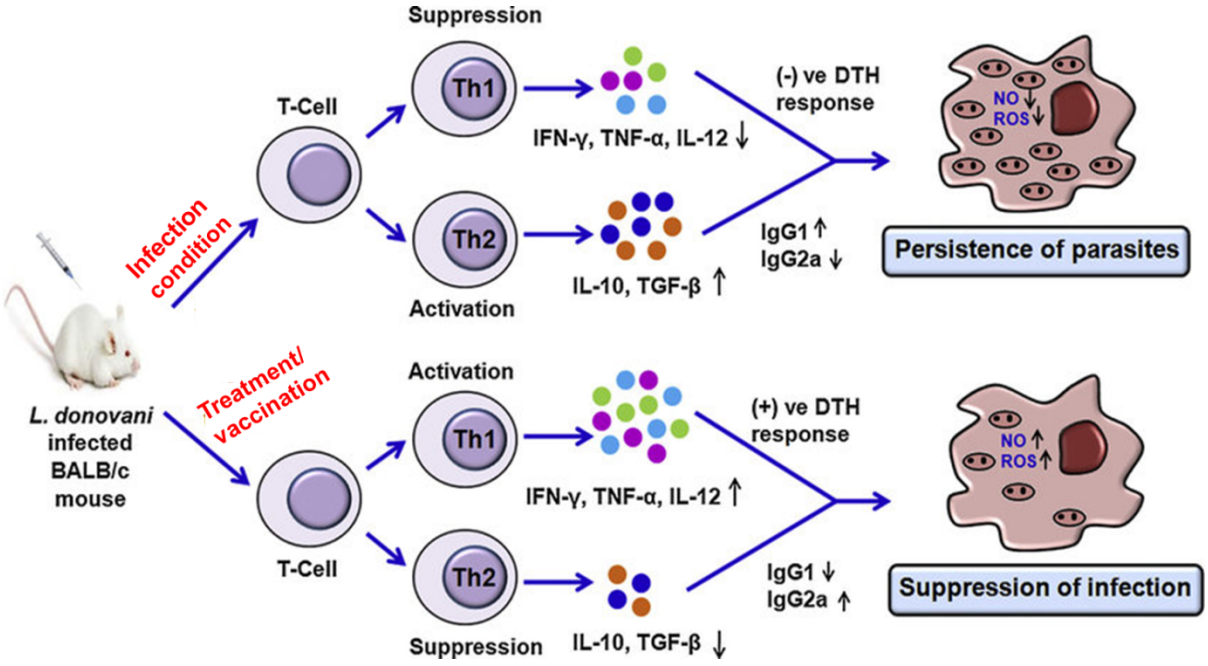

Figure: 4.2.9: Overview of immune responses from *Leishmania donovani*-infected BALB/c mice throughout infection establishment and infection eradication following immunization (Pramanik *et al.*, 2019).

Due to its high immunogenicity, as determined by the VaxiJen v2.0 server, the Tuzin protein was selected as the antigen for the current vaccine investigation. It has an average antigenic score of 0.7108, and its non-allergenic properties were confirmed using the AllerTOPv.2.0 server. After eight weeks of testing, the parasite burden in the spleens of several groups of mice was measured. The findings showed that the group of mice that were immunized with Tuzin had a markedly reduced amount of parasites in their spleens when compared to the control group. In normal mice with *L. donovani* hepatic infections, tissue granulomas form around parasitized resident macrophages (Kupffer cells) in the liver. The immune system recognizes and responds to these structures, which are surrounded by T cells that secrete

cytokines and blood monocytes that are effective against *Leishmania* parasites (Murray, 2001). However, our findings showed that the Tuzin-immunized group had fewer and smaller granulomas in their liver tissue, as evidenced by H&E staining, compared to the infected control group.

The Th2 type of immune response is indicated by the IgG1 response, whereas the Th1 response, which is protective, is indicated by the IgG2a antibody response (Kaur *et al.*, 2013). It is possible that the positive impact of the IgG2a response is negated by the IgG1 response. Only when the IgG1 reaction decreases can the IgG2a response have a positive effect. Our study revealed that the Tuzin vaccinated group had significantly higher estimated IgG2a antibody titers and lower IgG1 levels compared to the control groups. These findings suggest that Tuzin triggers the human immune system in the presence of a parasite. The results also indicate that a protective immune response against *L. donovani* requires higher levels of IgG2a than IgG1 and a low level of IgG1.

IL-10 is believed to play a key role in promoting the progression of VL by priming host macrophages to enhance parasite survival and development. The reduction of TNF-α and NO production can lead to macrophages developing resistance to activation signals, which in turn can impede the elimination of amastigotes. Research has demonstrated that inhibiting IL-10 in VL serum can stop the replication of *L. donovani* in macrophages and boost the IFN response by antigen-stimulated PBMC (Nylén *et al.*, 2007). To further understand the association between the immune response phenotype and the level of protection in mice, a study was conducted to evaluate the IFN-γ and IL-10 levels as indicators of Th1 and Th2 cells. The findings showed that the Tuzin-vaccinated group had significantly reduced expression of IL-10 compared to the control group, while IFN-γ levels remained the same. This suggests that Tuzin protein can provide partial protection against leishmaniasis, and the viability of intracellular parasites during visceral leishmaniasis is determined by the IFN-γ/IL-10 ratio. In the presence of a high IFN-γ/IL-10 ratio, the immune response shifts to the Th1 immunological phenotype, which supports protective immunity (Jajarmi *et al.*, 2019).. The Tuzin challenged group showed a much higher IFN-γ/IL-10 ratio than the infected control group, indicating a Th1-type immune response and supporting protective immunity.

The host is protected by stimulating the macrophages to create ROS and nitric oxide (NO) for the oxidative destruction of intracellular amastigotes (Dayakar *et al.*, 2019). The superoxide anion (O_2^-) and nitric oxide (NO) prevent *Leishmania* infection. Superoxide is created by the oxidative burst of macrophages in response to phagocytosis during the early stages of *Leishmania* infection (Carneiro *et al.*, 2016). In our results, Splenocytes from Tuzin vaccinated mice group showed increasing trend of NO and intracellular ROS level upon stimulation with CLA of *L. donovani* as compared with the other groups which indicates the Tuzin might help to eliminate the parasite. The characteristic of active VL in both human and animals is impairment of the cell-mediated immune response. Effective vaccine-induced immunity depends on the antigen-specific T-cell response being restored (Karmakar *et al.*, 2021). In our findings, The Tuzin-vaccinated and infected control groups showed no appreciable difference in T cell proliferation. However, more research is required to comprehend the underlying mechanism fully.

Objective 3: To determine the role of the Tuzin gene in the survival and infectivity of *L. donovani* by knockdown approach

The Tuzin over expression and knockdown construct successfully generated

4.3.1 Generation of Overexpression (OE) and Knock down (KD) construct for Tuzin

The Tuzin gene was cloned into pEGFP-C1 vector successfully in sense and anti-sense orientation for overexpression and knockdown, respectively and the both Tuzin OE and Tuzin KD construct was confirmed by double digestion with *HindIII* and *BamHI* restriction (Figure 4.4.1). .

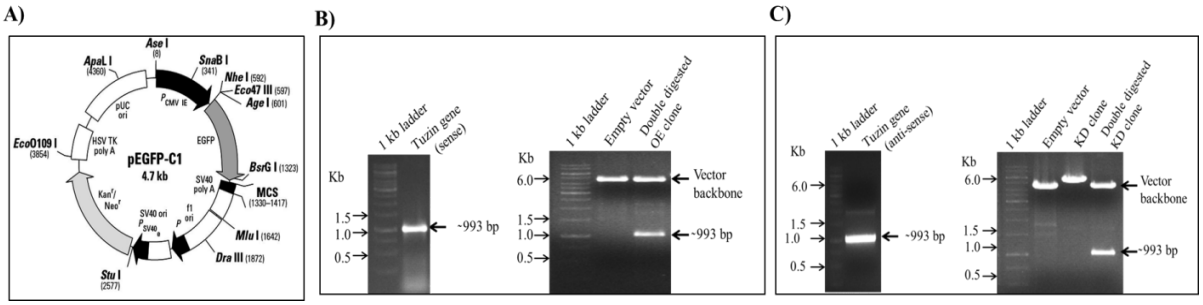

Figure 4.3.1: Knockdown and overexpression of Tuzin gene in *L. donovani* parasite: A) Amplification and confirmation of Tuzin OE clone; B) Amplification and confirmation of Tuzin KD clone

The Tuzin OE and Tuzin KD construct was successfully generated in sense and anti-sense orientation into the pEGFP-C1 vector and confirmed by double digestion. The confirmed construct of both constructs was transfected *into L. donovani* parasites by electroporation method as mentioned in methodology. Then the transfected parasites were maintained under 50 µg/ml G418 antibiotic and checked the transfection efficiency by fluorescence microscopy.`

4.3.2 Knockdown of Tuzin Confirmation by PCR

An equal number of DD8 WT, Tuzin OE, and Tuzin KD parasites were used to isolate total RNA. The Takara Prime script 1st strand DNA synthesis kit was used to create cDNA from 1 µg of total RNA, and the amplified cDNA was then utilized as a template for PCR using full-length Tuzin gene primers (Figure 4.3.2). The results indicate that the Tuzin gene was partially depleted because the intensity of the band in Tuzin KD was lower than in DD8 WT

Tuzin OE. The positive control for ensuring that the template was used at the same concentration involved the utilization of primers specific to the β-actin gene.

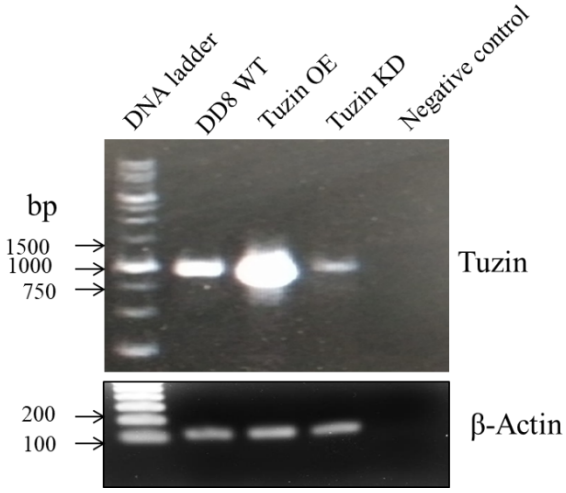

Figure 4.3.2: PCR for the confirmation of Tuzin KD: 1% Agarose gel showing the amplification of Tuzin gene in WT, Tuzin OE and Tuzin KD parasite with Tuzin specific primer and β-Actin primers

4.3.3 Immunoblotting confirms that Tuzin depletion was successful

The immunoblotting of an equal number of parasite lysates from DD8 WT, Tuzin OE, and Tuzin KD using an anti-Tuzin antibody, as described in the technique, revealed tuzin inhibition. When compared to WT and Tuzin OE parasites, Tuzin KD had lower band intensity (Figure 4.3.4A). The same blot was stripped and re-probed with anti-β tubulin following the second development, and the band intensity was the same for all samples, indicating similar volume loading. This result implied that the Tuzin gene had been successfully knocked down, and densitometry analysis confirmed that the Tuzin knockdown impacted the level of Tuzin expression (Figure 4.3.4B).

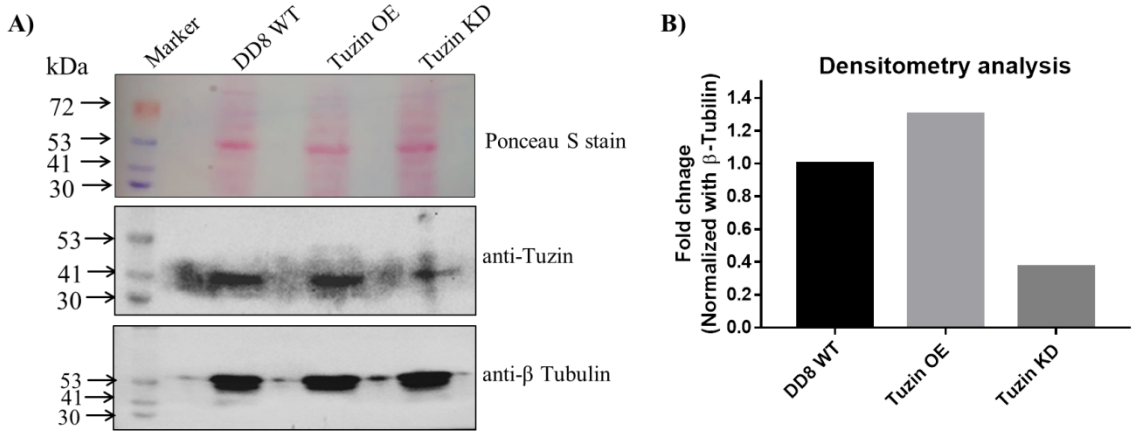

Figure 4.3.3: Immunoblotting analysis of *L. donovani* transfected parasites with Tuzin OE, and Tuzin KD construct: (A) western blot of crude lysate of DD8 WT, Tuzin OE with anti-Tuzin antibody and anti-β tubulin antibody. (B) Densitometry analysis of the western blot

4.3.4 Immunofluorescence assay to validate transfection and Tuzin depletion in *L. donovani* parasites

Immunofluorescence assay was employed to investigate transfection and Tuzin depletion in *L. donovani* transfectants, where the use of methanol permeabilization allowed the primary and secondary antibodies to bind to Tuzin present in the parasites. The plasmid pEGFP-C1's fluorescence confirms that it was successfully transfected into the parasites by demonstrating its existence. The AlexaFluor-555 fluorochrome coupled to a secondary antibody produces orange fluorescence with maximum 555 nm absorption and a maximum 580 nm emission. Tuzin expression is indicated by orange fluorescence, but orange fluorescence's absence indicates Tuzin depletion. Figure 4.3.4 shows Panel 1- bright field, panel 2- GFP fluorescence, Panel 3- Alexa Fluor 555 fluorochrome fluorescence, Panel 4- DAPI fluorescence, and Panel 5- Merged. There are no background artifacts, as evidenced by row A, where preabsorbed antibody control (without primary antibody) failed to show orange fluorescence. The plasmid has been successfully transfected into the parasites when B, C, and D exhibit green fluorescence, and they also exhibit orange fluorescence, which signals the expression of Tuzin. DAPI was used to label the nucleus and the kinetoplast. The overall result shows that the Tuzin KD parasites show less fluorescence when compared with WT DD8, and Tuzin OE parasites indicate that the Tuzin gene is partially depletion.

Interestingly, we found the altered morphology in Tuzin KD parasites, so to check the morphology of parasites, we performed Scanning electronic microscopy.

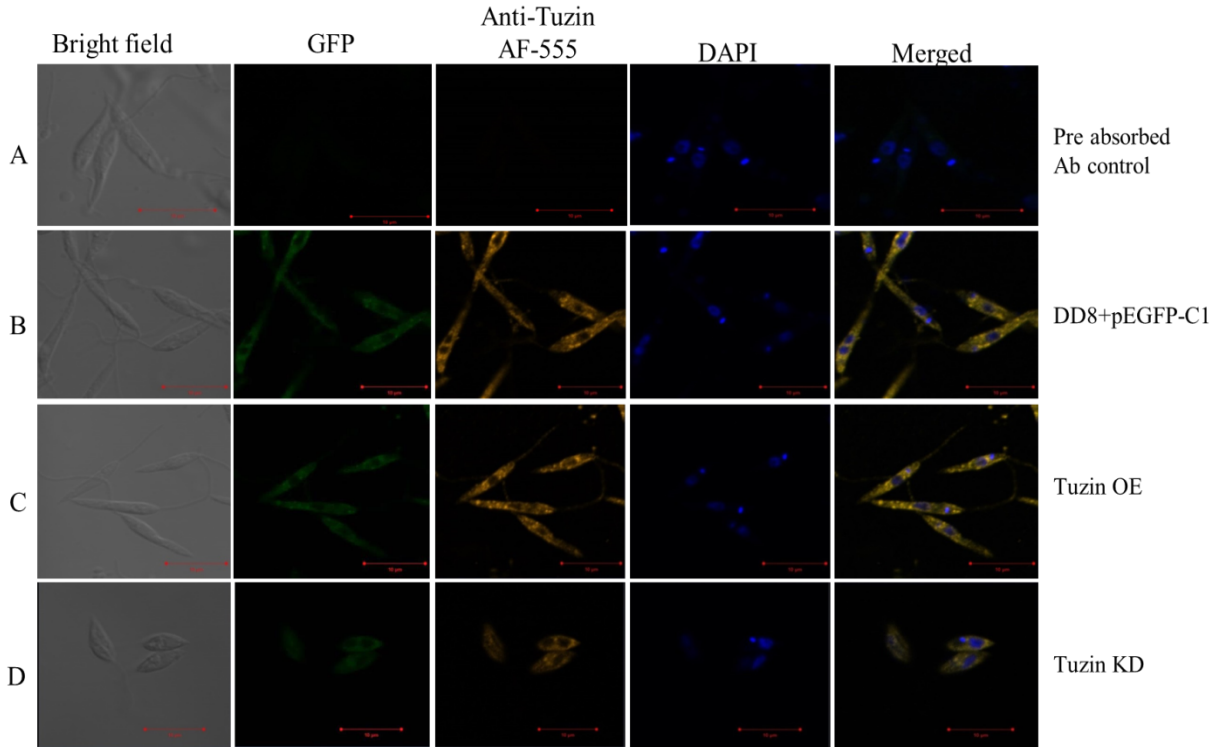

Figure 4.3.4: Immunofluorescence assay of *L. donovani* transfectants: Localization of LdTuzin protein in *L. donovani* promastigotes. Anti-Tuzin antibodies were used in immunofluorescence microscopy as the primary antibody and anti-rabbit IgG conjugated with Alexa Fluor 555 as the secondary antibody. With DAPI, the kinetoplast and nucleus were detected. The Panel 1- bright field, panel 2- GFP fluorescence, Panel 3- Alexa Fluor 555 fluorochrome fluorescence, Panel 4- DAPI, and Panel 5- Merged. A- Wild type DD8 parasite pre-absorbed antibody control (without anti-Tuzin antibody), B- Empty vector (DD8+pEGFP-C1) transfected parasite, C- Tuzin Overexpression parasites (DD8 with Tuzin pEGFP-C1 construct) and D- Knock down parasite (Tuzin KD) transfected parasite.

4.3.5 Effect of Tuzin OE and KD on Growth rate of *L. donovani*

To know the effect of Tuzin KD on growth rate we estimated the growth as mentioned in methodology. The growth rates of Tuzin KD and Tuzin OE parasites were compared with that of the wild-type parasites (Figure 4.3.5). The both Tuzin KD and Tuzin OE did not have any significant effect on promastigote multiplication.

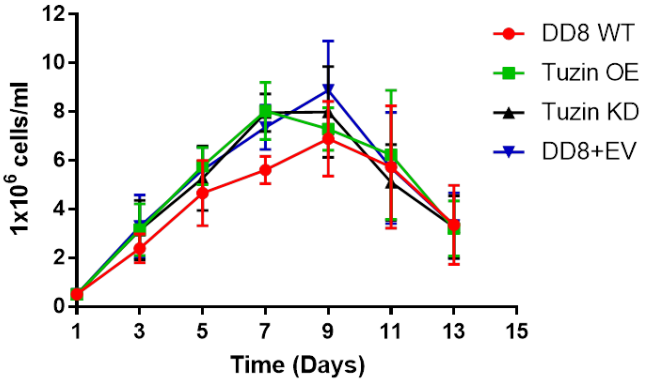

Figure 4.3.5: Effects of Tuzin OE and Tuzin KD growth on DD8 parasite. The data are mean values ± SD from two independent experiments.

4.3.6 Role of Tuzin in the morphology of parasites

The SEM analysis of the parasite cell morphology revealed that the WT, Tuzin OE, and DD8 EV parasites have a thin and elongated structure with healthy flagella (Figure 4.3.6). In contrast, Tuzin KD parasites exhibit morphological modifications, including the spindle-shaped structure and shorter flagella. The changed morphology in Tuzin KD parasites raised the possibility that it may contribute to their virulence and infectivity.

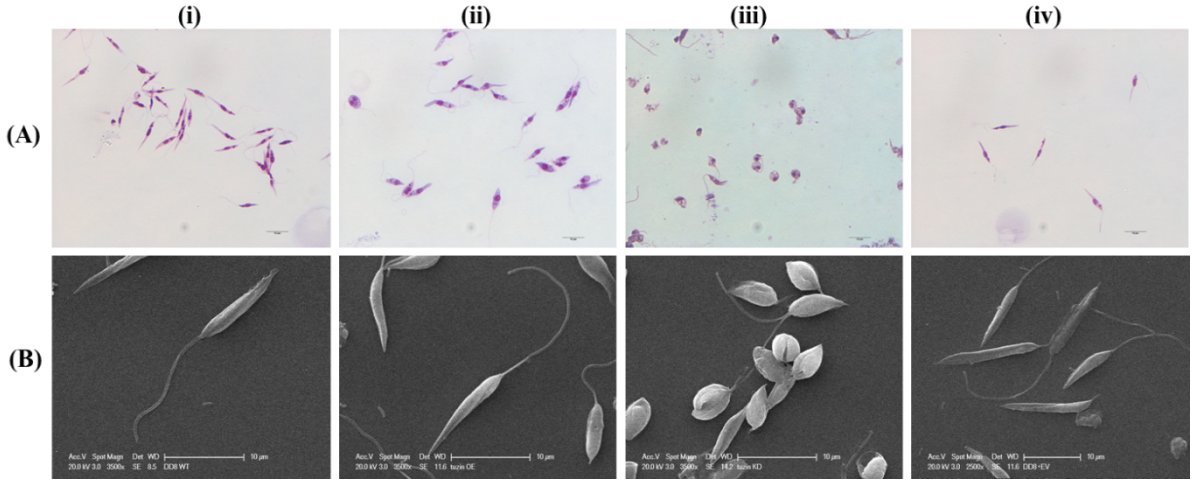

Figure 4.3.6: Role of Tuzin in parasite morphology: (A) Giemsa stain. (B) Morphological alterations of Tuzin KD mutant promastigotes observed under SEM micrographs, (i) SEM micrograph of wild type promastigotes showing a slender and elongated structure with healthy flagella, (ii) image of Tuzin OE showing cell morphology almost similar to DD8

WT, (iii) the image of Tuzin KD parasite demonstrating a much-altered morphology and a shorter flagella, and (iv) DD8 parasite transfected with pEGFP-C1 vector showed similar morphology as WT DD8.

4.3.7 Tuzin KD prevents the parasite uptake by THP-1 macrophages

The THP-1 cells were stimulated with PMA, infected with various *L. donovani* parasite groups, stained with Giemsa stain, and observed under a microscope (Figure 4.3.6A). Next, the intracellular amastigote was counted in 100 macrophages for each group. Afterward, the phagocytic index was determined. The results of the phagocytic index were 534.7 ± 17.64, 571.2 ± 22.2, 405.7 ± 17.02, and 552 ± 13.24, respectively in THP-1 (Figure 4.3.7B). The phagocytic index was considerably lower in Tuzin KD-infected THP-1 cells than wild-type DD8 cells, but Tuzin OE-infected macrophages showed no discernible difference from WT. The findings indicated that Tuzin could play a role in the contagiousness of the parasite.

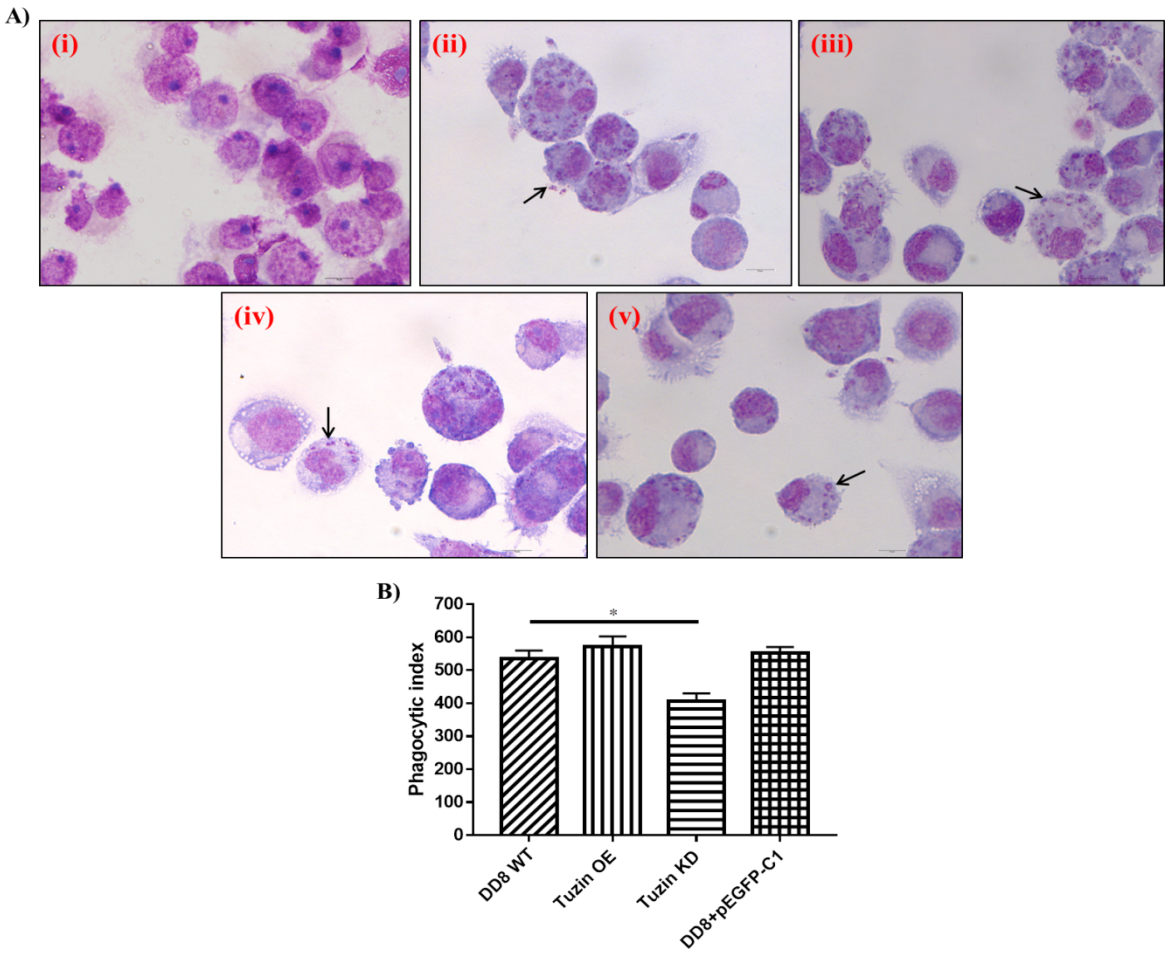

Figure 4.3.7: Phagocytic index of THP-1 macrophages: The activated THP-1 macrophages infected with different groups of parasites. (A) Giemsa stain of THP 1 macrophage (i) Naïve THP-1 macrophage (MΦ), (ii) THP-1 Φ infected with DD8 wild *L. donovani* parasites, (iii) THP-1 MΦ infected with Tuzin OE parasites, (iv) THP-1 MΦ infected with Tuzin KD parasites, and (v) THP-1 MΦ infected with DD8 parasites containing pEGFP-C1 vector. Phagocytic Index (PI) was calculated in each group from 100 macrophages. PI = (Total number of engulfed cells/Total number of counted MΦ) X (Number of MΦ's containing engulfed cells/Total number of counted MΦ) X 100.

3.4.8 Immunoblotting assay for iNOS and Arginase in infected THP-1 macrophages

The multiplication of *Leishmania* parasites can only occur in macrophages, which are crucial in determining whether the immune response will be controlled or aggravated, ultimately leading to clinical symptoms. Macrophages can be classified into two primary phenotypes - M1 and M2. M1 is characterized by its pro-inflammatory nature and ability to kill microorganisms, whereas M2 is a subtype that promotes inflammation resolution and tissue repair by exhibiting anti-inflammatory and regulatory properties. The differentiation of macrophages towards either M1 or M2 phenotype is primarily regulated by genes such as iNOS, arginase-1, and CD206, among others (Tomiotto-Pellissier et al., 2018). In VL patients, the levels of blood arginase are significantly higher, while NO levels are lower. Recent research has shown that the monocytes/macrophages of VL patients exhibit a regulatory M2 phenotype characterized by high levels of IL-10, CD163, and CXCL14, with lower oxidative burst and antigen presentation (Roy et al., 2018).

The cells were lysed by RIPA buffer and loaded with an equal sample of crude lysate. The western blot used an anti-iNOS antibody and anti-Arginase-I antibody (Figure 4.3.8). According to the western blot data, Tuzin KD-infected macrophages express less iNOS than WT- and Tuzin OE-infected macrophages. In Tuzin KD-infected macrophages, arginase expression was not noticeable.

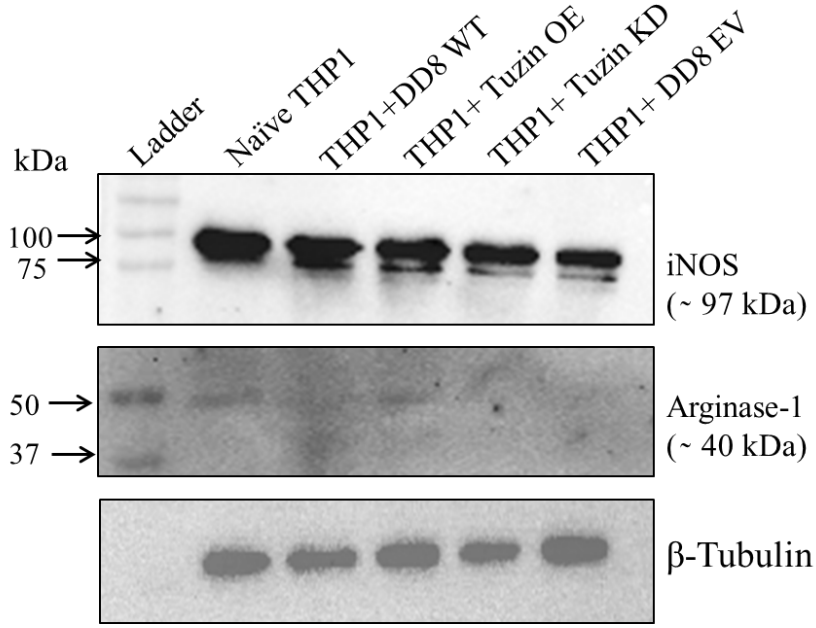

Figure 4.3.8: Western blot for iNOS and Arginase in THP-1 infected macrophage: The equal number of infected THP-1 MΦ was taken and lysed by RIPA buffer and performed western blot by using anti-iNOS antibody and anti-Arginase-I antibody. The anti-β-Tubulin antibody was used as a positive control.

To loosen the knot caused by Tuzin's episomal inhibition, the pEGFP-C1 mammalian expression vector carrying the antisense Tuzin construct was employed. Transfectants were selected using the neomycin-targeting G418 drug, and confirmation of transfection was achieved by utilizing the GFP expressed through the EGFP gene. Moreover, rabbits were used to produce the antibody against *L. donovani* Tuzin. Western blotting validated the different Tuzin expression levels, and our findings demonstrated that the Tuzin KD parasite expressed itself less than wild-type parasites. In order to determine the impact of Tuzin KD on the growth rate, we evaluated the growth; nevertheless, Tuzin KD had no appreciable impact on promastigote multiplication. The Tuzin gene is partially depleted, as evidenced by the Tuzin KD parasites' reduced fluorescence compared to WT DD8 parasites, according to the IFA. We noticed the altered morphology of Tuzin KD parasites, which is interesting. The SEM examination of the parasite cell morphology demonstrated that the WT, Tuzin OE, and DD8 EV parasites have thin, elongated structures with healthy flagella. In contrast, the spindle-shaped structure and shorter flagella are two morphological modifications seen in Tuzin KD parasites. It was speculated that The Tuzin gene might play a role in the virulence

and infectivity of *Leishmania*. The phagocytic index was significantly lower in Tuzin KD-infected THP-1 cells than in DD8 cells that were wild-type, whereas Tuzin OE-infected macrophages did not differ noticeably from WT. These findings suggested that Tuzin may contribute to the parasite's infectivity.

In animal models, *Leishmania*-infected lymphocytes release, TGF-β which causes the arginine pool to be switched from iNOS to arginase to form polyamines, which aids the parasite's proliferation (Iniesta *et al.*, 2001). *Leishmania* is found inside macrophages in the mammalian host. The parasite's survival within these cells depends on its ability to avoid several microbicidal defenses, including the regulation of inducible nitric oxide synthase (iNOS) that controls the production of nitric oxide (NO). For the parasite to reproduce, L-arginine must be available for both arginase and iNOS, which need it as a substrate. In order to avoid the iNOS-dependent killing mechanism in macrophages, the *L. donovani* infection typically stimulates the production of arginase, a protein similar to IL-10. Thus, macrophages are involved in both the parasites' survival and demise during *Leishmania* pathogenesis, where they play a multifaceted function (Dayakar *et al.*, 2019). According to data from multiple research, human monocytes are first polarised to an M1-like phenotype before switching to M2-like repair macrophages in response to changes in the microenvironment, and vice versa (Atri *et al.*, 2018). Our findings indicated that compared to WT- and Tuzin OE-infected macrophages, Tuzin KD-infected macrophages express less iNOS. There was no discernible arginase expression in Tuzin KD-infected macrophages.

Chapter: V
Summary

The poor are the most affected by Leishmaniasis, which is a significant worldwide public health issue. The standard medications are expensive, poisonous, and resistant. Since VL is currently not curable, a new strategy for managing the illness is urgently required. Although genomic, immunologic, and animal models have begun to provide insights into Visceral Leishmaniasis, its underlying causes are still not well comprehended. Tuzin protein was chosen as an antigen for the vaccine and diagnostic candidate in the current investigation due to its immunogenic character. By employing an in silico study with the PSIPRED tool, the location of the Tuzin protein was identified. The findings showed that the Tuzin protein was transmembrane, with its C-terminus positioned in the extracellular space and it's N-terminus inside the cytoplasm. Tuzin protein was selected as the antigen for the vaccination supported by the VaxiJen v2.0 server. Tuzin has a robust antigenic profile with an average antigenic score of 0.7108. The AllerTOPv.2.0 server was used to confirm Tuzin's non-allergenic properties.

In our study, we were successfully cloning the *Leishmania donovani* Tuzin gene into the pET28a vector, allowing for gene expression in *E. coli* Rosetta (DE3) strains. Successful expression, purification, and antibody production of the recombinant Tuzin protein were verified by western blot. Studies on the localization of tuzin in parasites revealed that the Tuzin protein was expressed in both stages of the *L. donovani* parasite *(*promastigote and amastigote), confirming by immunofluorescences assay (Confocal microscopy). The anti-Tuzin antibody titer was significantly higher in the serum of VL patients than that of treated patients when the diagnostic potential of the recombinant Tuzin protein was tested using ELISA with VL sera. Tuzin protein demonstrated 85% and 92% sensitivity and specificity against anti-Tuzin antibodies in human patient serum, suggesting that it may be used to identify active VL.

After being administered tuzin protein as a form of immunization, the BALB/c mice were exposed to the *L. donovani* metacyclic parasite. The mice were then euthanized eight weeks following the exposure, and blood, liver, and spleen were collected for use in subsequent experiments. The parasite burden was estimated, and it was found that the Tuzin immunized group had a significantly reduced parasite load compared to infected control mice. The quantity of IgG1 (Th2 specific) and IgG2a (Th1 specific) antibodies in mouse serum was then measured. Tuzin causes a cellular immune response during parasite infection, as shown

by the fact that Tuzin-vaccinated mice had elevated IgG2a titers but no noticeable change in IgG1 titers. In addition, since the development of granulomas is a characteristic feature of parasite elimination, we assessed the frequency of their occurrence in liver tissue samples obtained from both control and Tuzin-vaccinated animals. We observed a decrease in granulomas in the Tuzin challenged group. The development of loose and small granulomas further demonstrates that the parasites have been eradicated in immunized groups. On the other hand, the granuloma structure is compact and tight in the infected group.

To confirm this, we employed RT-qPCR to assess the mRNA expression levels of Th1-specific cytokine IFN-γ and Th2-specific cytokine IL-10 in the spleen tissue of both infected and immunized mice. Equal amounts of IFN-γ essential for parasite eradication were present in both the vaccinated and control mice. In contrast, anti-inflammatory cytokine (IL-10) expression was lower in Tuzin-challenged animals than in control mice, essential for the parasite's survival. The ratio of IFN-γ and IL-10 also indicates the degree of VL healing. Due to Tuzin's ability to suppress the IL-10 cytokine in immunized mice, this ratio is more significant in Tuzin-challenged animals, suggesting that Tuzin causes an immunological response those results in protective immunity. As a result, immunization with Tuzin protein may guard against *Leishmania* infection by boosting macrophage anti-leishmanial activity, indicating that Tuzin immunization may trigger the beneficial Th1 immune response against *Leishmania* parasites in these BALB/c mice. Based on our research findings, we did not observe any distinguishable variation in the expansion of T cells between the Tuzin-vaccinated group and the infected control group. However, more investigation is necessary to understand the underlying mechanism thoroughly.

Using the pEGFP-C1 vector, we successfully cloned the tuzin gene construct in both sense and antisense orientations, resulting in the overexpression (OE) and knockdown (KD) Tuzin mutant parasites. The electroporation technique effectively transfected the pEGFP-C1 vector's sense and antisense constructs into the *L. donovani* parasite. The G418 antibiotic drug pressure of 50 μg/ml was used to sustain and select the transfectant parasites. The PCR and western blotting confirmed the various Tuzin expression levels, and our results showed that the Tuzin KD parasite expressed itself less than wild-type parasites. Tuzin KD had no discernible effect on promastigote multiplication, according to our analysis of the growth rate to assess Tuzin KD's effect on it.

We then used immunofluorescence to measure the degree of Tuzin expression in parasites of the wild-type DD8, Tuzin OE, and Tuzin KD strains. We found that Tuzin KD showed lower expression of Tuzin. Interestingly, we also saw that the KD parasite's form had changed. Hence, to provide further evidence, we examined the morphology of parasites using SEM. The SEM analysis of the parasite cell morphology revealed that the WT, Tuzin OE, and DD8 EV parasites have thin, elongated structures with healthy flagella. Nevertheless, Tuzin KD parasites exhibit two morphological alterations, including a spindle-shaped structure and shorter flagella. The Tuzin gene was thought to contribute to the virulence and contagiousness of *Leishmania*. The phagocytic index was considerably lower in Tuzin KD-infected THP-1 cells than in wild-type DD8 cells but not statistically different from WT in Tuzin OE-infected macrophages. The results indicated that Tuzin could potentially play a role in the parasite's ability to cause infection.

Chapter: VI
References

Ababa, A. and Ababa, A. (2001). 1 Short Report A fast agglutination screening test (FAST) for the detection of anti- *Leishmania* antibodies. 400–401.

Abdellahi, L., Iraji, F., Mahmoudabadi, A. and Hejazi, S. H. (2022). Vaccination in leishmaniasis: A review article. *Iranian Biomedical Journal* **26**, 1–35. doi:10.52547/ibj.26.1.35.

Ah, M. S., El-tourn, I. A., Satti, M. and Ghalib, H. W. (1992). Kala-azar : a comparative study of parasitological agglutination test in diagnosis methods and the direct. *Tropical Medicine*.

Akhoundi, M., Downing, T., Votýpka, J., Kuhls, K., Lukeš, J., Cannet, A., Ravel, C., Marty, P., Delaunay, P., Kasbari, M., Granouillac, B., Gradoni, L. and Sereno, D. (2017). *Leishmania* infections: Molecular targets and diagnosis. *Molecular Aspects of Medicine* **57**, 1–29. doi:10.1016/j.mam.2016.11.012.

Annang, F., Pérez-Moreno, G., García-Hernández, R., Cordon-Obras, C., Martín, J., Tormo, J. R., Rodríguez, L., De Pedro, N., Gómez-Pérez, V., Valente, M., Reyes, F., Genilloud, O., Vicente, F., Castanys, S., Ruiz-Pérez, L. M., Navarro, M., Gamarro, F. and González-Pacanowska, D. (2015). High-throughput screening platform for natural product-based drug discovery against 3 neglected tropical diseases: Human African trypanosomiasis, leishmaniasis, and chagas disease. *Journal of Biomolecular Screening* **20**, 82–91. doi:10.1177/1087057114555846.

Ansari, N. A., Kumar, R., Gautam, S., Nylén, S., Singh, O. P., Sundar, S. and Sacks, D. (2011). IL-27 and IL-21 Are Associated with T Cell IL-10 Responses in Human Visceral Leishmaniasis. *The Journal of Immunology* **186**, 3977–3985. doi:10.4049/jimmunol.1003588.

Arunima Biswas, Arijit Bhattacharya, S. K. and P. K. D. (2011). Expression of IL-10-triggered STAT3-dependent IL-4R is required for induction of arginase.pdf.

Asad, M., Sabur, A., Shadab, M., Das, S., Kamran, M., Didwania, N. and Ali, N. (2019). EB1-3 chain of IL-35 along with TGF-β synergistically regulate anti-leishmanial immunity. *Frontiers in Immunology* **10**, 1–12. doi:10.3389/fimmu.2019.00616.

Asilian, A., Sadeghinia, A., Faghihi, G., Momeni, A. and Amini Harandi, A. (2003). The efficacy of treatment with intralesional meglumine antimoniate alone, compared with that of cryotherapy combined with the meglumine antimoniate or intralesional sodium stibogluconate, in the treatment of cutaneous leishmaniasis. *Annals of Tropical Medicine and Parasitology* **97**, 493–498. doi:10.1179/000349803225001373.

Atri, C., Guerfali, F. Z. and Laouini, D. (2018). Role of human macrophage polarization in inflammation during infectious diseases. *International Journal of Molecular Sciences* **19**,. doi:10.3390/ijms19061801.

Balasegaram, M., Ritmeijer, K., Lima, M. A., Burza, S., Ortiz Genovese, G., Milani, B., Gaspani, S., Potet, J. and Chappuis, F. (2012). Liposomal amphotericin B as a treatment for human leishmaniasis. *Expert Opinion on Emerging Drugs* **17**, 493–510. doi:10.1517/14728214.2012.748036.

Bamorovat, M., Sharifi, I., Tavakoli Oliaee, R., Jafarzadeh, A. and Khosravi, A. (2021). Determinants of Unresponsiveness to Treatment in Cutaneous Leishmaniasis: A Focus on Anthroponotic Form Due to *Leishmania* tropica. *Frontiers in Microbiology* **12**, 1–15. doi:10.3389/fmicb.2021.638957.

Basselin, M., Denise, H., Coombs, G. H. and Barrett, M. P. (2002). Resistance to pentamidine in *Leishmania* mexicana involves exclusion of the drug from the mitochondrion. *Antimicrobial Agents and Chemotherapy* **46**, 3731–3738. doi:10.1128/AAC.46.12.3731-3738.2002.

Basu, R., Bhaumik, S., Basu, J. M., Naskar, K., De, T. and Roy, S. (2009). Kinetoplastid Membrane Protein-11 DNA Vaccination Induces Antimonial-Sensitive and -Resistant Strains of Leishmania.

Belkaid, Y., Hoffmann, K. F., Mendez, S., Kamhawi, S., Udey, M. C., Wynn, T. A. and Sacks, D. L. (2001). The role of interleukin (IL)-10 in the persistence of *Leishmania major* in the skin after healing and the therapeutic potential of anti-IL-10 receptor antibody for sterile cure. *Journal of Experimental Medicine* **194**, 1497–1506. doi:10.1084/jem.194.10.1497.

Besteiro, S., Williams, R. A. M., Coombs, G. H. and Mottram, J. C. (2007). Protein turnover and differentiation in Leishmania. *International Journal for Parasitology* **37**, 1063–1075. doi:10.1016/j.ijpara.2007.03.008.

Boelaert, M., Rijal, S., Regmi, S., Singh, R., Karki, B., Jacquet, D., Chappuis, F., Campino, L., Desjeux, P., Le Ray, D., Koirala, S. and Van der Stuyft, P. (2004). A comparative study of the effectiveness of diagnostic tests for visceral leishmaniasis. *The American journal of tropical medicine and hygiene* **70**, 72–7.

Bogdan, C. and Röllinghoff, M. (1999). How do protozoan parasites survive inside macrophages? *Parasitology Today* **15**, 22–28. doi:10.1016/S0169-4758(98)01362-3.

Bowles, D., Britch, S., Linthicum, K. and Johnson, R. (2015). Sand Flies (Diptera: Psychodidae: Phlebotominae): Significance, Surveillance, and Control in Contingency Operations. *Armed Forces Pest Management Board* 72.

Bray, D. P., Alves, G. B., Dorval, M. E., Brazil, R. P. and Hamilton, J. G. C. (2010). Synthetic sex pheromone attracts the leishmaniasis vector Lutzomyia longipalpis to experimental chicken sheds treated with insecticide. *Parasites and Vectors* **3**, 1–11. doi:10.1186/1756-3305-3-16.

Burns, J. M., Shreffler, W. G., Benson, D. R., Ghalib, H. W., Badaro, R. and Reed, S. G. (1993). Molecular characterization of a kinesin-related antigen of Leishmania chagasi that detects specific antibody in African and American visceral leishmaniasis. *Proceedings of the National Academy of Sciences* **90**, 775–779. doi:10.1073/pnas.90.2.775.

Carneiro, P. P., Conceição, J., Macedo, M., Magalhães, V., Carvalho, E. M. and Bacellar, O. (2016). The role of nitric oxide and reactive oxygen species in the killing of *Leishmania braziliensis* by monocytes from patients with cutaneous leishmaniasis. *PLoS ONE* **11**, 1–16. doi:10.1371/journal.pone.0148084.

Carter, K. C., Hutchison, S., Henriquez, F. L., Légaré, D., Ouellette, M., Roberts, C. W. and Mullen, A. B. (2006). Resistance of *Leishmania donovani* to sodium stibogluconate is related to the expression of host and parasite γ-glutamylcysteine

synthetase. *Antimicrobial Agents and Chemotherapy* **50**, 88–95. doi:10.1128/AAC.50.1.88-95.2006.

Carvalho, E. M., Barral, A., Pedral-sampaio, D., Barral-netto, M., The, S., Diseases, I., Mar, N., Carvalho, E. M., Barral, A., Pedral-sampaio, D. and Barral-netto, M. (1992). Immunologic Markers of Clinical Evolution in Children Recently Infected with *Leishmania donovani* chagasi Roberto Badaró , Heonir Rocha and Warren D . Johnson Jr . Published by : Oxford University Press Stable URL : http://www.jstor.org/stable/30112059 Imm. **165**, 535–540.

Carvalho, L. P., Passos, S., Schriefer, A. and Carvalho, E. M. (2012). Protective and pathologic immune responses in human tegumentary leishmaniasis. *Frontiers in Immunology* **3**, 1–9. doi:10.3389/fimmu.2012.00301.

Chappuis, F., Sundar, S., Hailu, A., Ghalib, H., Rijal, S., Peeling, R. W., Alvar, J. and Boelaert, M. (2007). Visceral leishmaniasis: What are the needs for diagnosis, treatment and control? *Nature Reviews Microbiology* **5**, 873–882. doi:10.1038/nrmicro1748.

Coelho, A. C., Gentil, L. G., da Silveira, J. F. and Cotrim, P. C. (2008). Characterization of *Leishmania* (*Leishmania*) *amazonensis* promastigotes resistant to pentamidine. *Experimental Parasitology* **120**, 98–102. doi:10.1016/j.exppara.2008.03.018.

Colombo, A. L., Azevedo Melo, A. S., Crespo Rosas, R. F., Salomão, R., Briones, M., Hollis, R. J., Messer, S. A. and Pfaller, M. A. (2003). Outbreak of Candida rugosa candidemia: An emerging pathogen that may be refractory to amphotericin B therapy. *Diagnostic Microbiology and Infectious Disease* **46**, 253–257. doi:10.1016/S0732-8893(03)00079-8.

Conde, L., Maciel, G., de Assis, G. M., Freire-de-Lima, L., Nico, D., Vale, A., Freire-de-Lima, C. G. and Morrot, A. (2022). Humoral response in Leishmaniasis. *Frontiers in Cellular and Infection Microbiology* **12**, 1–8. doi:10.3389/fcimb.2022.1063291.

Coser, E. M., Ferreira, B. A., Branco, N., Yamashiro-Kanashiro, E. H., Lindoso, J. A. L. and Coelho, A. C. (2020). Activity of paromomycin against *Leishmania*

amazonensis: Direct correlation between susceptibility in vitro and the treatment outcome in vivo. *International Journal for Parasitology: Drugs and Drug Resistance* **14**, 91–98. doi:10.1016/j.ijpddr.2020.08.001.

Costa, A. S. A., Costa, G. C., de Aquino, D. M. C., de Mendonça, V. R. R., Barral, A., Barral-Netto, M. and Caldas, A. de J. M. (2012). Cytokines and visceral leishmaniasis: A comparison of plasma cytokine profiles between the clinical forms of visceral leishmaniasis. *Memorias do Instituto Oswaldo Cruz* **107**, 735–739. doi:10.1590/S0074-02762012000600005.

Crocker, P. R., Blackwell, J. M. and Bradley, D. J. (1984). Transfer of innate resistance and susceptibility to *Leishmania donovani* infection in mouse radiation bone marrow chimaeras. *Immunology (Oxford)* **52**, 417–422.

Cunningham, J., Hasker, E., Das, P., El Safi, S., Goto, H., Mondal, D., Mbuchi, M., Mukhtar, M., Rabello, A., Rijal, S., Sundar, S., Wasunna, M., Adams, E., Menten, J., Peeling, R., Khanal, B., Das, M., Oliveira, E., de Assis, T. M., Bhaskar, K. R., Huda, M. M., Hassan, M., Abdoun, A. O., Awad, A., Osman, M., Prajapati, D. K., Gidwani, K., Tiwary, P., Paniago, A. M. M., Sanchez, M. C. A., Celeste, B. J., Jacquet, D., Magiri, C., Muia, A., Kesusu, J., Ageed, A. F., Galal, N., Osman, O. S., Gupta, A. K., Bimal, A. S. and Das, V. N. R. (2012). A global comparative evaluation of commercial immunochromatographic rapid diagnostic tests for visceral leishmaniasis. *Clinical Infectious Diseases* **55**, 1312–1319. doi:10.1093/cid/cis716.

Dayakar, A., Chandrasekaran, S., Veronica, J. and Maurya, R. (2016). Leptin induces the phagocytosis and protective immune response in *Leishmania donovani* infected THP-1 cell line and human PBMCs. *Experimental Parasitology* **160**, 54–59. doi:10.1016/j.exppara.2015.12.002.

Dayakar, A., Chandrasekaran, S., Kuchipudi, S. V. and Kalangi, S. K. (2019). Cytokines: Key determinants of resistance or disease progression in visceral leishmaniasis: Opportunities for novel diagnostics and immunotherapy. *Frontiers in Immunology* **10**,. doi:10.3389/fimmu.2019.00670.

De Trez, C., Magez, S., Akira, S., Ryffel, B., Carlier, Y. and Muraille, E. (2009). iNOS-producing inflammatory dendritic cells constitute the major infected cell type during the chronic *Leishmania major* infection phase of C57BL/6 resistant mice. *PLoS Pathogens* **5**,. doi:10.1371/journal.ppat.1000494.

de Vries, H. J. C., Reedijk, S. H. and Schallig, H. D. F. H. (2015). Cutaneous Leishmaniasis: Recent Developments in Diagnosis and Management. *American Journal of Clinical Dermatology* **16**, 99–109. doi:10.1007/s40257-015-0114-z.

Deris, S., Delavari, M. and Hooshyar, H. *(2022). Medical Parasitology & Leishmania* Vaccines : A Narrative Review on Last Decade Developments. *Aras Part Medical International Press* **3**, 3–8. doi:10.34172/ijmpes.2022.02.

Desjeux, P., Ghosh, R. S., Dhalaria, P., Strub-Wourgaft, N. and Zijlstra, E. E. (2013). Report of the post Kala-Azar dermal leishmaniasis (PKDL) consortium meeting, New Delhi, India, 27-29 June 2012. *Parasites and Vectors* **6**, 1–21. doi:10.1186/1756-3305-6-196.

dos Santos Meira, C. and Gedamu, L. (2021). Protective or Detrimental? The Role of Host Immunity in Leishmaniasis. *Advances in Clinical Immunology, Medical Microbiology, COVID-19, and Big Data* 151–185.

Elmahallawy, E. K., Sampedro Martínez, A., Rodriguez-Granger, J., Hoyos-Mallecot, Y., Agil, A., Navarro Mari, J. M. and Gutierrez Fernández, J. (2014). Diagnosis of leishmaniasis. *Journal of Infection in Developing Countries* **8**, 961–972. doi:10.3855/jidc.4310.

Engwerda, C. R., Ato, M. and Kaye, P. M. (2004). Macrophages, pathology and parasite persistence in experimental visceral leishmaniasis. *Trends in Parasitology* **20**, 524–530. doi:10.1016/j.pt.2004.08.009.

Faleiro, R. J., Kumar, R., Hafner, L. M. and Engwerda, C. R. (2014). Immune Regulation during Chronic Visceral Leishmaniasis. *PLoS Neglected Tropical Diseases* **8**,. doi:10.1371/journal.pntd.0002914.

Garrido-Jareño, M., Sahuquillo-Torralba, A., Chouman-Arcas, R., Castro-Hernández, I., Molina-Moreno, J. M., Llavador-Ros, M., Gómez-Ruiz, M. D., López-Hontangas, J. L., Botella-Estrada, R., Salavert-Lleti, M. and Pemán-García, J. (2020). Cutaneous and mucocutaneous leishmaniasis: Experience of a Mediterranean hospital. *Parasites and Vectors* **13**, 1–7. doi:10.1186/s13071-020-3901-1.

Gasim, S., Elhassan, A. M., Khalil, E. A. G., Ismail, A., Kadaru, A. M. Y., Kharazmi, A. and Theander, T. G. (1998). High levels of plasma IL-10 and expression of IL-10 by keratinocytes during visceral leishmaniasis predict subsequent development of post-kala- azar dermal leishmaniasis. *Clinical and Experimental Immunology* **111**, 64–69. doi:10.1046/j.1365-2249.1998.00468.x.

Gatto, M., Borim, P. A., Wolf, I. R., da Cruz, T. F., Mota, G. A. F., Braz, A. M. M., Amorim, B. C., Valente, G. T., Golim, M. de A., Venturini, J., Junior, J. P. A., Pontillo, A. and Sartori, A. (2020). Transcriptional analysis of THP-1 cells infected with *leishmania infantum* indicates no activation of the inflammasome platform. *PLoS Neglected Tropical Diseases* **14**, 1–24. doi:10.1371/journal.pntd.0007949.

Ghalib, H. W., Piuvezam, M. R., Skeiky, Y. A. W., Siddig, M., Hashim, F. A., El-Hassan, A. M., Russo, D. M. and Reed, S. G. (1993). Interleukin 10 production correlates with pathology in human *Leishmania donovani* infections. *Journal of Clinical Investigation* **92**, 324–329. doi:10.1172/JCI116570.

Ghorbani, M. and Farhoudi, R. (2018). Leishmaniasis in humans: Drug or vaccine therapy? *Drug Design, Development and Therapy* **12**, 25–40. doi:10.2147/DDDT.S146521.

Gibson, M. E. (1983). The identification of kala azar and the discovery of *leishmania donovani*. *Medical History* **27**, 203–213. doi:10.1017/S0025727300042691.

Gluenz, E., Wheeler, R. J., Hughes, L. and Vaughan, S. (2015). Scanning and three-dimensional electron microscopy methods for the study of *Trypanosoma brucei* and *Leishmania mexicana* flagella. *Methods in Cell Biology* **127**, 509–542. doi:10.1016/bs.mcb.2014.12.011.

Gurung, P. and Kanneganti, T. D. (2015). Innate immunity against *Leishmania* infections. *Cellular Microbiology* **17**, 1286–1294. doi:10.1111/cmi.12484.

Habtemariam, S. (2003). In vitro antileishmanial effects of antibacterial diterpenes from two Ethiopian Premna species: P. schimperi and P. oligotricha. *BMC Pharmacology* **3**, 1–6. doi:10.1186/1471-2210-3-6.

Hailu, A., Schoone, G. J., Diro, E., Tesfaye, A., Techane, Y., Tefera, T., Assefa, Y., Genetu, A., Kebede, Y., Kebede, T. and Schallig, H. D. F. H. (2006). Field evaluation of a fast anti-*Leishmania* antibody detection assay in Ethiopia. *Transactions of the Royal Society of Tropical Medicine and Hygiene* **100**, 48–52. doi:10.1016/j.trstmh.2005.07.003.

Hawn, T. R., Ozinsky, A., Underhill, D. M., Buckner, F. S., Akira, S. and Aderem, A. (2002). *Leishmania major* activates IL-1α expression in macrophages through a MyD88-dependent pathway. *Microbes and Infection* **4**, 763–771. doi:10.1016/S1286-4579(02)01596-4.

Huang, F., Xu, D., Esfandiari, E. and Sands, W. (2013). Cutting Edge: Mice Defective in Fas Are Highly Susceptible to.

Hurdayal, R. and Brombacher, F. (2014). The role of IL-4 and IL-13 in cutaneous leishmaniasis. *Immunology Letters* **161**, 179–183. doi:10.1016/j.imlet.2013.12.022.

Iborra, S., Solana, J. C., Requena, J. M. and Soto, M. (2018). Vaccine candidates against *leishmania* under current research. *Expert Review of Vaccines* **17**, 323–334. doi:10.1080/14760584.2018.1459191.

Ikeogu, N. M., Akaluka, G. N., Edechi, C. A., Salako, E. S., Onyilagha, C., Barazandeh, A. F. and Uzonna, J. E. (2020). *Leishmania* immunity: Advancing immunotherapy and vaccine development. *Microorganisms* **8**, 1–21. doi:10.3390/microorganisms8081201.

Iniesta, V., Gómez-Nieto, L. C. and Corraliza, I. (2001). The inhibition of arginase by Nω-hydroxy-L-arginine controls the growth of *Leishmania* inside macrophages.

Journal of Experimental Medicine **193**, 777–783. doi:10.1084/jem.193.6.777.

Jackson, A. P. (2010). The evolution of amastin surface glycoproteins in trypanosomatid parasites. *Molecular Biology and Evolution* **27**, 33–45. doi:10.1093/molbev/msp214.

Jain, K. and Jain, N. K. (2013). Novel therapeutic strategies for treatment of visceral leishmaniasis. *Drug Discovery Today* **18**, 1272–1281. doi:10.1016/j.drudis.2013.08.005.

Jajarmi, V., Salehi-Sangani, G., Mohebali, M., Khamesipour, A., Bandehpour, M., Mahmoudi, M. and Zahedi-Zavaram, H. (2019). Immunization against *Leishmania major* infection in BALB/c mice using a subunit-based DNA vaccine derived from TSA, LmSTI1, KMP11, and LACK predominant antigens. *Iranian Journal of Basic Medical Sciences* **22**, 1493–1501. doi:10.22038/ijbms.2019.14051.

Jaramillo, M., Gomez, M. A., Larsson, O., Shio, M. T., Topisirovic, I., Contreras, I., Luxenburg, R., Rosenfeld, A., Colina, R., McMaster, R. W., Olivier, M., Costa-Mattioli, M. and Sonenberg, N. (2011). *Leishmania* repression of host translation through mTOR cleavage is required for parasite survival and infection. *Cell Host and Microbe* **9**, 331–341. doi:10.1016/j.chom.2011.03.008.

Jhingran, A., Chawla, B., Saxena, S., Barrett, M. P. and Madhubala, R. (2009). Paromomycin: Uptake and resistance in *Leishmania donovani*. *Molecular and Biochemical Parasitology* **164**, 111–117. doi:10.1016/j.molbiopara.2008.12.007.

Kangussu-Marcolino, M. M., De Paiva, R. M. C., Araújo, P. R., De Mendonça-Neto, R. P., Lemos, L., Bartholomeu, D. C., Mortara, R. A., Darocha, W. D. and Teixeira, S. M. R. (2013). Distinct genomic organization, mRNA expression and cellular localization of members of two amastin sub-families present in *Trypanosoma cruzi*. *BMC Microbiology* **13**,. doi:10.1186/1471-2180-13-10.

Karmakar, S., Ismail, N., Oliveira, F., Oristian, J., Zhang, W. W., Kaviraj, S., Singh, K. P., Mondal, A., Das, S., Pandey, K., Bhattacharya, P., Volpedo, G., Gannavaram, S., Satoskar, M., Satoskar, S., Sastry, R. M., Oljuskin, T., Sepahpour, T., Meneses, C., Hamano, S., Das, P., Matlashewski, G., Singh, S.,

Kamhawi, S., Dey, R., Valenzuela, J. G., Satoskar, A. and Nakhasi, H. L. (2021). Preclinical validation of a live attenuated dermotropic *Leishmania* vaccine against vector transmitted fatal visceral leishmaniasis. *Communications Biology* **4**, 1–14. doi:10.1038/s42003-021-02446-x.

Kato, K. C., Morais-Teixeira, E., Reis, P. G., Silva-Barcellos, N. M., Salaün, P., Campos, P. P., Corrêa-Junior, J. D., Rabello, A., Demicheli, C. and Frézard, F. (2014). Hepatotoxicity of pentavalent antimonial drug: Possible role of residual sb(3) and protective effect of ascorbic acid. *Antimicrobial Agents and Chemotherapy* **58**, 481–488. doi:10.1128/AAC.01499-13.

Kaur, T., Thakur, A. and Kaur, S. (2013). Protective immunity using MPL-A and autoclaved *Leishmania donovani* as adjuvants along with a cocktail vaccine in murine model of visceral leishmaniasis. *Journal of Parasitic Diseases* **37**, 231–239. doi:10.1007/s12639-012-0171-7.

Kaye, P. M. and Aebischer, T. (2011). Visceral leishmaniasis: Immunology and prospects for a vaccine. *Clinical Microbiology and Infection* **17**, 1462–1470. doi:10.1111/j.1469-0691.2011.03610.x.

Kaye, P. and Scott, P. (2011). Leishmaniasis: Complexity at the host-pathogen interface. *Nature Reviews Microbiology* **9**, 604–615. doi:10.1038/nrmicro2608.

Kedzierski, L. (2010). Leishmaniasis vaccine: Where are we today? *Journal of Global Infectious Diseases* **2**, 177. doi:10.4103/0974-777x.62881.

Kemp, M., Kurtzhals, J. A. L., Bendtzen, K., Poulsen, L. K., Hansen, M. B., Koech, D. K., Kharazmi, A. and Theander, T. G. (1993). *Leishmania donovani*-reactive Th1- and Th2-like T-cell clones from individuals who have recovered from visceral leishmaniasis. *Infection and Immunity* **61**, 1069–1073. doi:10.1128/iai.61.3.1069-1073.1993.

Kemp, K., Kemp, M., Kharazmi, A., Ismail, A., Kurtzhals, J. A. L., Hviid, L. and Theander, T. G. (1999). Leishmania-specific T cells expressing interferon-gamma (IFN-γ) and IL- 10 upon activation are expanded in individuals cured of visceral

leishmaniasis. *Clinical and Experimental Immunology* **116**, 500–504. doi:10.1046/j.1365-2249.1999.00918.x.

Khamesipour, A., Rafati, S., Davoudi, N., Maboudi, F. and Modabber, F. (2006). Leishmaniasis vaccine candidates for development: A global overview. *Indian Journal of Medical Research* **123**, 423–438.

Kharazmi, A., Kemp, K., Ismail, A., Gasim, S., Gaafar, A., Kurtzhals, J. A. L., El Hassan, A. M., Theander, T. G. and Kemp, M. (1999). T-cell response in human leishmaniasis. *Immunology Letters* **65**, 105–108. doi:10.1016/S0165-2478(98)00132-1.

Khatun, M., Alam, S. M. S., Khan, A. H., Hossain, M. A., Haq, J. A., Alam Jilani, M. S., Rahman, M. T. and Karim, M. M. (2017). Novel PCR primers to diagnose visceral leishmaniasis using peripheral blood, spleen or bone marrow aspirates. *Asian Pacific Journal of Tropical Medicine* **10**, 753–759. doi:10.1016/j.apjtm.2017.08.002.

Kumar, R. and Nylén, S. (2012). Immunobiology of visceral leishmaniasis. *Frontiers in Immunology* **3**, 1–10. doi:10.3389/fimmu.2012.00251.

Kumar, A., Pandey, S. C. and Samant, M. (2020). A spotlight on the diagnostic methods of a fatal disease Visceral Leishmaniasis. *Parasite Immunology* **42**, 0–2. doi:10.1111/pim.12727.

Kumar, V., Ghosh, S., Roy, K., Pal, C. and Singh, S. (2021). Deletion of Glutamine Synthetase Gene Disrupts the Survivability and Infectivity of *Leishmania donovani*. *Frontiers in Cellular and Infection Microbiology* **11**, 1–16. doi:10.3389/fcimb.2021.622266.

Lakshmi, B. S., Wang, R. and Madhubala, R. (2014a). *Leishmania* genome analysis and high-throughput immunological screening identifies tuzin as a novel vaccine candidate against visceral leishmaniasis. *Vaccine* **32**, 3816–3822. doi:10.1016/j.vaccine.2014.04.088.

Lakshmi, B. S., Wang, R. and Madhubala, R. (2014b). *Leishmania* genome analysis and high-throughput immunological screening identifies tuzin as a novel vaccine candidate

against visceral leishmaniasis. *Vaccine* **32**, 3816–3822. doi:10.1016/j.vaccine.2014.04.088.

Lehnhardt Pires, C., Rodrigues, S. D., Bristot, D., Gaeta, H. H., De Oliveira Toyama, D., Farias, W. R. L. and Toyama, M. H. (2013). Evaluation of macroalgae sulfated polysaccharides on the *Leishmania* (*L.*) *amazonensis* promastigote. *Marine Drugs* **11**, 934–943. doi:10.3390/md11030934.

Lima, Y. and Abass, K. S. (2020). Morphology, Life Cycle, Pathogenesis and Virulence Factors of Genus Leishmania : a Review. *Plant Archives* **20**, 4057–4060.

Loría-Cervera, E. N. and Andrade-Narváez, F. J. (2014). Review: Animal models for the study of leishmaniasis immunology. *Revista do Instituto de Medicina Tropical de Sao Paulo* **56**, 1–11. doi:10.1590/S0036-46652014000100001.

Mann, S., Frasca, K., Scherrer, S., Henao-Martínez, A. F., Newman, S., Ramanan, P. and Suarez, J. A. (2021). A Review of Leishmaniasis: Current Knowledge and Future Directions. *Current Tropical Medicine Reports* **8**, 121–132. doi:10.1007/s40475-021-00232-7.

Marcondes, M. and Day, M. J. (2019). Current status and management of canine leishmaniasis in Latin America. *Research in Veterinary Science* **123**, 261–272. doi:10.1016/j.rvsc.2019.01.022.

Matlashewski, G., Das, V. N. R., Pandey, K., Singh, D., Das, S., Ghosh, A. K., Pandey, R. N. and Das, P. (2013). Diagnosis of Visceral Leishmaniasis in Bihar India: Comparison of the rK39 Rapid Diagnostic Test on Whole Blood Versus Serum. *PLoS Neglected Tropical Diseases* **7**, 5–8. doi:10.1371/journal.pntd.0002233.

McCall, L. I. and Matlashewski, G. (2010). Localization and induction of the A2 virulence factor in Leishmania: Evidence that A2 is a stress response protein. *Molecular Microbiology* **77**, 518–530. doi:10.1111/j.1365-2958.2010.07229.x.

McCall, L. I., Zhang, W. W. and Matlashewski, G. (2013). Determinants for the Development of Visceral Leishmaniasis Disease. *PLoS Pathogens* **9**,.

doi:10.1371/journal.ppat.1003053.

Melby, P. C., Chandrasekar, B., Zhao, W. and Coe, J. E. (2001a). The Hamster as a Model of Human Visceral Leishmaniasis: Progressive Disease and Impaired Generation of Nitric Oxide in the Face of a Prominent Th1-Like Cytokine Response. *The Journal of Immunology* **166**, 1912–1920. doi:10.4049/jimmunol.166.3.1912.

Melby, P. C., Tabares, A., Restrepo, B. I., Cardona, A. E., McGuff, H. S. and Teale, J. M. (2001b). *Leishmania donovani*: Evolution and architecture of the splenic cellular immune response related to control of infection. *Experimental Parasitology* **99**, 17–25. doi:10.1006/expr.2001.4640.

Miralles, G. D., Stoeckle, M. Y., McDermott, D. F., Finkelman, F. D. and Murray, H. W. (1994). Th1 and Th2 cell-associated cytokines in experimental visceral Leishmaniasis. *Infection and Immunity* **62**, 1058–1063. doi:10.1128/iai.62.3.1058-1063.1994.

Mohapatra, T. M., Singh, D. P., Sen, M. R., Bharti, K. and Sundar, S. (2010). Comparative evaluation of rK9, rK26 and rK39 antigens in the serodiagnosis of Indian visceral leishmaniasis. *Journal of Infection in Developing Countries* **4**, 114–117. doi:10.3855/jidc.544.

Monzote, L. (2009). Current treatment of leishmaniasis: a review. *Open Antimicrob Agents J* **1**, 9–19.

Mugasa, C. M., Laurent, T., Schoone, G. J., Basiye, F. L., Saad, A. A., El Safi, S., Kager, P. A. and Schallig, H. D. F. H. (2010). Simplified molecular detection of *leishmania* parasites in various clinical samples from patients with leishmaniasis. *Parasites and Vectors* **3**, 1–6. doi:10.1186/1756-3305-3-13.

Müller, I., Pedrazzlni, T., Kropf, P., Louis, J. and Milon, G. (1991). Establishment of resistance to *Leishmania major* infection in susceptible BALB/c mice requires parasite-specific CD8+ T cells. *International Immunology* **3**, 587–597. doi:10.1093/intimm/3.6.587.

Muniaraj, M. (2014). The lost hope of elimination of Kala-azar (visceral leishmaniasis) by 2010 and cyclic occurrence of its outbreak in India, blame falls on vector control practices or co-infection with human immunodeficiency virus or therapeutic modalities? *Tropical Parasitology* **4**, 10. doi:10.4103/2229-5070.129143.

Murray, H. W. (2001). Tissue granuloma structure-function in experimental visceral leishmaniasis. *International Journal of Experimental Pathology* **82**, 249–267. doi:10.1046/j.1365-2613.2001.00199.x.

Murray, H. W. (2005). Interleukin 10 receptor blockade - Pentavalent antimony treatment in experimental visceral leishmaniasis. *Acta Tropica* **93**, 295–301. doi:10.1016/j.actatropica.2004.11.008.

Murray, H. W., Stern, J. J., Welte, K., Rubin, B. Y., Carriero, S. M. and Nathan, C. F. (1987). Experimental visceral leishmaniasis: production of interleukin 2 and interferon-gamma, tissue immune reaction, and response to treatment with interleukin 2 and interferon-gamma. *Journal of immunology (Baltimore, Md. : 1950)* **138**, 2290–7.

Murray, H. W., Jungbluth, A., Ritter, E., Montelibano, C. and Marino, M. W. (2000). Visceral Leishmaniasis in mice devoid of tumor necrosis factor and response to treatment. *Infection and Immunity* **68**, 6289–6293. doi:10.1128/IAI.68.11.6289-6293.2000.

Murray, H. W., Lu, C. M., Mauze, S., Freeman, S., Moreira, A. L., Kaplan, G. and Coffman, R. L. (2002). Interleukin-10 (IL-10) in experimental visceral leishmaniasis and IL-10 receptor blockade as immunotherapy. *Infection and Immunity* **70**, 6284–6293. doi:10.1128/IAI.70.11.6284-6293.2002.

Nicolas, L., Prina, E., Lang, T. and Milon, G. (2002). Real-time PCR for detection and quantitation of *Leishmania* in mouse tissues. *Journal of Clinical Microbiology* **40**, 1666–1669. doi:10.1128/JCM.40.5.1666-1669.2002.

Nylén, S. and Sacks, D. (2007). Interleukin-10 and the pathogenesis of human visceral leishmaniasis. *Trends in Immunology* **28**, 378–384. doi:10.1016/j.it.2007.07.004.

Nylén, S., Maurya, R., Eidsmo, L., Das Manandhar, K., Sundar, S. and Sacks, D. (2007). Splenic accumulation of IL-10 mRNA in T cells distinct from CD4 +CD25+ (Foxp3) regulatory T cells in human visceral leishmaniasis. *Journal of Experimental Medicine* **204**, 805–817. doi:10.1084/jem.20061141.

Opperdoes, F. R. (2019). Visceral leishmaniasis , Kala Azar , or dum dum fever.

Pal, M., Ejeta, I., Girma, A., Dave, K. and Dave, P. (2022). Etiology, Clinical Spectrum, Epidemiology, Diagnosis, Public Health Significance and Control of Leishmaniasis: A Comprehensive Review. *Acta Scientific Microbiology* 110–121. doi:10.31080/asmi.2022.05.1071.

Pandey, R. K., Ojha, R., Devender, M., Sebastian, P., Namdeo, M., Kumbhar, B. V., Sundar, S., Maurya, R. and Prajapati, V. K. (2022). Febrifugine dihydrochloride as a new oral chemotherapeutic agent against visceral leishmaniasis infection. *Experimental Parasitology* **236**–**237**, 108250. doi:10.1016/j.exppara.2022.108250.

Paris, C., Loiseau, P. M., Bories, C. and Bréard, J. (2004). Miltefosine Induces Apoptosis-Like Death in *Leishmania donovani* Promastigotes. *Antimicrobial Agents and Chemotherapy* **48**, 852–859. doi:10.1128/AAC.48.3.852-859.2004.

Peacock, C. S., Seeger, K., Harris, D., Murphy, L., Ruiz, J. C., Quail, M. A., Peters, N., Adlem, E., Tivey, A., Aslett, M., Kerhornou, A., Ivens, A., Fraser, A., Rajandream, M. A., Carver, T., Norbertczak, H., Chillingworth, T., Hance, Z., Jagels, K., Moule, S., Ormond, D., Rutter, S., Squares, R., Whitehead, S., Rabbinowitsch, E., Arrowsmith, C., White, B., Thurston, S., Bringaud, F., Baldauf, S. L., Faulconbridge, A., Jeffares, D., Depledge, D. P., Oyola, S. O., Hilley, J. D., Brito, L. O., Tosi, L. R. O., Barrell, B., Cruz, A. K., Mottram, J. C., Smith, D. F. and Berriman, M. (2007). Comparative genomic analysis of three *Leishmania* species that cause diverse human disease. *Nature Genetics* **39**, 839–847. doi:10.1038/ng2053.

Perez, L. E., Chandrasekar, B., Saldarriaga, O. A., Zhao, W., Arteaga, L. T., Travi, B. L. and Melby, P. C. (2006). Reduced Nitric Oxide Synthase 2 (NOS2) Promoter

Activity in the Syrian Hamster Renders the Animal Functionally Deficient in NOS2 Activity and Unable to Control an Intracellular Pathogen. *The Journal of Immunology* **176**, 5519–5528. doi:10.4049/jimmunol.176.9.5519.

Pramanik, A., Paik, D., Pramanik, P. K. and Chakraborti, T. (2019). Serine protease inhibitors rich Coccinia grandis (L.) Voigt leaf extract induces protective immune responses in murine visceral leishmaniasis. *Biomedicine and Pharmacotherapy* **111**, 224–235. doi:10.1016/j.biopha.2018.12.053.

Quinnell, R. J. and Courtenay, O. (2009). Transmission, reservoir hosts and control of zoonotic visceral leishmaniasis. *Parasitology* **136**, 1915–1934. doi:10.1017/S0031182009991156.

Rabaan, A. A., Bakhrebah, M. A., Mohapatra, R. K., Farahat, R. A., Dhawan, M., Alwarthan, S., Aljeldah, M. and Shammari, B. R. Al (2023). Omics Approaches in Drug Development against Leishmaniasis : Current Scenario and Future Prospects. 1–20.

Rafati, S., Hassani, N., Taslimi, Y., Movassagh, H., Rochette, A. and Papadopoulou, B. (2006). Amastin peptide-binding antibodies as biomarkers of active human visceral leishmaniasis. *Clinical and Vaccine Immunology* **13**, 1104–1110. doi:10.1128/CVI.00188-06.

Raj, S., Sasidharan, S., Balaji, S. N., Dubey, V. K. and Saudagar, P. (2020). Review on natural products as an alternative to contemporary anti-leishmanial therapeutics. *Journal of Proteins and Proteomics* **11**, 135–158. doi:10.1007/s42485-020-00035-w.

Raman, V. S., Duthie, M. S., Fox, C. B., Matlashewski, G. and Reed, S. G. (2012). Adjuvants for *Leishmania* vaccines: From models to clinical application. *Frontiers in Immunology* **3**, 1–15. doi:10.3389/fimmu.2012.00144.

Raymond, F., Boisvert, S., Roy, G., Ritt, J. F., Légaré, D., Isnard, A., Stanke, M., Olivier, M., Tremblay, M. J., Papadopoulou, B., Ouellette, M. and Corbeil, J. (2012). Genome sequencing of the lizard parasite *Leishmania* tarentolae reveals loss of genes associated to the intracellular stage of human pathogenic species. *Nucleic Acids Research* **40**, 1131–1147. doi:10.1093/nar/gkr834.

Reiner, S. L. and Locksley, R. M. (1995). The regulation of immunity to *Leishmania major*. *Annual Review of Immunology* **13**, 151–177. doi:10.1146/annurev.iy.13.040195.001055.

Reiner, S. L. and Seder, R. A. (1995). T helper cell differentiation in immune response. *Current Opinion in Immunology* **7**, 360–366. doi:10.1016/0952-7915(95)80111-1.

Reithinger, R. and Dujardin, J. C. (2007). Molecular diagnosis of leishmaniasis: Current status and future applications. *Journal of Clinical Microbiology* **45**, 21–25. doi:10.1128/JCM.02029-06.

Reithinger, R., Dujardin, J. C., Louzir, H., Pirmez, C., Alexander, B. and Brooker, S. (2007). Cutaneous leishmaniasis. *Lancet Infectious Diseases* **7**, 581–596. doi:10.1016/S1473-3099(07)70209-8.

Robledo, S. M., Murillo, J., Arbeláez, N., Montoya, A., Ospina, V., Jürgens, F. M., Vélez, I. D. and Schmidt, T. J. (2022). Therapeutic Efficacy of Arnica in Hamsters with Cutaneous Leishmaniasis Caused by *Leishmania braziliensis* and L. tropica. *Pharmaceuticals* **15**, 1–19. doi:10.3390/ph15070776.

Rochette, A., McNicoll, F., Girard, J., Breton, M., Leblanc, É., Bergeron, M. G. and Papadopoulou, B. (2005). Characterization and developmental gene regulation of a large gene family encoding amastin surface proteins in *Leishmania* spp. *Molecular and Biochemical Parasitology* **140**, 205–220. doi:10.1016/j.molbiopara.2005.01.006.

Roy, S., Mukhopadhyay, D., Mukherjee, S., Moulik, S., Chatterji, S., Brahme, N., Pramanik, N., Goswami, R. P., Saha, B. and Chatterjee, M. (2018). An IL-10 dominant polarization of monocytes is a feature of Indian Visceral Leishmaniasis. *Parasite Immunology* **40**, 0–2. doi:10.1111/pim.12535.

Roy, L., Uranw, S., Cloots, K., Smekens, T., Kiran, U. and Pyakurel, U. R. (2022). *Status of susceptibility of the visceral leishmaniasis vector , Phlebotomus (Diptera : Psychodidae : Phlebotominae), to insecticides used for vector control in Nepal*.

Sadlova, J., Seblova, V., Votypka, J., Warburg, A. and Volf, P. (2015). Xenodiagnosis of

Leishmania donovani in BALB/c mice using Phlebotomus orientalis: A new laboratory model. *Parasites and Vectors* **8**, 1–8. doi:10.1186/s13071-015-0765-x.

Salguero, F. J., Garcia-Jimenez, W. L., Lima, I. and Seifert, K. (2018). Histopathological and immunohistochemical characterisation of hepatic granulomas in *Leishmania donovani*-infected BALB/c mice: A time-course study. *Parasites and Vectors* **11**, 1–9. doi:10.1186/s13071-018-2624-z.

Santulli-Marotto, S., Gervais, A., Fisher, J., Strake, B., Ogden, C. A., Riveley, C. and Giles-Komar, J. (2015). Discovering molecules that regulate efferocytosis using primary human macrophages and high content imaging. *PLoS ONE* **10**, 1–21. doi:10.1371/journal.pone.0145078.

Shailendra Yadav, a, b Jitendra Kuldeep, c Mohammad I. Siddiqi, b, c Neena Goyala, B. (2020). TCP1_ Subunit Is Indispensable for Growth and Infectivity of *Leishmania donovani*. *Antimicrobial Agents and Chemotherapy* 1–18. doi:https://doi.org/10.1128/AAC.00669-20.

Sharma, U. and Singh, S. (2008). Insect vectors of Leishmania: Distribution, physiology and their control. *Journal of Vector Borne Diseases* **45**, 255–272.

Singh, O. P. and Sundar, S. (2015). Developments in diagnosis of visceral leishmaniasis in the elimination era. *Journal of Parasitology Research* **2015**,. doi:10.1155/2015/239469.

Späth, G. F. and Beverley, S. M. (2001). A lipophosphoglycan-independent method for isolation of infective *Leishmania* metacyclic promastigotes by density gradient centrifugation. *Experimental Parasitology* **99**, 97–103. doi:10.1006/expr.2001.4656.

Srivastava, P., Dayama, A., Mehrotra, S. and Sundar, S. (2011). Diagnosis of visceral leishmaniasis. *Transactions of the Royal Society of Tropical Medicine and Hygiene* **105**, 1–6. doi:10.1016/j.trstmh.2010.09.006.

Steverding, D. (2017). The history of leishmaniasis. *Parasites and Vectors* **10**, 1–10. doi:10.1186/s13071-017-2028-5.

Stober, C. B., Lange, U. G., Roberts, M. T. M., Alcami, A. and Blackwell, J. M. (2005).

IL-10 from Regulatory T Cells Determines Vaccine Efficacy in Murine *Leishmania major* Infection . *The Journal of Immunology* **175**, 2517–2524. doi:10.4049/jimmunol.175.4.2517.

Sudarshan, M., Weirather, J. L., Wilson, M. E. and Sundar, S. (2011). Study of parasite kinetics with antileishmanial drugs using real-time quantitative PCR in Indian visceral leishmaniasis. *Journal of Antimicrobial Chemotherapy* **66**, 1751–1755. doi:10.1093/jac/dkr185.

Sundar, S. and Olliaro, P. L. (2007). Miltefosine in the treatment of leishmaniasis: Clinical evidence for informed clinical risk management. *Therapeutics and Clinical Risk Management* **3**, 733–740. doi:10.2147/tcrm.s12160453.

Sundar, S., Reed, S. G., Singh, V. P., Kumar, P. C. K. and Murray, H. W. (1998). Rapid accurate field diagnosis of Indian visceral leishmaniasis. *Lancet* **351**, 563–565. doi:10.1016/S0140-6736(97)04350-X.

Sundar S, R. M. (2002). Laboratory diagnosis of visceral leishmaniasis. Clin Diagn Lab Immunol. *Clinacal And Diagnostic Laboratory Immunology* **9**, 951–8. doi:10.1128/CDLI.9.5.951.

Tavares, G. S. V., Mendonça, D. V. C., Pereira, I. A. G., Oliveira-Da-Silva, J. A., Ramos, F. F., Lage, D. P., MacHado, A. S., Carvalho, L. M., Reis, T. A. R., Perin, L., Carvalho, A. M. R. S., Ottoni, F. M., Ludolf, F., Freitas, C. S., Bandeira, R. S., Silva, A. M., Chávez-Fumagalli, M. A., Duarte, M. C., Menezes-Souza, D., Alves, R. J., Roatt, B. M. and Coelho, E. A. F. (2020). A clioquinol-containing Pluronic®F127 polymeric micelle system is effective in the treatment of visceral leishmaniasis in a murine model. *Parasite* **27**,. doi:10.1051/parasite/2020027.

Teixeira, S. M. R., Kirchhoff, L. V. and Donelson, J. E. (1995). Post-transcriptional elements regulating expression of mRNAs from the amastin/tuzin gene cluster of *Trypanosoma cruzi*. *Journal of Biological Chemistry* **270**, 22586–22594. doi:10.1074/jbc.270.38.22586.

Teng, Z., Zhang, Q., Yang, H., Kato, K., Yang, W., Lu, Y. R., Liu, S., Wang, C.,

Yamakata, A., Su, C., Liu, B. and Ohno, T. (2021). Atomically dispersed antimony on carbon nitride for the artificial photosynthesis of hydrogen peroxide. *Nature Catalysis* **4**, 374–384. doi:10.1038/s41929-021-00605-1.

Thakur, C. P., Kanyok, T. P., Pandey, A. K., Sinha, G. P., Zaniewski, A. E., Houlihan, H. H. and Olliaro, P. (2000). A prospective randomized, comparative, open-label trial of the safety and efficacy of paromomycin (aminosidine) plus sodium stibogluconate versus sodium stibogluconate alone for the treatment of visceral leishmaniasis. *Transactions of the Royal Society of Tropical Medicine and Hygiene* **94**, 429–431. doi:10.1016/S0035-9203(00)90130-5.

Thakur, S., Joshi, J. and Kaur, S. (2020). Leishmaniasis diagnosis: an update on the use of parasitological, immunological and molecular methods. *Journal of Parasitic Diseases* **44**, 253–272. doi:10.1007/s12639-020-01212-w.

Tiuman, T. S., Santos, A. O., Ueda-Nakamura, T., Filho, B. P. D. and Nakamura, C. V. (2011). Recent advances in leishmaniasis treatment. *International Journal of Infectious Diseases* **15**,. doi:10.1016/j.ijid.2011.03.021.

Tomiotto-Pellissier, F., Bortoleti, B. T. da S., Assolini, J. P., Gonçalves, M. D., Carloto, A. C. M., Miranda-Sapla, M. M., Conchon-Costa, I., Bordignon, J. and Pavanelli, W. R. (2018). Macrophage Polarization in Leishmaniasis: Broadening Horizons. *Frontiers in Immunology* **9**, 1–12. doi:10.3389/fimmu.2018.02529.

Trevethan, R. (2017). Sensitivity, Specificity, and Predictive Values: Foundations, Pliabilities, and Pitfalls in Research and Practice. *Frontiers in Public Health* **5**, 1–7. doi:10.3389/fpubh.2017.00307.

van Griensven, J. and Diro, E. (2019). Visceral Leishmaniasis: Recent Advances in Diagnostics and Treatment Regimens. *Infectious Disease Clinics of North America* **33**, 79–99. doi:10.1016/j.idc.2018.10.005.

Varani, S., Ortalli, M., Attard, L., Vanino, E., Gaibani, P., Vocale, C., Rossini, G., Cagarelli, R., Pierro, A., Billi, P., Mastroianni, A., Cesare, S. Di, Codeluppi, M., Franceschini, E., Melchionda, F., Gramiccia, M., Scalone, A. and Gentilomi, G. A.

(2017). Serological and molecular tools to diagnose visceral leishmaniasis : 2-years ' experience of a single center in Northern Italy. 1–10.

Varma, N. and Naseem, S. (2010). Hematologic changes in visceral Leishmaniasis/Kala Azar. *Indian Journal of Hematology and Blood Transfusion* **26**, 78–82. doi:10.1007/s12288-010-0027-1.

Vélez, I. D., Gilchrist, K., Arbelaez, M. P., Rojas, C. A., Puerta, J. A., Antunes, C. M. F., Zicker, F. and Modabber, F. (2005). Failure of a killed *Leishmania amazonensis* vaccine against American cutaneous leishmaniasis in Colombia. *Transactions of the Royal Society of Tropical Medicine and Hygiene* **99**, 593–598. doi:10.1016/j.trstmh.2005.04.002.

Veress, B., Omer, A. and Satir, A. A. (1977). Morphology of the spleen and lymph nodes.

Vermelho, A. B., Supuran, C. T., Cardoso, V., Menezes, D., Rocha, J., Silva, D. A., Luiz, J., Ferreira, P., Claudia, A., Amaral, F. and Rodrigues, I. a Leishmaniasis : Possible New Strategies for Treatment. doi:10.5772/57388.

Veronica, J., Chandrasekaran, S., Dayakar, A., Devender, M., Prajapati, V. K., Sundar, S. and Maurya, R. (2019). Iron superoxide dismutase contributes to miltefosine resistance in *Leishmania donovani*. *FEBS Journal* **286**, 3488–3503. doi:10.1111/febs.14923.

Vidal, S., Tremblay, M. L., Govoni, G., Gauthier, S., Sebastiani, G., Malo, D., Skamene, E., Olivier, M., Jothy, S. and Gros, P. (1995). The ity/lsh/bcg locus: Natural resistance to infection with intracellular parasites is abrogated by disruption of the nrampl gene. *Journal of Experimental Medicine* **182**, 655–666. doi:10.1084/jem.182.3.655.

Waller, R. F. and McConville, M. J. (2002). Developmental changes in lysosome morphology and function *Leishmania* parasites. *International Journal for Parasitology* **32**, 1435–1445. doi:10.1016/S0020-7519(02)00140-6.

Zhang, W. W., Ghosh, A. K., Mohamath, R., Whittle, J., Picone, A., Lypaczewski, P.,

Ndao, M., Howard, R. F., Das, P., Reed, S. G. and Matlashewski, G. (2018). Development of a sandwich ELISA to detect *Leishmania* 40S ribosomal protein S12 antigen from blood samples of visceral leishmaniasis patients. *BMC Infectious Diseases* **18**, 1–11. doi:10.1186/s12879-018-3420-2.

Zijlstra, E. E. (2016). The immunology of post-kala-azar dermal leishmaniasis (PKDL). *Parasites and Vectors* **9**, 1–9. doi:10.1186/s13071-016-1721-0.

Zijlstra, E. E., Alves, F., Rijal, S., Arana, B. and Alvar, J. (2017). Post-kala-azar dermal leishmaniasis in the Indian subcontinent: A threat to the South-East Asia Region Kala-azar Elimination Programme. *PLoS Neglected Tropical Diseases* **11**, 1–16. doi:10.1371/journal.pntd.0005877.

Publications

The FEBS Journal

FEBS PRESS science publishing by scientists

Iron superoxide dismutase contributes to miltefosine resistance in *Leishmania donovani*

Jalaja Veronica[1], Sambamurthy Chandrasekaran[1], Alti Dayakar[1], Moodu Devender[1], Vijay Kumar Prajapati[2], Shyam Sundar[3] and Radheshyam Maurya[1]

1 Department of Animal Biology, School of Life Sciences, University of Hyderabad, India
2 Department of Biochemistry, School of Life Sciences, Central University of Rajasthan, Ajmer, India
3 Department of Medicine, IMS, Banaras Hindu University, Varanasi, India

Keywords
iron superoxide dismutase; *Leishmania donovani*; miletfosine; proteome; resistant

Correspondence
R. Maurya, Department of Animal Biology, School of Life Sciences, University of Hyderabad, Prof. C.R. Rao Road, Gachibowli, Hyderabad 500046, India
Tel: +91 402 3134532
E-mails: rmusl@uohyd.ernet.in, radhemaurya@rediffmail.com

(Received 3 June 2018, revised 19 February 2019, accepted 10 May 2019)

doi:10.1111/febs.14923

The emergence of drug-resistant *Leishmania* is the major challenge to management of visceral leishmaniasis (VL) in areas in which this parasite is endemic. Miltefosine has been widely used against VL, but the emergence of resistant strains could impose a significant threat in the near future. The present study used high-throughput proteomics to determine whether proteins are differentially expressed in miltefosine-resistant (BHU875) and -sensitive (DD8) *Leishmania donovani* strains. Comparative proteomic analysis revealed up-regulation of iron superoxide dismutase (FeSODA) in the resistant BHU875 strain compared to the drug-sensitive DD8 strain. In accordance with the proteomic data, BHU875 showed higher FeSODA enzymatic activity relative to the sensitive strain. Molecular characterization of BHU875 parasites in which the gene encoding FeSODA was silenced demonstrated that drug sensitivity was restored and the intracellular survival of the parasite was lowered. This suggests that FeSODA activity plays a part in miltefosine resistance. Our study provides a drug target that could be used to overcome miltefosine resistance or help in rational redesigning of miltefosine-based therapy to combat *Leishmania* infection.

Introduction

Visceral leishmaniasis (VL), one of the most severe clinical forms of leishmaniasis, is caused by a protozoan parasite *Leishmania donovani* in the Indian subcontinent. The disease symptoms include recurrent bouts of fever, gradual weight loss, fatigue, anemia, hepatomegaly, and splenomegaly. The life-threatening disease is responsible for ~ 40 000 deaths per annum in the Indian subcontinent [1] and has been categorized by World Health Organization as one of the neglected tropical diseases. Few antileishmanial drugs are available to treat VL such as sodium stibogluconate, amphotericin B, paromomycin, and miltefosine. The development of resistance against these drugs limits their clinical efficacy [2] and also abandons VL elimination. Miltefosine (Milt), the only promising oral drug, is used to control leishmaniasis in endemic areas of the Indian subcontinent [3,4]. Miltefosine (hexadecylphosphocholine), an analog of phosphatidylcholine, was originally developed as an anticancer drug [5,6] and fortuitously found to have an antileishmanial activity [7,8]. The internalization of Milt in parasite is thought to be either by an endocytic pathway or by a nonendocytic pathway through flippase activity [9]. The leishmanicidal action of Milt against the parasite remains to be an enigma. However, previous reports suggest that it exerts an apoptosis-like death [10,11],

Abbreviations
ABC, ATP-binding cassette; ASFesodA, antisense FesodA; DMEM, Dulbecco's modified Eagle's medium; EPB, electroporation buffer; FeSODA, iron superoxide dismutase; KD, knockdown; LGT, lateral gene transfer; MFI, mean fluorescence intensity; Milt/MIL, miltefosine; NBT, nitroblue tetrazolium; PI, propidium iodide; ROS, reactive oxygen species; VL, visceral leishmaniasis; WT, wild-type.

frontiers in Immunology

REVIEW
published: 18 June 2021
doi: 10.3389/fimmu.2021.649359

COVID-19 Severity in Obesity: Leptin and Inflammatory Cytokine Interplay in the Link Between High Morbidity and Mortality

Radheshyam Maurya[1]*, *Prince Sebastian*[1], *Madhulika Namdeo*[1], *Moodu Devender*[1] *and Arieh Gertler*[2]

[1] Department of Animal Biology, School of Life Sciences, University of Hyderabad, Hyderabad, India, [2] Institute of Biochemistry, Food Science and Nutrition, The Hebrew University of Jerusalem, Rehovot, Israel

OPEN ACCESS

Edited by:
Alexandros Tsoupras,
University of Limerick, Ireland

Reviewed by:
Markus Xie,
Genentech, United States
Viviana Parreño,
National Agricultural Technology Institute, Argentina
Matteo A. Russo,
San Raffaele Pisana (IRCCS), Italy
Nicolò Merendino,
University of Tuscia, Italy

***Correspondence:**
Radheshyam Maurya
rmusl@uohyd.ac.in;
rmusl@uohyd.ernet.in

Specialty section:
This article was submitted to Nutritional Immunology, a section of the journal Frontiers in Immunology

Received: 04 January 2021
Accepted: 31 May 2021
Published: 18 June 2021

Citation:
Maurya R, Sebastian P, Namdeo M, Devender M and Gertler A (2021) COVID-19 Severity in Obesity: Leptin and Inflammatory Cytokine Interplay in the Link Between High Morbidity and Mortality. Front. Immunol. 12:649359. doi: 10.3389/fimmu.2021.649359

Obesity is one of the foremost risk factors in coronavirus infection resulting in severe illness and mortality as the pandemic progresses. Obesity is a well-known predisposed chronic inflammatory condition. The dynamics of obesity and its impacts on immunity may change the disease severity of pneumonia, especially in acute respiratory distress syndrome, a primary cause of death from SARS-CoV-2 infection. The adipocytes of adipose tissue secret leptin in proportion to individuals' body fat mass. An increase in circulating plasma leptin is a typical characteristic of obesity and correlates with a leptin-resistant state. Leptin is considered a pleiotropic molecule regulating appetite and immunity. In immunity, leptin functions as a cytokine and coordinates the host's innate and adaptive responses by promoting the Th1 type of immune response. Leptin induced the proliferation and functions of antigen-presenting cells, monocytes, and T helper cells, subsequently influencing the pro-inflammatory cytokine secretion by these cells, such as TNF-α, IL-2, or IL-6. Leptin scarcity or resistance is linked with dysregulation of cytokine secretion leading to autoimmune disorders, inflammatory responses, and increased susceptibility towards infectious diseases. Therefore, leptin activity by leptin long-lasting super active antagonist's dysregulation in patients with obesity might contribute to high mortality rates in these patients during SARS-CoV-2 infection. This review systematically discusses the interplay mechanism between leptin and inflammatory cytokines and their contribution to the fatal outcomes in COVID-19 patients with obesity.

Keywords: COVID-19, leptin, obesity, inflammation, cytokine, mortality

INTRODUCTION

Obesity is marked as redundant fat accumulation in the body. Obesity is considered an increased circulating fatty acid that is causing low-grade chronic inflammation due to macrophages' chemoattraction and its expansion in the adipose tissue (1, 2). An individual with obesity presents with increased TNF-α cytokine, changed T-cell subset, and suppressed T-cell responses

Experimental Parasitology 236-237 (2022) 108250

Contents lists available at ScienceDirect

Experimental Parasitology

journal homepage: www.elsevier.com/locate/yexpr

Febrifugine dihydrochloride as a new oral chemotherapeutic agent against visceral leishmaniasis infection

Rajan Kumar Pandey [a], Rupal Ojha [a], Moodu Devender [b], Prince Sebastian [b], Madhulika Namdeo [b], Bajarang Vasant Kumbhar [c], Shyam Sundar [d], Radheshyam Maurya [b], Vijay Kumar Prajapati [a,*]

[a] Department of Biochemistry, School of Life Sciences, Central University of Rajasthan, NH-8, Bandarsindri, Kishangarh Ajmer, 305817, Rajasthan, India
[b] Department of Animal Biology, School of Life Science, University of Hyderabad, Hyderabad, India
[c] Department of Biological Sciences, Sunandan Divatia School of Science, NMIMS University (Deemed), Vile Parle, Mumbai, India
[d] Department of Medicine, Institute of Medical Sciences, Banaras Hindu University, Varanasi, 221005, UP, India

ARTICLE INFO

Keywords:
Visceral leishmaniasis
Febrifugine
Miltefosine
Drug repurposing
BALB/c mice

ABSTRACT

Visceral leishmaniasis (VL) is the deadliest form of leishmaniasis without a safer treatment option. This study implies drug repurposing to find a novel antileishmanial compound, namely febrifugine dihydrochloride (FFG) targeting *Leishmania* antioxidant system. Starting with virtual screening revealed the high binding affinity and lead likeness of FFG against the trypanothione reductase (TR) enzyme of *Leishmania donovani,* followed by experimental validation. The promastigotes inhibition assay gave the IC50 concentration of FFG and Miltefosine (positive control) as 7.16 ± 1.39 nM and 11.41 ± 0.29 μM, respectively. Their CC_{50} was found as 451 ± 12.73 nM and 135.9 ± 5.94 μM, respectively. FFG has been shown to increase the reactive oxygen species (ROS), leading to apoptosis-like cell death among *L. donovani* promastigotes. Spleen touch biopsy resulted in 62% and 55% decreased parasite load with FFG and miltefosine treatment, respectively. Cytokine profiling has shown an increased proinflammatory cytokine response post-FFG treatment. Moreover, FFG is safe on the liver toxicity parameter in mice post-treatment.

1. Introduction

Visceral leishmaniasis (VL) or kala-azar is the fatal form of leishmaniasis caused by the obligate intracellular protozoan parasite of genus *Leishmania,* mainly *L. donovani* and *L. infantum* (Terefe et al., 2015). The former affects the population of the Indian subcontinent and Africa, while later affects the population of the Mediterranean basin, South and Central America (Torres-Guerrero et al., 2017). Sandflies, mainly *Phlebotomus argentipes* and *Lutzomyia longipalpis* are the vectors to spread this disease severity in the old world (Indian subcontinent and Africa) and the new world (Mediterranean basin, South and Central America), respectively (Maroli et al., 2013). VL targets the cells of the reticuloendothelial system, and increasing parasite load leads to the swelling of the liver and spleen (Alemayehu and Alemayehu, 2017). Its symptoms include fever, weight loss, anemia, hepatosplenomegaly, and thrombocytopenia (Lainson and Shaw, 1978). Even after such a severe clinical manifestation, none of the vaccine candidates have been registered to prevent this disease. The treatment of VL only relies upon the countable number of chemotherapeutic drugs. These drugs are pentavalent antimonials, amphotericin B, Miltefosine, and paromomycin.

Antimonial has been the first-line treatment for the VL since the 1970s; later on, a gradual decrease in its clinical efficacy and more than 70% resistance within only two decades restricted its use in the Bihar state of India. Later, amphotericin B (AmB) was introduced as a second-line treatment, yet soon it turned into a mainline treatment. Still, it has shown resistance and adverse events like myocarditis, infusion reaction, hypokalemia, and nephrotoxicity (Messori et al., 2013). Further, paromomycin was reported from Kenya in the 1990s, having good efficacy and showing side effects like pain at the injection site. At the same time, few patients experienced reversible ototoxicity (2%) and hepatotoxicity (6%) (Sundar et al., 2007). Later in 2002s, Miltefosine was approved as the first oral antileishmanial drug in India but was also associated with various adverse events like gastrointestinal toxicity, recurrent hepatotoxicity, nephrotoxicity, and teratogenicity (Sundar et al., 2012).

* Corresponding author.
E-mail address: vkprajapati@curaj.ac.in (V.K. Prajapati).

https://doi.org/10.1016/j.exppara.2022.108250
Received 20 September 2021; Received in revised form 9 March 2022; Accepted 23 March 2022
Available online 4 April 2022

Anti-Plagiarism report

Deciphering the Tuzin protein of Leishmania donovani as a potential Diagnostic Marker and Vaccine Candidate against Visceral Leishmaniasis

by Moodu Devender

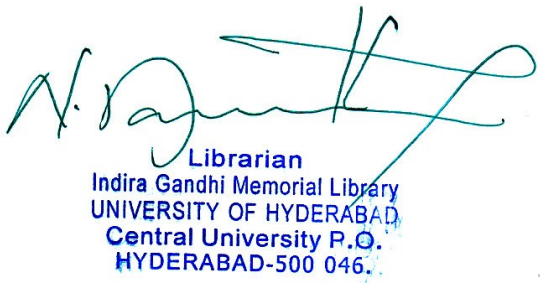

Submission date: 27-Mar-2023 05:17PM (UTC+0530)
Submission ID: 2047956992
File name: MOODU_DEVENDER.docx (321.62K)
Word count: 24328
Character count: 134339

Deciphering the Tuzin protein of Leishmania donovani as a potential Diagnostic Marker and Vaccine Candidate against Visceral Leishmaniasis

ORIGINALITY REPORT

8%	7%	4%	2%
SIMILARITY INDEX	INTERNET SOURCES	PUBLICATIONS	STUDENT PAPERS

PRIMARY SOURCES

1	dspace.uohyd.ac.in Internet Source	2%
2	Submitted to University of Hyderabad, Hyderabad Student Paper	1%
3	link.springer.com Internet Source	<1%
4	www.frontiersin.org Internet Source	<1%
5	studentsrepo.um.edu.my Internet Source	<1%
6	Shivani Thakur, Jyoti Joshi, Sukhbir Kaur. "Leishmaniasis diagnosis: an update on the use of parasitological, immunological and molecular methods", Journal of Parasitic Diseases, 2020 Publication	<1%
7	patents.google.com	

	Internet Source	<1%
8	www.freepatentsonline.com Internet Source	<1%
9	core.ac.uk Internet Source	<1%
10	hdl.handle.net Internet Source	<1%
11	erepository.uonbi.ac.ke:8080 Internet Source	<1%
12	www.jbc.org Internet Source	<1%
13	"Abstracts - Friday 27th July 2001", Scandinavian Journal of Immunology, 7/2001 Publication	<1%
14	Submitted to Birla Institute of Technology and Science Pilani Student Paper	<1%
15	dspace.uevora.pt Internet Source	<1%
16	Tushar Tukaram Dhumal, Rajender Kumar, Anindita Paul, Pradyot Kumar Roy, Prabha Garg, Sushma Singh. "Molecular explorations of the Leishmania donovani 6-phosphogluconolactonase enzyme, a key	<1%

player in the pentose phosphate pathway", Biochimie, 2022
Publication

17	qmro.qmul.ac.uk Internet Source	<1 %
18	www.patentguru.com Internet Source	<1 %
19	Submitted to KYUNG HEE UNIVERSITY Student Paper	<1 %
20	www.zora.uzh.ch Internet Source	<1 %
21	ALESSANDRO GRAPPUTO. "The voyage of an invasive species across continents: genetic diversity of North American and European Colorado potato beetle populations", Molecular Ecology, 10/10/2005 Publication	<1 %
22	etd.aau.edu.et Internet Source	<1 %
23	pure.rug.nl Internet Source	<1 %
24	theses.gla.ac.uk Internet Source	<1 %
25	www.ncbi.nlm.nih.gov Internet Source	<1 %

26	Submitted to Dublin City University Student Paper	<1%
27	Submitted to Ivy Tech Community College Central Office Student Paper	<1%
28	Submitted to Jawaharlal Nehru University (JNU) Student Paper	<1%
29	"Development of recombinant vaccines to prevent the disease caused by the respiratory viruses SARS-CoV-2, hMPV, and hRSV", Pontificia Universidad Catolica de Chile, 2022 Publication	<1%
30	Alti Dayakar, Sambamurthy Chandrasekaran, Jalaja Veronica, Vadloori Bharadwaja, Radheshyam Maurya. "Leptin regulates Granzyme-A, PD-1 and CTLA-4 expression in T cell to control visceral leishmaniasis in BALB/c Mice", Scientific Reports, 2017 Publication	<1%
31	Kumar, Rajiv, and Susanne NylÃ©n. "Immunobiology of visceral leishmaniasis", Frontiers in Immunology, 2012. Publication	<1%
32	Biology of C Reactive Protein in Health and Disease, 2016. Publication	<1%

33	M. SAMANT. "Proteophosphoglycan is differentially expressed in sodium stibogluconate-sensitive and resistant Indian clinical isolates of Leishmania donovani", Parasitology, 08/2007 Publication	<1 %
34	Submitted to Universiti Malaysia Terengganu UMT Student Paper	<1 %
35	journals.plos.org Internet Source	<1 %
36	jpet.aspetjournals.org Internet Source	<1 %
37	thurj.org Internet Source	<1 %
38	Ahmad Shabanizadeh, Mohammad Reza Rahmani, Aliakbar Yousefi-Ahmadipour, Fatemeh Asadi, Mohammad Kazemi Arababadi. "Mesenchymal Stem Cells: The Potential Therapeutic Cell Therapy to Reduce Brain Stroke Side Effects", Journal of Stroke and Cerebrovascular Diseases, 2021 Publication	<1 %
39	J DEGROOT, M RUIS, J SCHOLTEN, J KOOLHAAS, W BOERSMA. "Long-term effects of social stress on antiviral immunity in pigs", Physiology & Behavior, 2001	<1 %

	Publication	
40	aem.asm.org Internet Source	<1 %
41	citeseer.ist.psu.edu Internet Source	<1 %
42	ourarchive.otago.ac.nz Internet Source	<1 %
43	Submitted to University of Sydney Student Paper	<1 %
44	Venuprasad, K.. "CD28 signaling in neutrophil induces T-cell chemotactic factor(s) modulating T-cell response", Human Immunology, 200301 Publication	<1 %
45	Zhang, Chun-Ying, Juan Zhou, Bin Ding, Xiao-Jun Lu, Yu-Ling Xiao, Xiao-Su Hu, and Ying Ma. "Phylogenetic analysis of lack gene sequences for 22 Chinese Leishmania isolates", Infection Genetics and Evolution, 2013. Publication	<1 %
46	minerva-access.unimelb.edu.au Internet Source	<1 %
47	repository.ubn.ru.nl Internet Source	<1 %
48	www.mdpi.com Internet Source	<1 %

49	www.science.org Internet Source	<1%
50	Dan Yan Zhu, Xiao Zhao Deng, Long Feng Jiang, Wen Xiao et al. "Potential Role of Hepatitis C Virus Alternate Reading Frame Protein in Negative Regulation of T-Bet Gene Expression", Inflammation, 2015 Publication	<1%
51	Parul Tripathi, Vinod Singh, Sita Naik. "Immune response to leishmania: paradox rather than paradigm", FEMS Immunology & Medical Microbiology, 2007 Publication	<1%
52	ulspace.ul.ac.za Internet Source	<1%

Exclude quotes	On	Exclude matches	< 14 words
Exclude bibliography	On		